THE UNIVERSITY *of* EDINBURGH

Roles of the microRNA pathway in cortical development.

By Tomasz Jan Nowakowski

Thesis submitted for the degree of doctor of philosophy at the University of Edinburgh

December 2011

DISCLAIMER

I (Tomasz Jan Nowakowski) performed all of the experiments presented in this thesis unless otherwise clearly stated in the text. No part of this work has been, or is being submitted for any other degree of qualification.

Signed:

Date:

Límites

“De estas calles que ahondan el poniente,
una habrá (no sé cual) que he recorrido
ya por última vez, indiferente
y sin adivinarlo, sometido”

Joge Luis Borges

I dedicate this Thesis to my father, Marian Nowakowski, whose determination and perseverance have inspired me to always choose the most challenging of the paths of life open to me.

ACKNOWLEDGEMENTS

First of all I wish to thank my supervisors David Price and Tom Pratt for allowing me to pursue my ideas and for their rigorous and critical review of work. Sincere thanks to Veronica van Heyningen for her time to provide good advice and mentoring at all stages of my work.

I am deeply indebted to Vassiliki Fotaki who has provided me mentoring, technical support, professional and personal advice.

Big thanks to Jane Quinn who fostered my scientific rigour and helping me ask important questions about experiments and project design.

I wish to thank members of the Price, Mason, Pratt, Kind and Spears laboratories for being such a very friendly environment to work in and for their technical support. In particular I wish to thank Michael Molinek, Rowena Smith and Alison Murray who inducted me into the know-how of cell and tissue culture techniques. I also wish to thank Trudi Gillespie for effortless attempts to teach me how to master confocal microscopy. I wish to thank the staff at the Hugh Robson Building Animal House who looked after my mice.

Furthermore, I wish to thank my fantastic friends who shared with me the time I spent in Edinburgh, particularly Julio Rodriguez- Andres, Robert Ekiert, Albert Sanchez- Ribalta, Ryota Iwasawa, Hayden Selvadurai, Lynne Harris, Manuela Marescotti Elise Malavasi and Marta Golonek- Ekiert.

Probably the greatest thanks should go to the unknown author of the assignment for Molecular Genetics 3 course during my Undergraduate education. This assignment incited my love for RNA interference and microRNAs and motivated me throughout this work.

I also wish to thank my parents Izabella and Marian and my sister Maria who are a wonderful family and who have supported my all the way. Special thanks also to Elzbieta Petlicka for her patience and understanding.

ABSTRACT

Dicer endoribonuclease catalyzes the maturation of microRNAs (miRNAs) from double stranded precursors. Studies conditionally inactivating Dicer in the mouse embryonic forebrain continue to shed light on the spectrum of biological processes subject to miRNA regulation.

This study looked at defects of brain development following a widespread ablation of Dicer in the early forebrain. The neuroepithelial stem cells failed to specify the radial glia appropriately around the time when the first postmitotic neurons begin to be generated in the neuroepithelium.

Ablation of Dicer in only a subset of radial glia was not accompanied by the early apoptosis observed in all other models of Dicer ablation in the cortex. This allowed the study of the role of miRNAs in regulating cell numbers in the cortex. The study revealed that generation of cortical cells is increased during postnatal development.

Finally, the study identified a miRNA which is able to negatively regulate the development of neuronal precursor cells of the developing cortex by targeting T-box transcription factor 2.

Together the results presented in this Thesis contribute to the understanding of the roles of endogenous RNA interference in the development of the brain.

TABLE OF CONTENTS

TABLE OF FIGURES

ABBREVIATIONS

DiI	1,1'-dioctadecyl-3,3,3',3'-tetramethylindocarbocyanine
DAPI	4'-6-Diamino-2-phenylindole
ANOVA	Analysis of variance
anr	Anterior neural ridge
AR	Antigen retrieval
Ago	Argonaute
aPKC	Atypical protein kinase C
Bmp	Bone morphogenetic protein
Blbp	Brain- lipid binding protein
BrdU	Bromodeoxyuridine
CoP	Comissural plate
CH	Cortical hem
CP	Cortical plate
Cux	Cut-like homeobox
cAMP	Cyclic adenosine monophosphate
CREB	cyclic AMP responsive element binding
CMV	Cytomegalovirus
DNA	Deoxyribonucleic acid
DAB	Diaminobenzidine
Dgcr	DiGeorge critical region
DIG	Digoxigenin
dTel	Doral telencephalon
DP	Dorsal pallium
dsRNA	Double- stranded RNA
Dcx	Doublecortin
E	Embryonic age (day)
EGFP	Enhanced green fluorescent protein
EDTA	Ethylenediaminetetraacetic acid

eIF4E	Eukaryotic initiation factor 4E
Fgf	Fibroblast growth factor
Fox	Forkhead box
GABA	Gamma-aminobutyric acid
GFAP	Glial fibrillary acidic protein
GLAST	Glutamate aspartate transporter
GFP	Greeen fluorescent protein
Hes	Hairy enhancer of split
HEK	Human embryonic kidney
hTh	Hypothalamus
INP	Intermediate neural progenitors
IPC	Intermediate progenitor cell
IZ	Intermediate zone
IRES	Internal ribosomal enrty site
IPC	Intraperitoneal
JAK	Just another kinase
LGE	Lateral ganglionic eminence
LP	Lateral pallium
LNA	Locked nucleic acid
MGE	Medial ganglionic eminence
MP	Medial pallium
mRNA	Messenger RNA
miRNA	MicroRNA
Me	Midbrain
N	Neural plate
NP	Neural progenitors
NE	Neuroepithelial stem cells
Ngn	Neurogenin
NRSF	Neuron restrictive silencing factor

NEB	New england biolabs
NMD	Nonsense mediated decay
NICD	Notch intracellular domain
nc	Notocord
OB	Olfactory bulb
Pax	Paired box
PFA	Paraformaldehyde
PBS	Phosphate buffered saline
pHH3	Phosphohistone 3
PAZ	Piwi- Argonaute- Zwille
piRNA	Piwi-interacting RNA
PABP	Poly- adenosine binding protein
Pol	Polymerase
PCR	Polymerase chain reaction
P	Postnatal age (day)
pre-miRNA	Precursor microRNA
POa	Preoptic area
pri-miRNA	Primary microRNA transcript
RG	Radial glia
REST	Repressor element-1 silencing transcription factor
RE1	Repressor element-1 silencing transcription factor
RA	Retinoic acid
RNase	Ribonuclease
RNA	Ribonucleic acid
RISC	RNA- Induced Silencing Complex
RMS	Rostral migratory stream
STAT	Signal transducer and activator of transcription
Shh	Sonic hedgehog
Sox	Sry- like box

SVZ	Subventricular zone
Tlx	Tailless
UTR	Untranslated region
VP	Ventral pallium
vTel	Ventral telencephalon
VZ	Ventricular zone
V	Volume
WM	White matter
YFP	Yellow fluorescent protein

CHAPTER 1:
General Introduction

1.1 Overview

Development of the brain is a complex and multi-stage process which requires a number of biological events taking place at the right time in the right place. At the molecular level, this involves high fidelity control of protein expression. Until recently the control of protein expression during development was mostly thought to take place at the level of their coding genes with transcription factors responding to signalling molecules and switching gene transcription on and off when necessary. However, recent advances in biology have greatly broadened our understanding of the complexity of factors which regulate the expression of genes. These include the roles of the "junk" DNA, epigenetic modifications, splicing, RNA editing, non-protein coding RNAs to name a few. This thesis focuses on the role of microRNA molecules in the control of biological processes and gene expression during the development of the cortex. This study investigated the role of the microRNA pathway during development by generating models of Dicer –deficient neuroepithelial cells and identifies a novel functional interaction between one of the non-coding RNAs and one of the key transcription factors regulating brain development. The introduction will initially provide an overview of mechanisms regulating the embryonic development of the cortex with a clear focus on mechanisms of progenitor cell development which regulate cortical cell number and diversity. The second part of the introduction will provide an overview of the RNA interference pathway with a focus on the known functions of Dicer and microRNAs in the developing mouse cortex.

1.2 Cortex development

1.2.1 Neural induction and anteroposterior patterning of the neural plate

Formation of the neural plate follows a highly stereotypical pattern in virtually all studied vertebrates. Most of the early experimental work elucidating the origins of the forebrain during development including the identification of key genetic networks was done in *Xenopus laevis*.

Transplantation experiments by Spemann and Mangold showed that the dorsal lip of the early blastopore is able to instruct the formation of the neural axis (Bouwmeester, 2001). The progeny of the Spemann's organiser migrate rostrally to give rise to the notochord. Cells of the notochord express a number of Bone morphogenetic protein (Bmp) antagonists such as Chordin, Noggin and Follistatin (Bouwmeester, 2001). These factors induce neural fate in the overlying ectoderm and the formation of the neural plate with cells undergoing pseudostratification (Figure 1.01). Clonal analysis experiments of single epiblast cells of the early embryo revealed that the early neural plate shows anteroposterior patterning (Lawson and Pedersen, 1992). The rostral section of the notochord, the prechordal plate produces factors, including Cerberus and Goosecoid (Piccolo et al., 1999; Steinbeisser et al., 1993) that instruct the neural plate to express genes, Lim1 and Otx2, which are necessary for development of anterior neural structures (Acampora et al., 1995; Matsuo et al., 1995; Shawlot and Behringer, 1995). Posterior neural plate is patterned by the posterior notochord, which expresses Brachyury and is a source of the Fibroblast growth factor (Fgf) signalling (Conlon and Smith, 1999; Kimelman and Kirschner, 1987).

These pathways were later found to be conserved in the mouse as well as other vertebrates and thanks to the development of technology to generate transgenic mice it was possible to verify their roles in mammalian development. Therefore, the next paragraph describing more in-depth mechanisms of forebrain specification and patterning is based largely on studies that were performed in mice.

Figure 1.01: Development and patterning of cerebral cortex. (A) Dorsal view of an E8 mouse embryo. Visible is the neural plate which will give rise to all structures of the central nervous system (N) (Sulik et al., 1994). (B) Open view of the neural plate, patterns indicate the expression of key regulators of the early development of the neural tube including the Fibroblast growth factor 8 (Fgf8) which is expressed at the anterior neural ridge (anr) and patterns the telencephalon by promoting the expression of Foxg1 (BF1) as well as at the boundary between the midbrain (me) and the hindbrain (rh). The expression of Sonic hedgehog (Shh) by the notochord (nc) and the prechordal plate (pcp) and acts to ventralise the central nervous system and induces the expression of ventral telencephalic marker Nkx2.1. Bone morphogenetic proteins are expressed at the periphery of the neural plate and promote the dorsalisation of the central nervous system (Rubenstein1998). (C) Side- view of the mouse brain at E10.5, after the neural tube closure, highlighting the key sources of morphogens, ventralising signals Fgf8, Shh and dorsalising signal Wnt1. Rhombomeres 1-7 are designated r1- r7 (Rubenstein et al., 1998). (D) The key telencephalic patterning centres are the cortical hem, source of BMPs and Wnts, the commissural plate (CoP) and the floor plate, which produces Sonic hedgehog. Key anatomical structures are annotated including the Cortex (Ctx), lateral ganglionic eminence (LGE), medial ganglionic eminence (MGE), midbrain (me) and the hypothalamus (hTh) (Rubenstein, 2011).

FIGURE 1.01

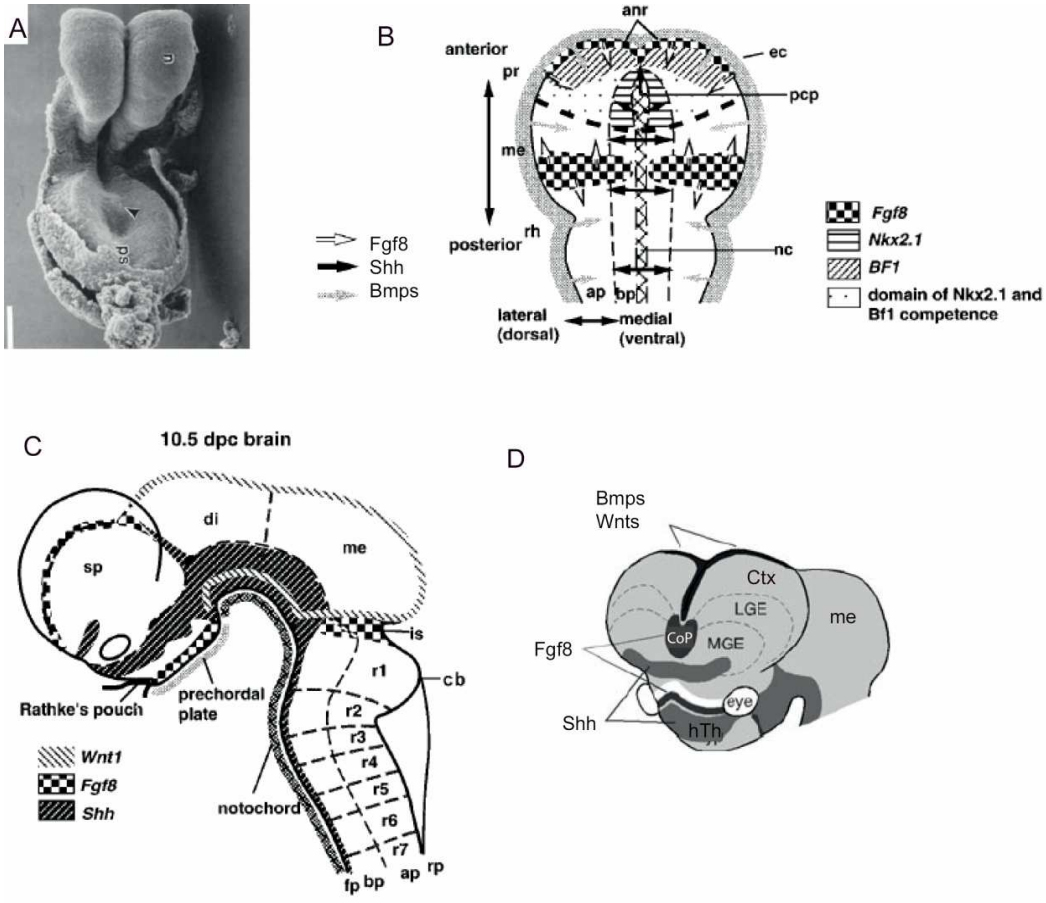
A
B
anr
anterior
pr
ec
pcp
me
posterior
rh
nc
ap
bp
lateral
(dorsal)
medial
(ventral)
Fgf8
Shh
Bmps
Fgf8
Nkx2.1
BF1
domain of Nkx2.1 and
Bf1 competence
C
10.5 dpc brain
di
me
sp
is
cb
r1
r2
r3
r4
r5
r6
r7
Rathke's pouch
prechordal
plate
notochord
fp
bp
ap
rp
Wnt1
Fgf8
Shh
D
Bmps
Wnts
Ctx
LGE
me
CoP
MGE
Fgf8
eye
Shh
hTh

1.2.2 Forebrain specification and its mediolateral patterning

The telencephalon is further specified by the Fibroblast growth factor 8 (Fgf-8), produced at the most anterior border between the neurectoderm and the non-neural ectoderm, which induces the expression of Foxg1 (Shimamura and Rubenstein, 1997). The medio-lateral patterning of the neural plate corresponds, following the anterior neuropore closure, to ventro-dorsal patterning of the telencephalon (Figure 1.01). One of the most powerful signalling molecules involved in this process is Sonic hedgehog (Shh) (Echelard et al., 1993). Notochord expresses Shh and stimulates the overlying neural plate to express Shh as well. The Shh signalling is required for normal patterning of the forebrain. The lateral neural plate (prospective dorsal area) expresses dorsalising factors including Bmps and Wnts (Borello and Pierani, 2010). The Shh signalling plays an important role in the specification of ventral fates in the forebrain. This is achieved through several mechanisms (Figure 1.02). First, Shh is known to induce the expression of Nkx2.1 (Ericson et al., 1995), which is expressed ventrally in the Medial Ganglionic Eminence (MGE). Second, the Shh signalling restricts the dorsalising activity of the Gli3 transcription factor, which is expressed throughout the telencephalon and mediates the dorsalising effects of the Bmp signal (Aoto et al., 2002). This also allows Fgfs, whose expression is inhibited by Gli3, to promote development of the ventral cell types (Kuschel et al., 2003; Theil et al., 1999).

Further regionalisation of the telencephalon involves expression of the transcription factors Pax6, Emx1 in the dorsal telencephalon and Gsh2 in the ventral telencephalon (Hebert and Fishell, 2008) (Figure 1.02). Cross- repression between Pax6 and Gsh2 establishes the boundary between the dorsal telencephalon (pallium) and the ventral telencephalon (subpallium). Pax6 is expressed in a rostro-lateral (high) to caudo-medial (low) gradient while Emx1 is expressed in an opposite gradient (Bishop et al., 2000). Expression of these transcription factors is restricted to the progenitor cells of the cortex, striatum and the globus pallidus and their action is required for normal development of the forebrain. The cortical progenitors will generate the excitatory neurons of the cortex, while all inhibitory neurons of the cortex will be generated in the ventral telencephalon and will migrate tangentially to populate the cortex.

Figure 1.02: Transcription factors and further specification of telencephalic fates. (A) Key transcription factors involved in the specification of different anatomical areas of the forebrain. The cortical hem (CH) will give rise to the Choroid Plexus. The medial pallium (MP) is specified by Lhx2 and will develop into the hippocampus. The dorsal pallium (DP) will give rise to the cortex and the progenitor identity is maintained by Gli3 induced expression of Emx1/2, Pax6 and Neurogenins 1 and 2 (Ngn1/2). The dorsal and ventral Lateral ganglionic eminences (dLGE and vLGE) are specified by transcription factors Gsh1/2, Mash1 (Ascl1) and Dlx1/2, which act in a cross-repressive loop with the transcription factors expressed dorsally (red arrows). The Medial ganglionic eminence is specified by Nkx2.1, Lhx6 and Lhx7 and will give rise to important structures such as for example the Globus pallidus. Other abbr. Lateral pallium (LP), Ventral pallium (VP), pre-optic area (POa) (figure from Schuurmans et al., 2004). (B) Key neuro- and glio- genic areas of the developing telencephalon. Patterning of cortical is regulated by neurogenins, Ngn1/2 and Gli3 and the progenitors will give rise to pyramidal neurons and astrocytes. Ventral progenitors including ones residing in the Lateral ganglionic eminence, Medial ganglionic eminence and the Pre-optic area are patterned by Mash1 (Ascl1) and Dlx1/2 and give rise to neurons producing the inhibitory neurotransmitter γ-aminobutyric acid (GABA) and oligodendrocytes (figure from Rowitch and Kriegstein, 2010).

FIGURE 1.02

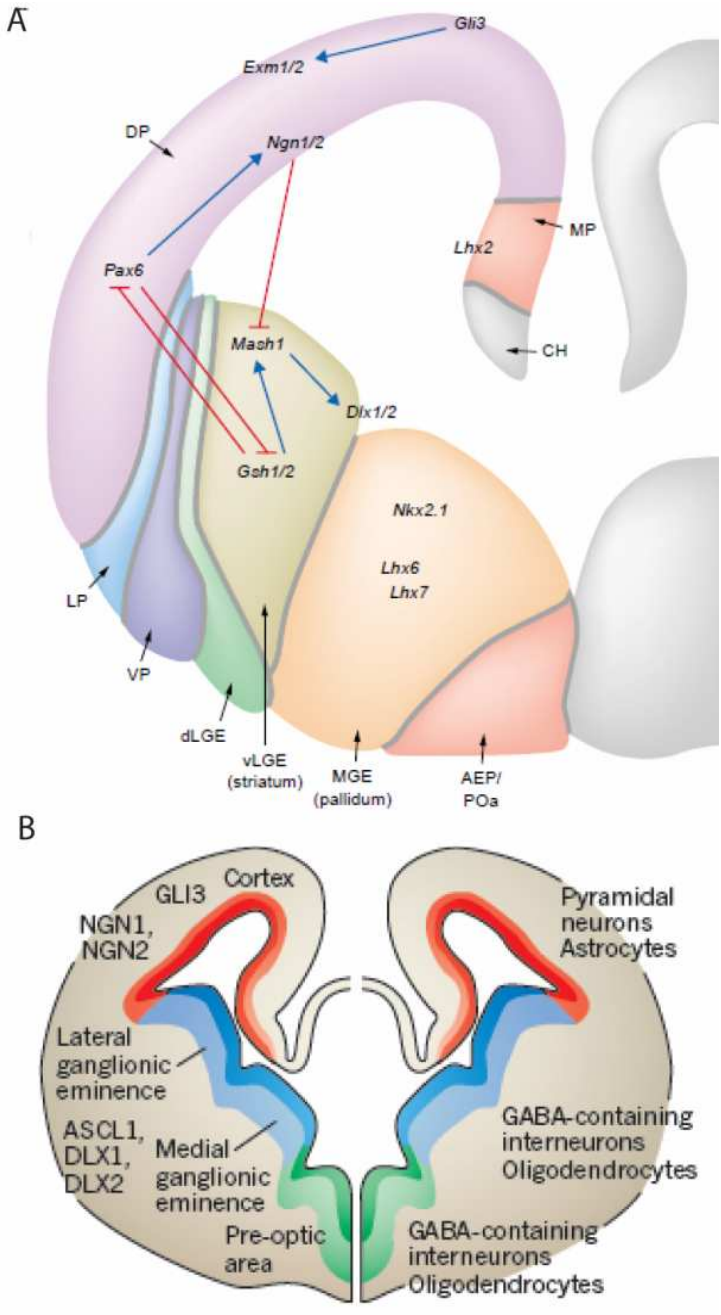
A
Gli3
Exm1/2
DP
Ngn1/2
MP
Lhx2
Pax6
CH
Mash1
Dlx1/2
Gsh1/2
Nkx2.1
Lhx6
Lhx7
LP
VP
dLGE
vLGE
(striatum)
MGE
(pallidum)
AEP/
POa
B
GLI3
Cortex
NGN1,
NGN2
Pyramidal
neurons
Astrocytes
Lateral
ganglionic
eminence
ASCL1,
DLX1,
DLX2
Medial
ganglionic
eminence
GABA-containing
interneurons
Oligodendrocytes
Pre-optic
area
GABA-containing
interneurons
Oligodendrocytes

Most of the mechanisms described above have been elucidated through numerous studies using transgenic animals where the expression of these genes is defective or absent. These could be described in further details, but instead the rest of the introduction will focus on the molecular and cellular aspects of development of the progenitor cells in the cortex.

1.2.3 Neuroepithelial stem cells and the Radial Glia

After the closure of the anterior neuropore at E9.5, the neuroepithelium is thought to consist of the neuroepithelial stem cells dividing only symmetrically and not producing any postmitotic cells (Misson et al., 1988; Voigt, 1989) (Figure 1.03).

During the time when most of the cortical neurons are born, between E10.5-E17.5 in mouse (Caviness, 1982), the neuroepithelium is thought to be composed mainly or only of the radial glial cells which are commonly referred to as the neural stem cells. The transition between the neuroepithelial stem cells and the radial glia involves progressive expression of glial proteins (Campbell, 2003; Pinto and Gotz, 2007). Morphologically, these two cell populations are similar with the radial processes spanning the thickness of the neuroepithelium (Figure 1.03). The RC2 antigen expression is restricted to the pial endfeet in the E9.0 neuroepithelium and becomes expanded by E11.0 (Misson et al., 1988). Similarly, the transition was later described to coincide with changes in the expression of Blbp and GLAST (Feng et al., 1994; Shibata et al., 1997).

Figure 1.03: Development of cortical neuroepithelium. (A) Graphical illustration demonstrating the neurogenesis and gliogenesis. Glia and neurons are born from the primary proliferative population, termed the neuroepithelial (NE) stem cells before E10.0 (green). Between E10.0 and E11.0 the NE stem cells transform into radial glia (RG, green) and begin to produce the first postmitotic neurons (N) (dark red) which contribute to the preplate. Between E11.5 and E17.5, following the split of the preplate into the subplate and the marginal zone, the neurons born from the radial glia contribute to the cortical plate. A subset of cells born from radial glia generate the secondary proliferative population, the intermediate progenitor cells (NP) which only have neurogenic potential. Early born neurons generate the deep layers of the cortex (red, organge) and late born progenitors give rise to the upper layer neurons (yellow). It is believed that the fate of cortical neurons is pre-determined in the neurogenic progenitors. During postnatal development, gliogenic progenitors (blue) together with the radial glia give rise to astrocytes (figure from Okano and Temple, 2009). (B) Schema outlining the molecular mechanisms governing the key aspects of the neuroepithelial stem cell and radial glia development. Factors promoting the transition of neuroepithelial stem cells transition into radial glia include the Notch, Neuregulin1 (Nrg1) signalling through ErbB receptor, the fibroblast growth factor 10 (Fgf10) and retinoic acid (RA). A number of factors have been demonstrated to promote the transformation of radial glia into astrocytes, most importantly the JAK-STAT signalling, the Notch signalling pathway, the and the polycomb group complex- (PcG) mediated epigenetic modification which inactivates Ngn1 (figure from Miyata et al., 2010).

FIGURE 1.03

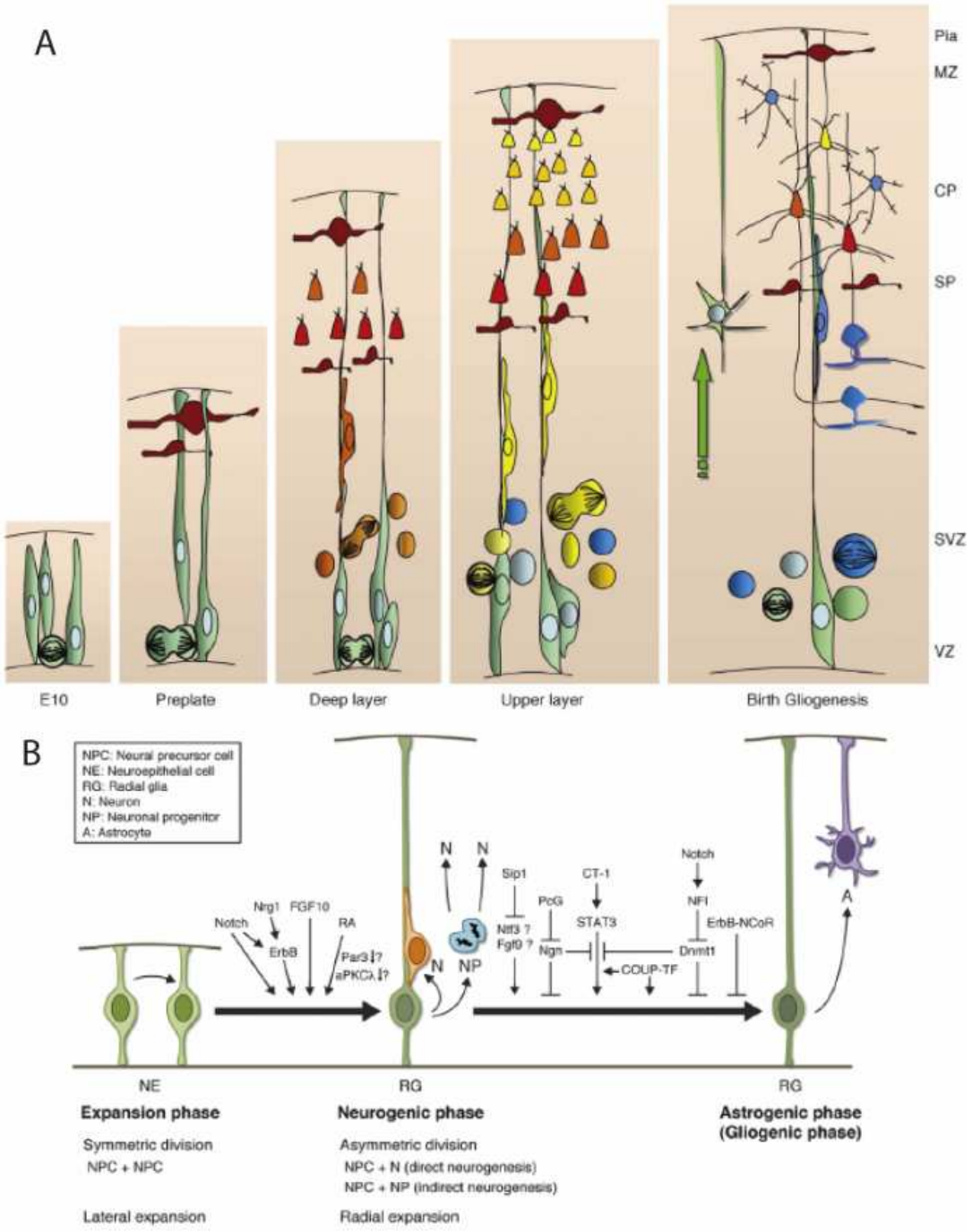
A
Pia
MZ
CP
SP
SVZ
VZ
E10
Preplate
Deep layer
Upper layer
Birth Gliogenesis
B
NPC: Neural precursor cell
NE: Neuroepithelial cell
RG: Radial glia
N: Neuron
NP: Neuronal progenitor
A: Astrocyte
Notch
Nrg1
FGF10
RA
ErbB
Par3⇕?
aPKCλ⇕?
N
NP
Sip1
Ntf3 ?
Fgf9 ?
PcG
Ngn
CT-1
STAT3
COUP-TF
Notch
NFI
Dnmt1
ErbB-NCoR
A
NE
RG
RG
Expansion phase
Neurogenic phase
Astrogenic phase
(Gliogenic phase)
Symmetric division
NPC + NPC
Asymmetric division
NPC + N (direct neurogenesis)
NPC + NP (indirect neurogenesis)
Lateral expansion
Radial expansion

However, molecular pathways which could be regulating this transition are very poorly understood. Injection of a retrovirus expressing activated form of Notch1 (NIC) into the E9.0 mouse embryos demonstrated that the Notch signalling pathway is involved in the early specification of the radial glia with premature expression of Blbp and RC2 (Gaiano et al., 2000). This was supported by the later findings that Blbp is an important target of the Notch signalling pathway with Blbp expression being diminished in Notch1, Notch3 double -knockout mice (Anthony et al., 2004). Activation of the Notch signalling was also demonstrated to be necessary for expression of Neuregulin1 receptor, ErbB2, signalling through which is necessary for the expression of the RC2 epitope and development and maintenance of the radial glia (Anton et al., 1997; Schmid et al., 2003) (Figure 1.03).

More recently, the fibroblast growth factor signalling through FGFR2 has been shown to corroborate with the Notch signalling pathway to establish the radial glia cell population and confer *in vitro* neurosphere forming ability to the progenitors (Yoon et al., 2004). Further analysis revealed that Fgf10 is particularly potent for this transformation to occur at the right time with *Fgf10* knockout mice showing a delayed expression of Blbp (Sahara and O'Leary, 2009) (Figure 1.03). Recently, sonic hedgehog signalling was also implicated in the process through the induction of expression of sry- homology box Sox9, whose precocious overexpression in E9.5 embryos confers neurosphere forming ability to dissociated progenitors prematurely (Scott et al., 2010). Together, these findings suggest that the early neuroepithelial stem cell to radial glia transition is an important event during development of the cortex and requires a coordinated activation of several signalling pathways.

It remains unclear to what extent the specification of the radial glia is necessary to generate postmitotic neurons. Premature specification of the radial glia by constitutive activation of the Notch signalling or by overexpression of Sox9 leads to early generation of postmitotic neurons (Gaiano et al., 2000; Scott et al., 2010). However, experiments aimed at abolishing the neuroepithelial stem cell to radial glia transition did not provide conclusive results. While normal capacity to produce postmitotic neurons was reported for the *Nrg1* knockout radial glia lacking RC2 expression (Schmid et al., 2003), conditional inactivation of Sox9 resulted in a reduced neurosphere forming ability of the progenitor cells and a reduced neuronal differentiation (Scott et al., 2010). Technical differences could, in part, account for

this difference, as the former study used slice cultures with 10% serum containing medium to assess neuronal differentiation, while the latter used a protocol which does not involve the use of serum to study the neurosphere formation, although medium containing 1% serum is used to study their differentiation (Reynolds and Weiss, 1996; Scott et al., 2010). Analysis of the *Fgf10* knockout mice, where the expression of Blbp and specification of the radial glia is delayed, suggested that neuronal differentiation is also delayed, although the assessment was made based on the expression of Tbr1 as opposed to TuJ1 in the other studies (Sahara and O'Leary, 2009).

For this and other reasons, it is important to adopt a unified nomenclature for the early progenitors of the embryonic cortex. For the purpose of this work the earliest progenitors normally present in the neuroepithelium which are not normally neurogenic will be referred to as the neuroepithelial stem cells. The neurogenic progenitors characterised by the strong expression of genes such as Sox9 and RC2 and give rise to the postmitotic neurons will be referred to as the radial glia.

1.2.4 Radial glia and postmitotic cells

Radial glia were initially identified as a population of cells each containing a single radial process spanning the thickness of the developing tissue and guiding the migration of postmitotic neurons to the cortical plate (Rakic, 1971; Rakic, 1972). During mouse development, the radial glia are specified from the neuroepithelial stem cells around the time when the neuroepithelium begins to generate postmitotic neurons (around E11). It was later observed that the radial glia not only guide differentiating neurons, but can also produce neurons directly during asymmetric cell divisions (Malatesta et al., 2000; Noctor et al., 2001).

Cell bodies of the radial glia undergo somal translocations (interkinetic nuclear migration), which are linked to their cell cycle (Fujita, 1963). Mitotic divisions of the radial glia are restricted to the ventricular edge and the positioning of the cell body during cell division is believed to be maintained by a number of proteins

(Lathia et al., 2007; Ohno, 2001). Precise molecular mechanisms regulating the fate decision of postmitotic cells remain unclear.

It is believed that symmetricity of the mitotic division of the radial glia is dependent on the inheritance of cell fate factors and it was proposed that the orientation of the mitotic spindle might be the determinant of their inheritance. Studies of central nervous system development in *Drosophila melanogaster* initially identified prospero to be such a factor with the par3/par6/aPKC protein complex involved in maintaining appropriate positioning of the spindle during cell division (Betschinger et al., 2003; Doe et al., 1991; Ohno, 2001). Following the exciting discovery that in the developing nervous system of *Drosophila melanogaster* the distribution of postmitotic cell fate factors is indeed linked to the positioning of the spindle during division (Kuchinke et al., 1998; Schober et al., 1999; Wodarz et al., 1999) it was proposed that perhaps these factors, all of which are high conserved, may also control cell fate decisions during the divisions of the radial glia in mammals (Wodarz and Huttner, 2003). However, the predicted rate of asymmetric cell divisions based on the anatomical observations that only a small fraction of cell divisions in mammals are horizontal to the ventricular edge (Smart, 1973) would be too small to explain the numbers of neurons generated in the mouse brain and it was later demonstrated that vertical cell divisions which would be expected to be symmetric based on the findings from *Drosophila melanogaster* can give rise to asymmetric divisions in mammals (Kosodo et al., 2004).

Studies investigating the role of the Notch signalling pathway have provided substantial evidence for the role of this pathway in the neuronal differentiation of the radial glia. Notch is a membrane bound-bound receptor for Delta and Jagged ligands and is involved in intercellular signalling (Kopan and Ilagan, 2009). Upon activation, the intracellular domain of Notch (NICD) is cleaved by Presenilin of the γ-secretase complex and, together with the recombining binding protein suppressor of hairless (RBP-J), activates the transcription of target genes, most importantly the hairy enhancer of split (*hes*) genes (Pierfelice et al., 2011). It was observed that the proneural genes Ngn2 and Mash1 are expressed in the neuroepithelium before the first postmiotic neurons are born (Bettenhausen et al., 1995; Hatakeyama et al., 2004). It was later shown that the Notch signalling effectors, particularly Hes1, are expressed in an oscillatory fashion due to the negative autoregulation of its own

promoter (Shimojo et al., 2008). The inhibition of Ngn2 expression by Hes1 induces an out of phase oscillation of Ngn2 protein in the radial glia (Figure 1.04). The proneural genes, such as Ngn2, are known to induce the expression of Delta1, a Notch ligand, and this stimulates the Notch signalling pathway in the neighbouring cells. As a result, there is a harmonic oscillation with some of the radial glia expressing proneural genes and some lacking their expression. This explains the salt and pepper pattern of expression of proneural genes in the ventricular zone of the developing telencephalon. Additional signals have been proposed to modulate the oscillatory behaviour of Hes1 including the just another kinase (JAK) – signal transducer and activator of transcription (STAT) signalling with the Jak inhibitor, AG490 shown to stabilize Hes1 expression (Shimojo et al., 2008). As a result of this, the neighbouring cells would then fail to receive the Notch signal and would be allowed to differentiate because of a sustained expression of proneural genes and stimulation of the Notch signalling in the precursor cell, preventing its differentiation (Pierfelice et al., 2011).

Apart from the Notch signalling pathway, there is a growing interest in the role of epigenetic silencing in neuronal differentiation. In particular, the repressor element-1 silencing transcription factor/ neuron restrictive silencing factor (REST/NRSF) has emerged as a powerful modulator of neuronal development, identity and function. REST and its cofactor CoREST recognise and bind the repressor element-1/ neuron restrictive silencer elements (RE1/NRSE) in the genome and recruit a number of enzymes involved in chromatin modifications such as histone deacetylases, the Swi/Snf complex or the MeCP2. Initially this mechanism was thought to be necessary primarily for the developing nervous system (Johnson et al., 2007; Otto et al., 2007), but later a number of functions outside the nervous system have been reported (Qureshi and Mehler, 2009).

However, it remains unclear how these findings will be reconciled with the studies demonstrating that at least some of the progenitors might show some degree of lineage restriction. Clonal analysis studies utilising a modified version of the Babe BOLAP retroviral vector (Cepko et al., 1998) to contain the cytomegalovirus (CMV) enhancer with chicken β-actin promoter (CAG) which is resistant to silencing in the E9.0 neuroepithelium (Gaiano et al., 1999) have provided some evidence that the neuroepithelium might show some lineage heterogeneity even before the radial glia

are specified with some of the clones consisting only of astrocytes at the end of corticogenesis (McCarthy et al., 2001). Nonetheless, mechanisms of fate selection could, in theory, be independent from the molecular control of proliferation and differentiation.

Figure 1.04: Role of the Notch signalling pathway in the maintenance of the radial glia. (A) Notch is a membrane receptor and the signalling through the Notch receptor induces the expression of hairy enhancer of split1 (Hes1), which negatively autoregulates its own promoter and this generates an oscillation of the Hes1 protein level. Hes1 inhibits the expression of Neuregulin2 (Ngn2), which is necessary to promote the expression of Notch ligand Delta-like1 (Dll1). (B) As a result of this pathway, populations of radial glial cells are heterogeneous in terms of their Notch activity with one radial glial cell "neural progenitor1" expressing Ngn2 and Dll1 and its neighbour "neural progenitor 2" expressing Hes1 (Shimojo et al., 2008). (C) To maintain sufficient levels of Notch signalling in the radial glia (BP), whose cell bodies are restricted to the ventricular zone (VZ), intermediate progenitors (INP) located in the subventricular zone (SVZ) and the postmitotic neurons provides the simulation. E3 ubiquitin ligase Mind bomb1 (Mib1) is necessary for the endocytosis of all known ligands of Notch including Delta like -1, 3 and 4 and Jagged 1 and 2, yet the knockout studies have shown that its presence is required for functional signalling (Koo et al., 2005). Image from (Pierfelice et al., 2011).

FIGURE 1.04

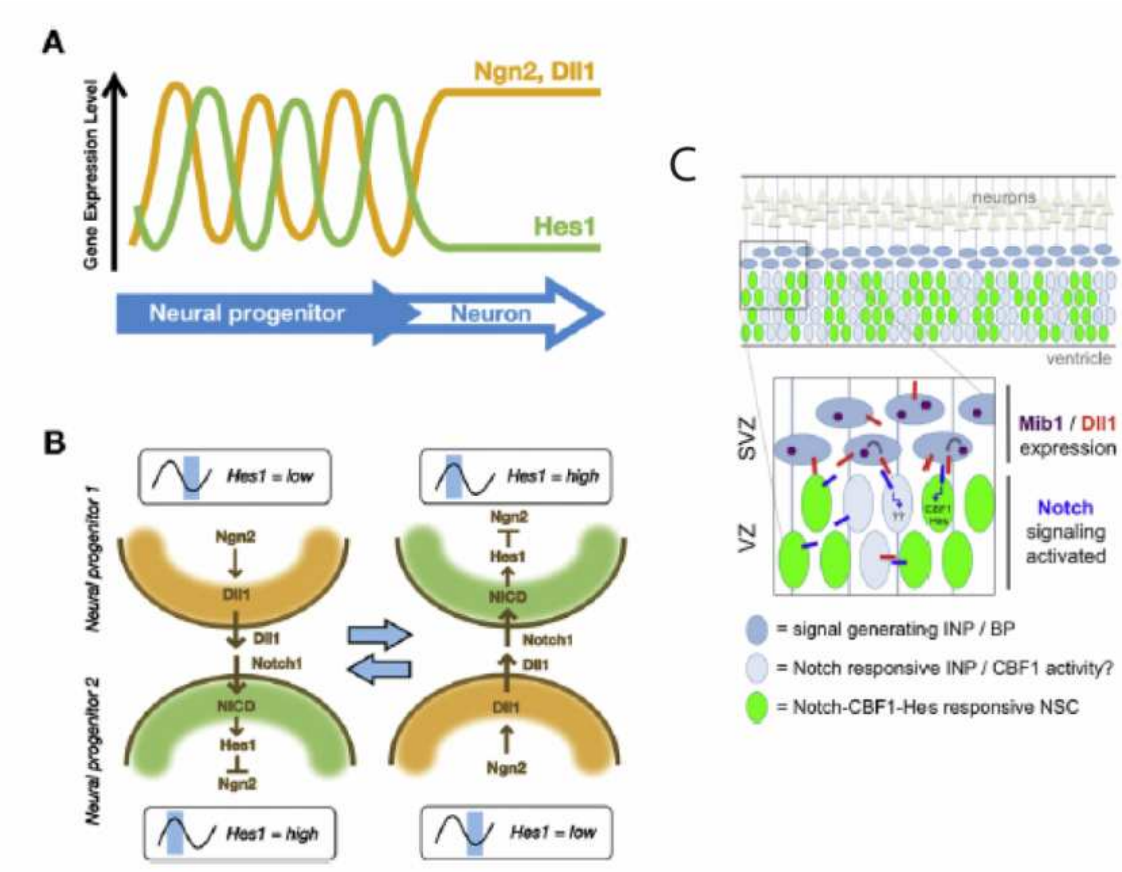
A
Gene Expression Level
Ngn2, Dll1
Hes1
Neural progenitor
Neuron
B
Neural progenitor 1
Neural progenitor 2
Hes1 = low
Hes1 = high
Ngn2
Dll1
Notch1
NICD
Hes1
Ngn2
Hes1 = high
Hes1 = low
C
neurons
ventricle
SVZ
VZ
Mib1 / Dll1
expression
Notch
signaling
activated
= signal generating INP / BP
= Notch responsive INP / CBF1 activity?
= Notch-CBF1-Hes responsive NSC

1.2.5 Differentiation of postmitotic cells

Initial identification of the radial glia by Rakic and co-workers suggested that the main role of the radial fibres is to guide the radial migration of the postmitotic neurons (Rakic, 1971; Rakic, 1972). The observation that, in addition, the radial glia produce neurons modified this hypothesis, but raised an important question which remains unanswered: what happens to the radial process during the asymmetric division of the radial glia. Studies from the Kriegstein laboratory using retrovirally infected radial glia expressing GFP reported that most postmitotic cells which inherit the radial (basal) process remain radial glial progenitors and the other cells differentiate (Noctor et al., 2001). However, findings using lipophilic dye DiI labelling of the radial glia showed that the inheritance of the radial process by cells which later express neuronal markers such as Hu, TuJ1, NeuN happens in approximately half of the cases (Miyata et al., 2001). This would be in line with the hypothesis put forward in 1970 by Morest (Morest, 1970) that neurons can be derived from cells containing the basal process by undergoing a somal translocation. Studies using the non-integrating adenoviral GFP expression vector would seem to support this hypothesis (Tamamaki et al., 2001). It is therefore a subject of further research to determine the exact cellular mechanisms taking place during neuronal differentiation of the radial glia. It is also unclear how a new radial process is established following a symmetric division of the radial glia.

It was later observed that neurons can also be generated via another pathway. A subset of postmitotic cells was found to divide once, twice or thrice more in the subventricular zone to amplify the neuronal output of the radial glia (Haubensak et al., 2004; Miyata et al., 2004; Noctor et al., 2004) (Figure 1.05). The subventricular zone is a histologically distinct region of the developing cortex previously observed to contain a number of abventricular cell divisions (Smart, 1976). At the molecular level it can be identified based on the expression of several markers including Tbr2 (Englund et al., 2005), svet1 (Tarabykin et al., 2001), Cux1 and Cux2 (Nieto et al., 2004; Zimmer et al., 2004), Satb2 (Britanova et al., 2005). Further analysis of expression of transcription factors which are involved in radial glia maintenance, such as Pax6, the intermediate progenitor marker Tbr2, proneural NeuroD1 and Tbr1, which is expressed in the postmitotic projection neurons, prompted postulation

of the hypothesis that the development of pyramidal projection neurons is regulated by sequential expression of these transcription factors (Hevner et al., 2006). It is unclear whether neurons born directly from the radial glia require the expression of Tbr2 at some stage. Data showing that Tbr2 is under direct transcriptional regulation by Ngn2 and the proposed role of Tbr2 in direct activation of NeuroD transcription would support such a hypothesis (Hevner et al., 2006; Lee et al., 2000; Ochiai et al., 2009). However, neurogenesis in the embryonic neocortex is not completely abolished in the conditional Tbr2 knockout mice (Arnold et al., 2008; Sessa et al., 2008). Therefore the molecular mechanisms regulating direct and indirect neurogenesis remain to be investigated.

Figure 1.05: Two modes of neurogenesis in cerebral cortex. Radial glia of the developing cortex express Pax6 and their cell bodies undergo interkinetic nuclear migration in the ventricular zone (VZ) in harmony with the phases of cell cycle with mitotic divisions taking place at the edge of the ventricle. Postmitotic cells can differentiate into neurons directly (left panel) and migrate through the subventricular zone (SVZ), the intermediate zone (IZ) and into the cortical plate (CP) or adopt an intermediate progenitor cell (IPC) fate, divide at the SVZ to amplify the neuronal output and then differentiate into neurons. The sequential expression of transcription factors Pax6, Tbr2, NeuroD and Tbr1 suggests that these transcription factors are necessary to drive the postmitotic cells through these stages. It is unclear if Tbr2 is involved in direct neurogenesis. Image from (Hevner, 2006).

FIGURE 1.05

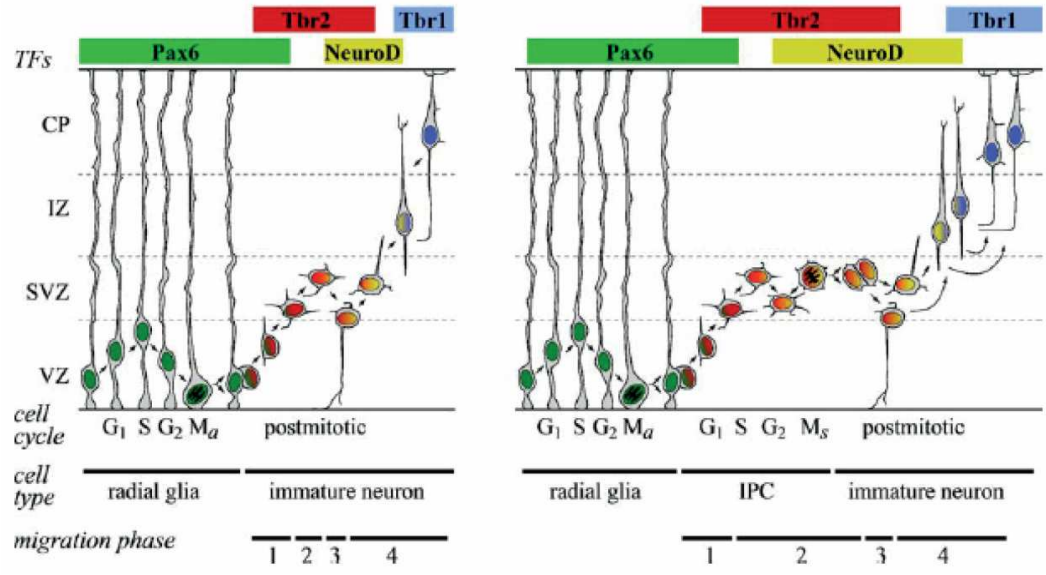
Tbr2
Tbr1
TFs
Pax6
NeuroD
CP
IZ
SVZ
VZ
cell cycle
G1 S G2 Ma
postmitotic
cell type
radial glia
immature neuron
migration phase
1 2 3 4
Tbr2
Tbr1
Pax6
NeuroD
G1 S G2 Ma
G1 S G2 Ms
postmitotic
radial glia
IPC
immature neuron
1 2 3 4

1.2.6 Cortical layer formation 1 – the preplate

The earliest born neurons of the cerebral cortex migrate to the pia and generate the preplate around E11.5, which later splits into the marginal zone and the subplate. The early neuronal population of the cortex includes mostly the transient population of Cajal-Retzius neurons, which are primarily born in the cortical hem and around the pallio-subpallial boundary (Bielle et al., 2005). At E11.5, the Cajal Retzius neurons can be identified by the expression of two markers, Reelin and Calretinin (Hevner et al., 2003). While most Cajal-Retzius cells are found to express both markers, some only express one at E11.5. At later stages the expression of Reelin and Calretinin in the developing cortex appears to overlap (Hevner et al., 2003). At late stages of corticogenesis, particularly after the first week of postnatal development in mouse, the Cajal Retzius cells disappear, which is mainly attributed to programmed cell death (Price et al., 1997; Wood et al., 1992). Substantial evidence has been provided to demonstrate the role of the Cajal Retzius cells in the laminar organisation of the cortex. The cortical lamination in mice lacking the fully functional Reelin protein, the “reeler” mice, is disrupted with the laminae found in an inverted order (Caviness, 1982; Rice and Curran, 2001; Rice et al., 2001; Tissir and Goffinet, 2003). It appears that while Reelin is important to promote migration of postmitotic neurons towards the pial surface at early stages of development, it is also required to prevent neurons from entering layer I of the cortex by inhibiting their migration (Dulabon et al., 2000; Trommsdorff et al., 1999). A molecular mechanism for the latter has recently been described, showing that Reelin inhibits the degradation of the activated Notch intracellular domain (NICD) (Hashimoto-Torii et al., 2008).

1.2.7 Cortical layer formation 2 – the cortical plate

Most cortical neurons are born as a result of 11 divisions of the progenitor cells between E11.5 and E17.5 (Caviness, 1982; Takahashi et al., 1996). The postmitotic neurons contributing to the cortical plate migrate through the intermediate zone and the subplate and enter the cortical plate. Neurons born earlier in development

contribute to deeper layers of the cortex than neurons born later (Angevine and Sidman, 1961; McConnell, 1995) (Figure 1.06). This inside-out pattern of corticogenesis has been extensively studied and the exact mechanisms controlling the development of this pattern are still unknown. Pioneering work involving the transplantation of the early cortical progenitors into an older brain and older progenitors into a younger brain revealed that the early progenitors are more multipotent and can generate neurons contributing to deep as well as superficial layers, while the later progenitors can only generate neurons contributing to the superficial layers (Desai and McConnell, 2000; Frantz and McConnell, 1996; McConnell and Kaznowski, 1991). It remains unclear what environmental factors could direct younger progenitors to generate more superficial neurons in the older neuroepithelium, or what cell-autonomous mechanisms could be progressively restricting the competence of the progenitors to generate neurons of diverse fates in the developing cortex. Recent studies using multipotent stem cells to generate cortical neurons found that differentiating mouse and human embryonic stem cells generate neurons of different subtypes in a temporal sequence which is similar to that of the cortical radial glia *in vivo* (Gaspard et al., 2008; Eiraku et al., 2008; Shi et al. 2012), suggesting that mechanisms regulating the diversity of cortical neurons could be intrinsic to the progenitor cells.

A number of transcription factors involved in the specification of various neuronal populations have recently been identified (Leone et al., 2008; Molyneaux et al., 2007) (Figure 1.06). These include Tbr1, Satb2 and Ctip2. Tbr1 is highly expressed in layer VI and, to a lesser extent, layer II/III. Mice lacking Tbr1 show multiple defects of the layer VI pyramidal neuron specification and axonal pathfinding (Hevner et al., 2001). Loss of Ctip2, which is expressed at high level in layer V of the adult mouse cortex, results in defects of development of corticospinal neurons (Arlotta et al., 2005). Satb2 was shown to be expressed in the developing and adult cortex (Britanova et al., 2005) and mice lacking its expression show defects in the development of upper layer neurons (Britanova et al., 2008). Recently published transcriptome analysis of cortical layers will undoubtedly provide further candidates for neuronal subtype specific genes and factors involved in cortical lamination (Belgard et al., 2011).

Figure 1.06: The cortical progenitors to cortical lamination. (A) Schema representing the radial expansion hypothesis predicts that the cortical surface area is dependent on the number of radial glia (NE/RG) in the tissue, all of which establish the radial unit as examined by Pasko Rakic and co-workers. Their proliferation is regulated by factors such as Pax6, Emx2, Id4 or Tlx as well as extrinsic signals including Wnt, Fgf and Shh. The laminar thickness of the cortex is determined by the amplification of neuronal output of the radial glia by intermediate progenitors in the subventricular zone (SVZ) (Pontious et al., 2008). (B) Initial examination of cortical layer markers in the embryonic cortex showed that the intermediate progenitor markers Svet1, Cux1, Cux2 are later expressed in the upper layer neurons of the cortex (Leone et al., 2008). (C) Recent studies have greatly expanded the knowledge about genes whose expression is enriched in certain cortical layers. The full potential of this analysis for the future understanding of cortical development remains to be explored (Molyneaux et al., 2007).

FIGURE 1.06

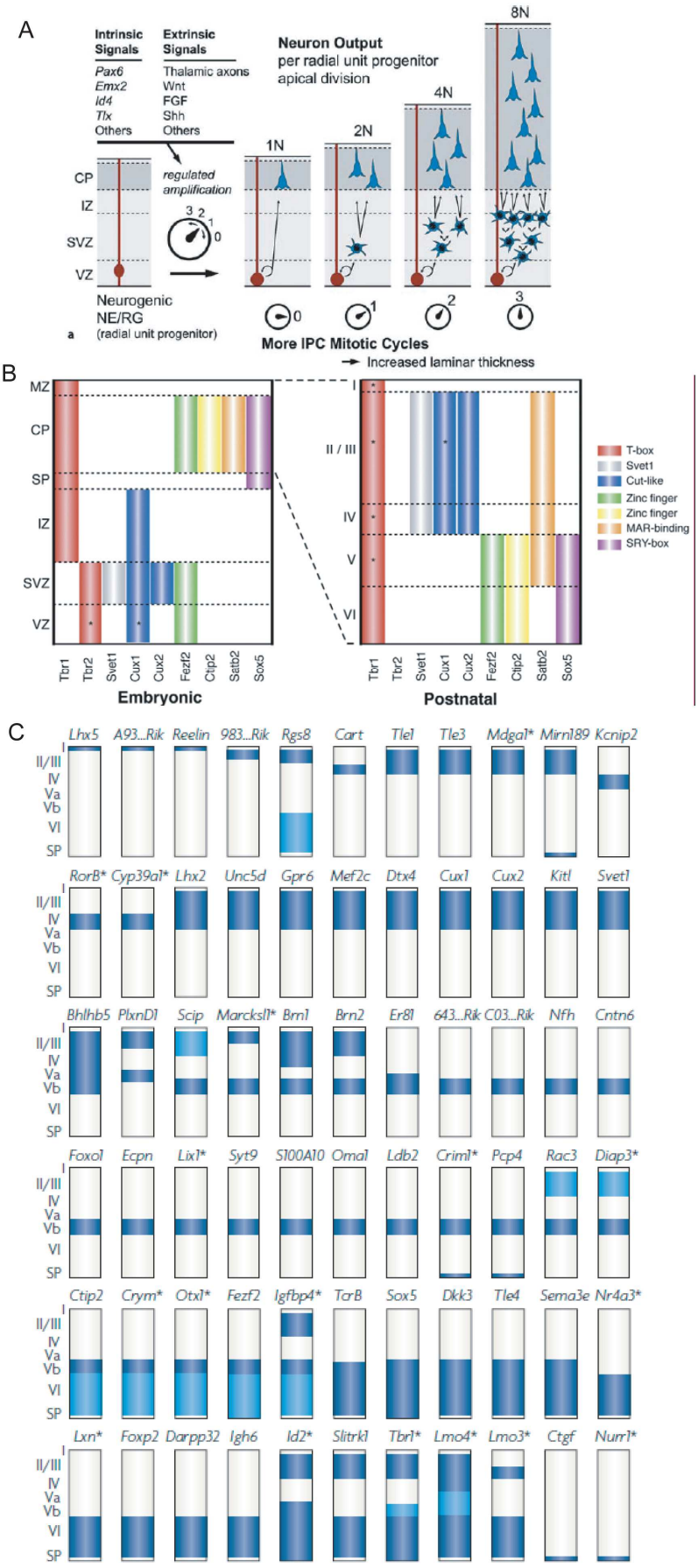
A
Intrinsic Signals
Extrinsic Signals
Pax6
Emx2
Id4
Tlx
Others
Thalamic axons
Wnt
FGF
Shh
Others
Neuron Output
per radial unit progenitor
apical division
1N
2N
4N
8N
regulated amplification
CP
IZ
SVZ
VZ
Neurogenic NE/RG
(radial unit progenitor)
a
More IPC Mitotic Cycles
Increased laminar thickness
B
MZ
CP
SP
IZ
SVZ
VZ
I
II / III
IV
V
VI
T-box
Svet1
Cut-like
Zinc finger
Zinc finger
MAR-binding
SRY-box
Tbr1
Tbr2
Svet1
Cux1
Cux2
Fezf2
Ctip2
Satb2
Sox5
Embryonic
Postnatal
C
Lhx5 A93...Rik Reelin 983...Rik Rgs8 Cart Tle1 Tle3 Mdga1* Mirn189 Kcnip2
RorB* Cyp39a1* Lhx2 Unc5d Gpr6 Mef2c Dtx4 Cux1 Cux2 Kitl Svet1
Bhlhb5 PlxnD1 Scip Marcksl1* Brn1 Brn2 Er81 643...Rik C03...Rik Nfh Cntn6
Foxo1 Ecpn Lix1* Syt9 S100A10 Oma1 Ldb2 Crim1* Pcp4 Rac3 Diap3*
Ctip2 Crym* Otx1* Fezf2 Igfbp4* TorB Sox5 Dkk3 Tle4 Sema3e Nr4a3*
Lxn* Foxp2 Darpp32 Igh6 Id2* Slitrk1 Tbr1* Lmo4* Lmo3* Ctgf Nurr1*
I
II/III
IV
Va
Vb
VI
SP

1.2.8 The role of intermediate progenitors in cortical lamination

The analysis of expression of cortical layer markers revealed an interesting pattern that genes such as the transcription factors Cux1 and Cux2, Satb2 and a non-coding RNA Svet1 (Britanova et al., 2005; Nieto et al., 2004; Tarabykin et al., 2001) (Figure 1.06) are expressed in the upper layers of the cortex are also expressed in the SVZ during development (Leone et al., 2008) and it was proposed that the intermediate progenitor cells could perhaps be responsible for the production of the superficial layer neurons. This is sometimes referred to as the "upper layer hypothesis". This hypothesis was further supported by the observation that in mice lacking Cux2, which is a negative regulator of intermediate progenitor proliferation, upper but not deep layers are expanded (Cubelos et al., 2008). Cross-species comparison of cortical anatomy would seem to support this hypothesis since a distinct subventricular zone is present only in mammals and its size relative to the ventricular zone is expanded in higher mammals and so is the relative thickness of upper to deep layers (Cheung et al., 2007; Molnar et al., 2006; Smart et al., 2002). Furthermore, sustained overexpression of Tbr2 was recently shown to promote the conversion of radial glia to intermediate progenitors and subsequent generation of upper- rather than deep- layer neurons (Sessa et al., 2008).

In vivo imaging experiments provided evidence that the subventricular progenitors also give rise to deep layer projection neurons (Haubensak et al., 2004). This observation, along with the fact that in the absence of Tbr2 the reduction of cortical thickness is profound both in the deep and upper layers of the cortex (Arnold et al., 2008; Sessa et al., 2008) provided ground to question the validity of the upper layer hypothesis.

A new hypothesis has been proposed that the neuronal composition and thickness of the cortical layers are controlled by two separate mechanisms, whereby the area of the cortical sheet depends on the number of radial glia, which establish the radial units of the cortex, while the cortical thickness is regulated by the intermediate progenitors, whose proliferation is key to the amplification of the neuronal numbers (Lui et al., 2011; Pontious et al., 2008). This could be supported by the observation that mice expressing a stabilized version of β-catenin or lacking caspase-9 show

abnormally increased cortical surface area leading to gyration of the mouse cerebral cortex (Chenn and Walsh, 2002; Kuida et al., 1998). This model would suggest that mechanisms regulating cortical area and thickness are independent from each other. However, it was recently shown that the stimulation of the Notch signalling in the radial glia by intermediate progenitors are instrumental to maintain the radial glia population (Figure 1.04) (Pierfelice et al., 2011; Yoon et al., 2008), suggesting that the various cortical progenitor populations can cross-regulate each other in the proliferative niche.

1.2.9 Amplification of neuronal output – radial glia to intermediate progenitors

Several molecules have been shown to be crucially involved in regulating the ratio of radial glia to intermediate progenitors. These mainly include positive regulators of intermediate progenitor identity. Mice lacking functional Pax6, Tbr2, Lrp6, Ngn2, Tlx, and Id4 show reduced numbers of intermediate progenitors relatively to radial glia progenitors leading, at least in some cases, to reduced cortical thickness (Quinn et al., 2007; Roy et al., 2004; Schuurmans and Guillemot, 2002; Sessa et al., 2008; Yun et al., 2004; Zhou et al., 2006). These changes can be linked to changes in cell cycle progression, as Tlx represses the transcription of cyclin- dependent kinase p21 and the tumour suppressor Pten whose overexpression in Tlx null mice leads to reduced cell cycle progression. Another important mechanism is the transcriptional regulation by Tbr2 of a currently unknown set of genes with loss and gain-of-function experiments showing opposing effects on the abundance of intermediate progenitors (Arnold et al., 2008; Sessa et al., 2008). Mechanisms of intermediate progenitor cell specification by Pax6 remain unclear (Quinn et al., 2007).

It is important to note that the loss of all of the above factors, except for Tbr2, leads to developmental abnormalities of both the primary and secondary proliferative populations in the cortex. Only the loss of Tbr2 seems to specifically decrease the abundance of intermediate progenitors but not the radial glia (Arnold et al., 2008; Sessa et al., 2008). It remains unclear why the radial glia are not affected given the recent discovery of the role intermediate progenitors play in driving the Hes1 oscillation in the radial glia (Yoon et al., 2008). It is possible that the presence of a

reduced number of intermediate progenitors provides sufficient stimulus to drive Hes1 oscillation and because the conditional loss of Tbr2 in the cortex does not deplete intermediate progenitors completely, it is possible that radial glia may be unaffected (Arnold et al., 2008; Sessa et al., 2008).

1.2.10 Gliogenesis

At the end of neurogenesis, the radial glia give rise to the astrocyte population. The molecular mechanisms remain largely unknown, but there is evidence that the astrogliogenesis may be controlled to a large extent by the same signalling pathways as those which promote radial glia specification (Figure 1.03). This is reflected in the expression of many radial glia markers including GFAP, Sox9 or S100β by immature and mature astrocytes. Overexpression of Notch has been shown to promote astrogenesis in the adult brain (Gaiano et al., 2000). Additionally, activation of the JAK-STAT signalling pathway promotes astrocyte differentiation with the STAT1/STAT3 transcription factors shown to directly bind the *Gfap* promoter and promote its transcription (Kamakura et al., 2004). In addition, the effectors of the Bmp- signalling pathway, the Smad1/Smad4 transcription factors, have been shown to bind to nearby sites and it is believed that they corroborate the activation of *Gfap* transcription (Nakashima et al., 1999). Experimental evidence using lipophilic dye DiI has provided evidence that the radial glia detach from the ventricular edge and transform directly into astrocytes (Voigt, 1989). Supportive of the view that astrocytes share the radial glial lineage is the fact that mature astrocytes can be dedifferentiated *in vitro* and *in vivo* particularly following the reintroduction of ErbB2 and express radial glia markers Nestin, Vimentin, Blbp and regain their neurosphere forming ability (Ghashghaei et al., 2007; Hunter and Hatten, 1995).

Recent studies have identified novel mechanisms regulating neuronal differentiation. These include epigenetic modification. For example, the Polycomb group protein complex was shown to be important for silencing the *Ngn1* locus. Inactivation of the complex results in the loss of silent chromatin marks, particularly the trimethylation of lysine 27 on histone 3, in the *Ngn1* locus. This prolongs cortical neurogenesis and

delays the terminal transdifferentation of the radial glia into astrocytes but does not prevent it (Hirabayashi et al., 2009).

Furthermore, the orphan nuclear receptor chicken ovalbumin upstream promoter transcription factors I and II (Coup-tf I/II) were recently demonstrated to promote the neuro- to glio- genic switch of the radial glia with double- knockout mice showing increased numbers of mature neurons in the cortex at the end of corticogenesis (Naka et al., 2008).

In the adult brain, astrocyte marker- expressing radial glia- like cells can be found in two regions of the brain that retain neurogenic capacity, the subventricular zone (largely studied by Alvarez-Buylla and co-workers) and the dentate gyrus (studied by Fred Gage and co-workers, see review (Ihrie and Alvarez-Buylla, 2011; Ming and Song, 2011)) (Figure 1.07). These populations are largely quiescent but upon depletion of amplifying cells they can be reactivated and re-populate the amplifying cells (Doetsch et al., 1999). The neurons born from the adult neurogenic progenitors contribute either the olfactory bulb or the granule cell layer of the dentate gyrus and recent experiments disrupting the Notch signalling provided evidence that the adult neurogenesis may have a functional role and can affect physiological function (Sakamoto et al., 2011).

Figure 1.07: Postnatal neurogenesis. Diagrams illustrate the neurogenic programmes in two neural stem cell niches in the adult brain, the subventricular zone (A) and the dentate gyrus (B) in the hippocampus. Substantial evidence has been provided demonstrating that the adult neural stem cells express a number of markers of cortical radial glia including Nestin, Vimentin, Sox2, Blbp or GFAP. (A) Neurons born at the adult SVZ (derived from ventral telencephalic progenitors) migrate through the rostral migratory stream (RMS) and differentiate into interneurons of the olfactory bulb (OB). The neurogenic programme retains evidence of its ventral telencephalic origin including the expression of the ventral telencephalic proneural transcription factor Mash1. Recent evidence suggests this process is important for olfaction (Sakamoto et al., 2011). (B) The neurons generated in the dentate gyrus contribute to the granule gell layer and the mature neurons project axons (mossy fibres) to the CA3 region of the hippocampus. Neurogenesis in the dentate gyrus involves the expression of Tbr2, which may be reminiscent of the hippocampal genesis from the medial pallium of the dorsal telencephalon. This process is thought to be involved in memory formation and storage (both images(Ming and Song, 2011)).

FIGURE 1.07

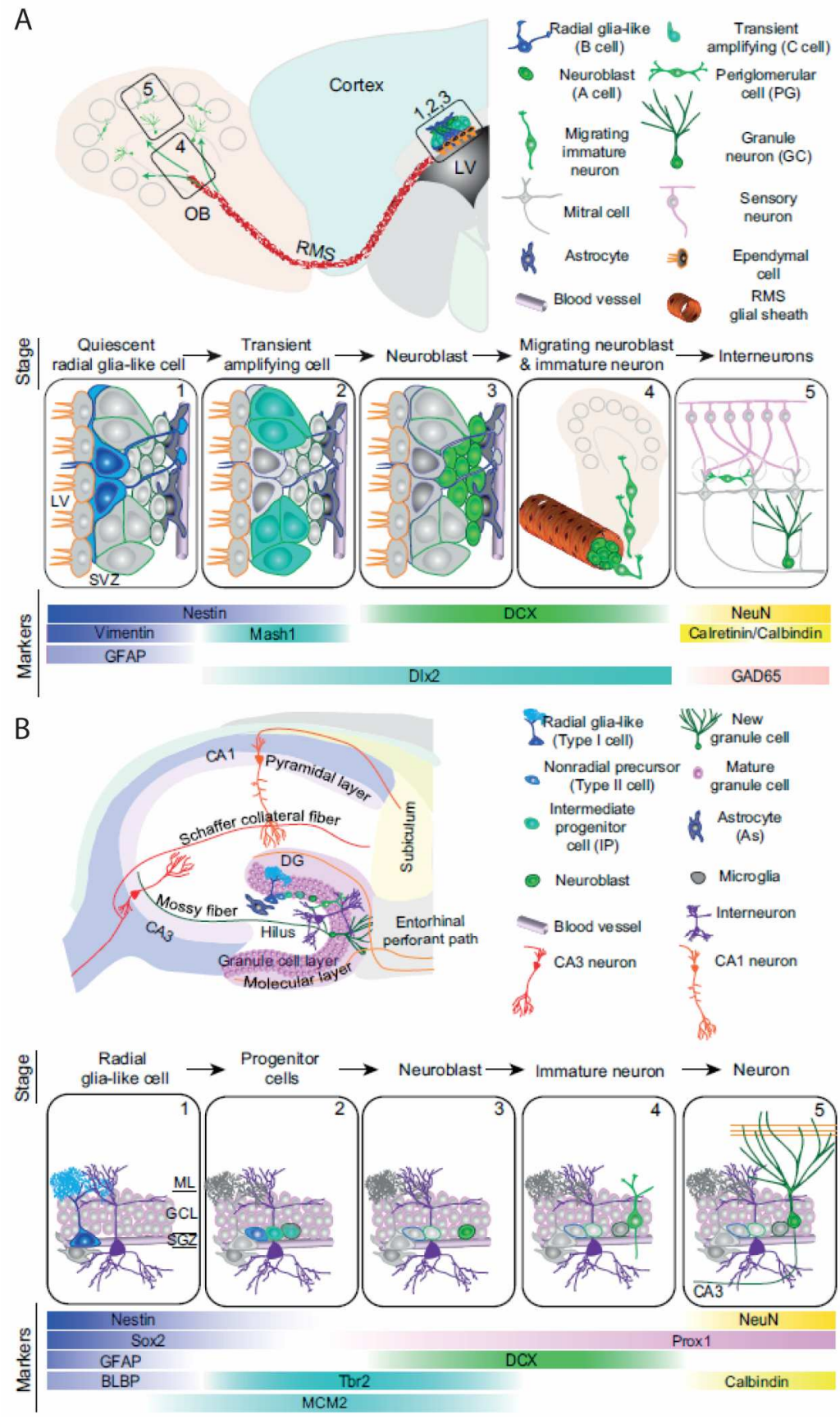
A
Cortex
1,2,3
LV
5
4
OB
RMS
Radial glia-like (B cell)
Transient amplifying (C cell)
Neuroblast (A cell)
Periglomerular cell (PG)
Migrating immature neuron
Granule neuron (GC)
Mitral cell
Sensory neuron
Astrocyte
Ependymal cell
Blood vessel
RMS glial sheath
Stage
Quiescent radial glia-like cell
Transient amplifying cell
Neuroblast
Migrating neuroblast & immature neuron
Interneurons
1
2
3
4
5
LV
SVZ
Markers
Nestin
Vimentin
GFAP
Mash1
DCX
Dlx2
NeuN
Calretinin/Calbindin
GAD65
B
CA1
Pyramidal layer
Schaffer collateral fiber
Subiculum
DG
Mossy fiber
CA3
Hilus
Granule cell layer
Molecular layer
Entorhinal perforant path
Radial glia-like (Type I cell)
New granule cell
Nonradial precursor (Type II cell)
Mature granule cell
Intermediate progenitor cell (IP)
Astrocyte (As)
Neuroblast
Microglia
Blood vessel
Interneuron
CA3 neuron
CA1 neuron
Stage
Radial glia-like cell
Progenitor cells
Neuroblast
Immature neuron
Neuron
1
2
3
4
5
ML
GCL
SGZ
CA3
Markers
Nestin
Sox2
GFAP
BLBP
Tbr2
MCM2
DCX
NeuN
Prox1
Calbindin

1.3 The microRNA pathway and the developing brain

1.3.1 Brief history of RNA interference

RNA interference was discovered in plants following failed attempts to overexpress Chalcone Synthase in pigmented petunias by introducing a chimeric transgene (Napoli et al., 1990). However, the generalised mechanism of RNA interference were not postulated until late 90's when Andrew Fire working with Craig Mello reported that double stranded RNAs can induce silencing of endogenous mRNA transcripts in *Caenorhabditis elegans* (Fire et al., 1998). The first endogenous non protein -coding RNA was discovered by Victor Ambros and co-workers to regulate developmental timing of transitions between larval stages of *Caenorhabditis elegans* (Ambros and Horvitz, 1987; Lee et al., 1993). This was followed by the observation by the Baulcombe lab that RNAs as small as 25 nucleotides can drive RNA interference (Hamilton et al., 1999). The endoribonuclease Dicer responsible for the synthesis of the small RNA molecules was discovered in the Hannon lab (Bernstein et al., 2001; Nicholson and Nicholson, 2002). Mouse lacking functional Dicer and the ability to synthesize small RNAs for silencing demonstrated the incredible importance of this pathway in mouse (Bernstein et al., 2003).

To date, several classes of small RNAs have been described (see review by Farazi et al., 2008) and some of these classes are only present in certain organisms, such as the trans-acting small interfering RNAs (tasiRNA) which are found only in plants. Best studied in mammalian systems are the 20-23 nucleotide microRNAs which are known for their regulation of protein coding transcripts and this class will be extensively described in this introduction. It has been believed for a long time that microRNAs are the only class of small RNAs in mammalian somatic cells and that the other main class of short RNAs, the piwi-interacting RNAs (piRNA) are only present in the germline where, by analogy to *Drosophila melanogaster*, they act to silence the activity of transposable elements (Aravin et al., 2007; Brennecke et al., 2003; Kuramochi-Miyagawa et al., 2008). However, a recent report identifying piRNAs in the brain sheds a new light on the study of non-coding RNAs in mammals (Lee et al., 2011). The discovery comes along with progress in identifying

the activity of human L1 elements in the neuronal precursors and the evidence that it may have functional implications for neuronal activity (Coufal et al., 2009; Muotri et al., 2005). Recent whole genome analyses provided further evidence that transposable elements may be more active in somatic cells than previously thought (Beck et al., 2010; Huang et al., 2010; Iskow et al., 2010) and their increased activity due to changes in RNA interference may be important in human diseases as shown with the accumulation of *Alu* elements in human cases of geographic atrophy (Kaneko et al., 2011).

1.3.2 Molecular mechanisms of microRNA biosynthesis and action

Most microRNA genes are present in the non-coding regions and are transcribed by Polymerase II, which produces a primary transcript containing the pre-miRNA hairpin with a partially complementary stem (Lee et al., 2004). As many miRNA loci are often found in close proximity of each other, the transcripts are commonly polycistronic (Lee et al., 2002). The miRNA gene transcripts are indistinguishable from protein coding RNAs in that they can be modified post- transcriptionally with common types of modification including m^7G capping and polyadenylation, RNA editing and ubiquitination (Du and Zamore, 2005; Kawahara et al., 2007; Rybak et al., 2009; Yang et al., 2006). The hairpins are recognised and cleaved by nuclear class II endoribonuclease Drosha, bound and exported to the cytoplasm by Exportin-5 (Lund et al., 2004; Yi et al., 2005; Yi et al., 2003). In the cytoplasm, the pre-miRNAs are recognised by the Piwi-Argonaute-Zwille (PAZ) domain (Cerutti et al., 2000) of the class III endoribonuclease Dicer and further enzymatic cleavage by catalytic residues in the antiparallel RNase III folds produces a mature double-stranded ~21nt RNA molecule (Du et al., 2008). The mature miRNA is then loaded on the RNA induced silencing complex (RISC) (Hutvagner and Zamore, 2002; Mourelatos et al., 2002; Parker and Sheth, 2007; Teixeira et al., 2005). It is then able to interact with protein coding RNAs with perfect or imperfect complementarity (Doench and Sharp, 2004). Little is known about this process, in particular whether all mRNAs are available for immediate silencing by mature miRNAs *in vivo*, or only some. The interaction between miRNA and its target is thought to be recognised by

the Argonaute proteins, which are the key proteins of the RISC complex (Martinez et al., 2002). This is believed to take place in the processing (P-) bodies in the cytoplasm (Ding et al., 2005) (Figure 1.08).

Figure 1.08: Summary of the RNA interference pathway in mammals. (A) Outline of the current understanding of the mechanisms and compartmentalisation of the miRNA pathway. Same as the protein coding genes, the miRNA coding genes are transcribed by RNA PolymeraseII (Pol II) to produce primary RNA transcripts (pri-miRNA), commonly polycistronic. The hairpins with double stranded RNA (dsRNA) stem loops are recognised and released by the Drosha- Pasha complex and exported to the cytoplasm by Exportin-5, where the dsRNA ends they are recognised by endoribonuclease Dicer. Other sources of dsRNA can also be incorporated including bidirectional transcription products. Dicer cleaves the pre-miRNA hairpin to release the mature double- stranded miRNA/miRNA* and mediates its association with the miRNA induced silencing complex (miRISC) which includes the Argonaute (Ago) proteins and the Gawky GW182 protein. The miRNA or miRNA* can then interact with the protein coding mRNAs (including ones in active translation). The interaction can lead to translational inhibition and mRNA storage or to the degradation of the mRNA by Dcp and Xrn1 exoribonuclease complex, which is closely associated with the nonsense mediated decay (NMD) machinery normally involved in the destruction of incorrectly spliced or aberrant mRNA (Pontes and Pikaard, 2008). (B – D) Schema representing best established effects of the miRNA – mRNA interaction(Fabian et al., 2010). (A) The binding of miRNA to the 3' untranslated region (UTR) of the protein coding mRNA and the association of miRISC with the poly-A- binding protein (PABP) induces block of initiation of protein translation either by repressing the recognition of the methyl-cap (m^7G) by eIF4E, or by repressing the recruitment of 60S ribosomal subunit upon the recognition of translation initiation codon AUG by the scanning 40S ribosomal subunit. (C) In cases when mRNA is in active translation, the miRISC can induce ribosome drop-off and protein degradation. (D) miRISC can recruit deadenylating enzymes such as CAF1, CCR4, NOT1, which is followed by decapping by DCP1/DCP2 and degradation of the mRNA.

FIGURE 1.08

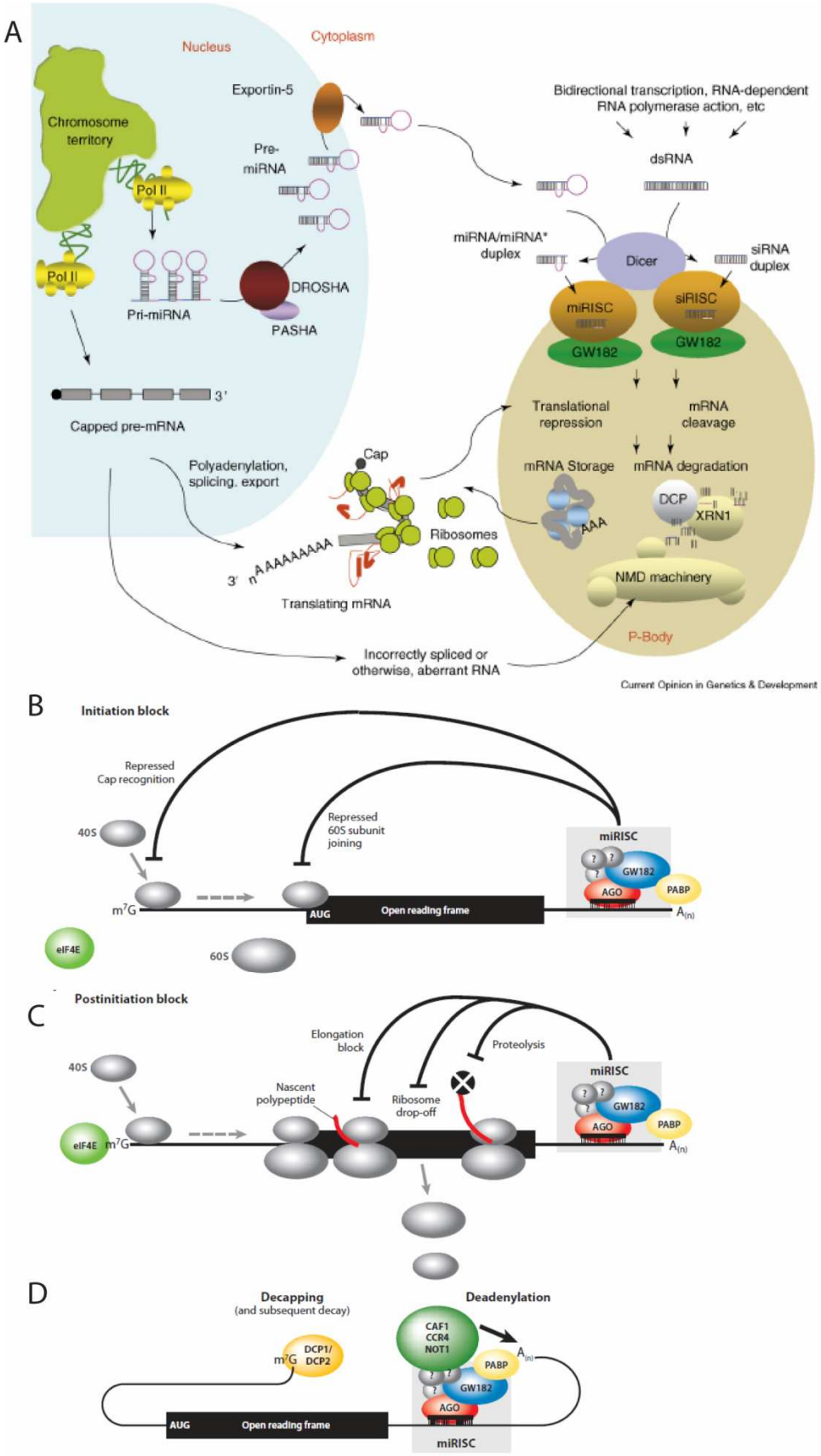
A
Nucleus
Cytoplasm
Exportin-5
Chromosome territory
Pre-miRNA
Pol II
Pol II
Pri-miRNA
DROSHA
PASHA
3'
Capped pre-mRNA
Polyadenylation, splicing, export
Bidirectional transcription, RNA-dependent RNA polymerase action, etc
dsRNA
miRNA/miRNA* duplex
Dicer
siRNA duplex
miRISC
siRISC
GW182
GW182
Translational repression
mRNA cleavage
mRNA Storage
mRNA degradation
DCP
XRN1
AAA
Cap
Ribosomes
3' nAAAAAAAAA
Translating mRNA
NMD machinery
P-Body
Incorrectly spliced or otherwise, aberrant RNA
Current Opinion in Genetics & Development
B
Initiation block
Repressed Cap recognition
40S
Repressed 60S subunit joining
miRISC
GW182
AGO
PABP
m7G
AUG
Open reading frame
A(n)
eIF4E
60S
C
Postinitiation block
Elongation block
Proteolysis
40S
Nascent polypeptide
Ribosome drop-off
miRISC
GW182
AGO
PABP
eIF4E
m7G
A(n)
D
Decapping
(and subsequent decay)
Deadenylation
CAF1
CCR4
NOT1
m7G
DCP1/
DCP2
A(n)
PABP
GW182
AGO
AUG
Open reading frame
miRISC

Several outcomes of the interaction between a microRNA and a protein coding mRNA have been proposed (Stefani and Slack, 2008). The interaction can result in the cleavage of the target mRNA, mainly believed to take place when the complementarity between the two RNA molecules is perfect. More commonly, the endogenous miRNAs are thought to hybridise to their targets with imperfect complementarity leading to inhibition of protein expression by one of several mechanisms. The binding of the miRNA and the RISC complex can interfere with the initiation of translation by obstructing the recruitment of eIF4E to the m^7G of the mRNA (Kiriakidou et al., 2007; Pillai et al., 2007; Thermann and Hentze, 2007). The binding can also initiate the drop-off of the ribosomes from mRNA during active translation (Nottrott et al., 2006; Petersen et al., 2006). Finally, recent evidence suggested that the RISC complex proteins such as GW182 which interact with Argonaute can recruit deadenylating enzymes, such as CAF1, to degrade the poly(A) tail and destabilize the mRNA (Chekulaeva et al., 2010; Fabian et al., 2009) (Figure 1.08). Most microRNAs are negative regulators of protein output and *in vitro* studies from mammalian systems suggest that while the short term action of miRNAs may be to inhibit protein translation (Fabian, 2009), the long term consequence is destabilisation and degradation of the target mRNA (Guo et al., 2010; Lim et al., 2005).

The 3' untranslated regions (3'UTRs) of protein coding genes have been found to harbour most of the known and predicted miRNA binding sites. Following the finding that a fully complementary 7 nt "seed" sequence (nt 2-8) of the mature miRNA is commonly sufficient to induce silencing (Xie et al., 2005), it was proposed that approximately every third human gene could be regulated with individual genes proposed to be regulated by a many miRNAs at the same time and a single miRNA proposed to regulate a number of mRNA transcripts (Lewis et al., 2005; Miranda et al., 2006). This of course means that in the absence of a given miRNA, other miRNAs with similar sequence could compensate for its loss. The exponentially increasing rates of discovery and annotation of novel miRNAs required a novel nomenclature system which was postulated primarily by Victor Ambros and other leading miRNA researchers (Ambros et al., 2003) as well as an online database dedicated to miRNA research, miRBase (Griffiths-Jones, 2004). It

also raised fears that a lot of miRNAs may be acting primarily as homeostatic factors rather than playing a role in biological pathways.

Nevertheless, mice knockout for specific miRNAs revealed specific and profound defects demonstrating the importance of this pathway in biology. The first miRNA to be deleted in mice, miR-1, expressed specifically in the heart was shown to be important in development with deletion of just one out of the two loci of this miRNA being sufficient for phenotypical changes (van Rooij et al., 2007; Zhao et al., 2007). Also, the deletion of the miR17-92 cluster was shown to cause significant disruption to normal development (Ventura et al., 2008). And yet, some mouse miRNA knockouts do not show any obvious phenotype (Park et al., 2010). This was also true for *Caenorhabditis elegans* (Miska et al., 2007) and it was proposed that most miRNAs are individually dispensable for development.

While disruptions in the levels of specific miRNAs have been shown to be associated with diseases, defects of the miRNA synthesis machinery, particularly the processing by Dicer, have also been demonstrated in several important diseases including the age-related macula degeneration (Kaneko et al., 2011), metastasis (Kumar et al., 2009; Martello et al., 2010) or schizophrenia (Beveridge et al., 2010; Santarelli et al., 2011). In addition, proteins known to be disrupted in human diseases including Fmrp and Dgcr8 were later found to interact with the key proteins of the miRNA pathway, such as Drosha and Argonaute (Caudy et al., 2002; Gregory et al., 2004), and their disruption leads to abnormal miRNA synthesis or function (Babiarz et al., 2011; Cheever and Ceman, 2009a; Cheever and Ceman, 2009b; Fenelon et al., 2011; Landgraf et al., 2007).

1.3.3 MicroRNAs in forebrain development – Part 1, lessons from Dicer knockouts

To bypass the early lethality in Dicer knockout mice (Bernstein et al., 2003), two transgenic lines of mice were generated containing LoxP cassettes flanking exons of *Dicer1* that encode parts of the RNase III folds necessary for processing of a pre-miRNA to a fully functional mature miRNA (Du et al., 2008; Macrae et al., 2006). Cliff Tabin's lab generated a line where exon 23 was flanked, encoding

approximately 90 residues of the RNase IIIb domain, while Gregory Hannon's lab flanked exons 22 and 23, which disrupts both RNase III domains (Harfe et al., 2005; Murchison et al., 2005).

Conditional *Dicer1*$^{fl/fl}$ mice were then crossed to mice expressing cre recombinase under the regulation of several different tissue specific promoters to ablate functional Dicer in the developing telencephalon (Fineberg et al., 2009). For the purpose of this introduction I will briefly review the key findings from each of the models of cortical Dicer mutant mice and I will subsequently point out similarities and differences between them. These and other cre- expressing lines have been used to delete Dicer in other parts of the central nervous system including the neural retina, the hippocampus and the spinal cord, but these studies will not be reviewed in this introduction.

1.3.3.1 Foxg1^{cre}

This is the earliest acting cre recombinase with expression driven by the endogenous *Foxg1* promoter starting from about E8.0 (Hebert, 2000). It was used by Tom Maniatis laboratory to provide *in vivo* evidence that miR124, a highly brain-enriched miRNA (Lagos-Quintana et al., 2002), targets a repressor of neuron-specific alternative splicing PTBP1. The analysis focused on the ventral telencephalon of E13.5 embryos and revealed that while the expression of PTBP1 in wild type embryos is restricted to the ventricular zone of the telencephalon, it can be detected in the postmitotic populations in the tissue lacking functional Dicer (Makeyev et al., 2007). It was additionally observed that the neuronal populations were misplaced throughout the ventral telencephalic wall, possibly due to the reported increase in rates of apoptotic cell death.

1.3.3.2 Emx1^{cre}

The cre recombinase driven by the Emx1 promoter was used to delete Dicer in the cortex with validated depletion of mature miR9 and miR124 by E10.5 (De Pietri Tonelli, 2008), though low levels of Dicer protein have been reported to persist until E13.5-E15.3 (Kawase-Koga, 2009).

During embryonic development of the cortex, the first phenotypic change reported in this model was the early apoptosis of postmitotic neurons starting from E12.5, which later also affected the progenitor cells. Expression of neuronal markers such as TuJ1 or Tbr1 was found initially normal in the cortex, prior to the onset of apoptosis, but with numerous disorganised axonal processes found in the cortical plate (De Pietri Tonelli, 2008). It was also shown that postmitotic neurons born following the loss of mature miRNAs display migration defects (Kawase-Koga, 2009). Cortex lacking functional Dicer also showed defects in the development of the deep layer neurons expressing markers such as Brn1 and Foxp2 as well as the reduced abundance of calretinin –expressing interneurons by P7 (De Pietri Tonelli, 2008).

No evidence of functional defects were observed in the progenitor populations before the onset of widespread apoptosis in the ventricular and subventricular zones at E14.5, which is followed by a reduction in the expression of markers of proliferative population such as Ngn2, Hes5, Tbr2, Pax6, Ki67 and radial glia markers Blbp, FABP7 and GLAST between E15.5-E16.5 (De Pietri Tonelli, 2008). However, it was later reported that the ability of the isolated neural stem cells to form neurospheres *in vitro* in the presence of FGF2 and EGF is compromised (Kawase-Koga et al., 2010).

1.3.3.3 Nes^{cre}

This line was found to disrupt normal levels of mature miRNAs by E13.5 with complete depletion of miR17-5p and miR181 by E18.5 (Kawase-Koga, 2009). In this line, the proportions of cells expressing postmitotic neuronal markers TuJ1 and Tbr1 are normal at E15.5 and the migration of neurons born on E13.5 was found to

be unaffected by the deletion (Kawase-Koga, 2009). In addition, expression of markers of the progenitor populations and the proportion of cells in S-phase relative to the size of the proliferative pool were not found to be different between control and Dicer deficient cortices (Kawase-Koga, 2009).

The onset of apoptosis in the progenitor cells between E16.5 and E18.5 coincides with defects in the size of the postmitotic population, particularly of the Tbr1 expressing subtype, as well as their ability to migrate to the cortical plate (Kawase-Koga, 2009).

1.3.3.4 Camk2^{cre}

The first cre expressing line used to ablate Dicer in the cortex was the *Camk2^{cre}*, which is known to be active from around E15.5 (Dragatsis and Zeitlin, 2000), but analysis of miRNA expression showed a reduction in the abundance of miR132 by P15 and a further loss by P21 in the cortex and the hippocampus. Key defects in the cortex included reduced brain size, attributed to apoptosis around P0, and axonal pathfinding defects, particularly in the anterior commissure (Davis et al., 2008).

1.3.3.5 Roles of Dicer in cortical development

To summarise the observations from studies investigating the phenotypes of Dicer deficient mouse cortex, the onset and severity of defects correlate with the timing of mature miRNA loss. All studies identified cell survival as one of the key biological processes which the ability to synthesise mature miRNAs is crucially required for. In addition, various defects following the depletion of mature miRNAs affect primarily the postmitotic neurons. This could tie in with the observation that mature neurons have particularly high rates of miRNA turnover (Krol et al., 2010a). It is intriguing that the function of radial glia and intermediate progenitors might be somehow able to escape the regulation by mature miRNAs, but it is plausible that miRNAs with

opposing effects on progenitor cell functions act to maintain homeostasis (Melton et al., 2010).

1.3.4 MicroRNAs in central nervous system development – Part 2, lessons from microRNA studies

While deletion of Dicer is a powerful tool for identifying biological processes which are dependent on mature miRNAs, the approach is very non-specific and it is difficult to identify specific target genes or individual miRNAs with non-redundant functions. It is also difficult to disentangle roles of miRNA whose expression in the brain is only transient in development or whose expression is upregulated towards the end of development (Smirnova et al., 2005).

Therefore, a more specific approach taken to understand the roles of miRNAs in cortical development has been to generate transgenic mice lacking functional miRNAs or to deliver vectors overexpressing candidate miRNAs (Meza-Sosa et al., 2012; Park et al., 2010). This introduction will focus on three miRNAs which have been demonstrated to play a functional role in the development of the cortex.

1.3.4.1 miR-134

So far only one study reported the role of this miRNA in cortical development and so relatively little is understood about the pathways which this miRNA could be involved in. MicroRNA overexpression and inhibition studies have provided substantial evidence that miR134 is important for neuronal migration and terminal differentiation by targeting Doublecortin and a Bmp antagonist, Chordin-like1 (Gaughwin et al., 2011). This finding may be of clinical importance in the future, as levels of mature miR134 have recently been reported to be elevated in post-mortem samples of human prefrontal cortex in cases of schizoaffective disorder and schizophrenia (Santarelli et al., 2011).

1.3.4.2 miR-124

This microRNA is one of the best studied microRNAs in the central nervous system. It is thought to be an important proneural miRNA with the expression primarily in the differentiating and mature neurons (Landgraf, 2007; Maiorano, 2009). Several mRNAs have been validated as targets of miR124 in the embryonic central nervous system, including splicing regulator PTBP1 (Makeyev et al., 2007) and components of the anti-neural repressor element-1 silencing transcription factor (REST) repressor complex (Visvanathan et al., 2007), the BAF53a and BAF45a subunits of the Swi/Snf neural progenitor complex (Yoo et al., 2009) involved in promoting proliferation of progenitor cells through the regulation of chromatin state (Lessard et al., 2007). In the adult brain, miR124 has shown to be expressed by the neuroblasts in the subventricular zone and the interaction with the target *Sox9* mRNA was shown to be important for postnatal neurogenesis (Cheng et al., 2009). Following the overexpression of miR124, cortical progenitors appear to differentiate prematurely (Maiorano, 2009) and the recent demonstration that overexpression of this miRNA together with miR9/9* (discussed below) is sufficient to induce a conversion of human fibroblasts into functional neurons provides important evidence that microRNAs can be extremely potent regulators of biological processes with prospects of future clinical applications (Yoo et al., 2011).

*1.3.4.3 miR-9/9**

Similarly to miR-124, miR9/9* was shown to target BAF53a and BAF45a (Yoo et al., 2009) and together with miR124 was shown to be a potent pro-neural miRNA (Yoo et al., 2011). This miRNAs also regulates the anti-neural REST and CoREST factors involved in establishing appropriate epigenetic modifications during neurogenesis (Packer et al., 2008). It was also shown to regulate the Tlx transcription factor, a step demonstrated to be important for neuronal differentiation of the radial glia (Zhao et al., 2009). Mice with deletions in miR9-2 and miR9-3 are hypomorphic for miR9 and the study investigating the phenotype of double-mutant mice demonstrated neuronal differentiation defects following miR9 depletion and

identified that key target mRNAs of miR9 encode important transcription factors such as Gsh2, Foxg1 and Meis2, providing further evidence for the role of miRNAs in the regulation of neuronal differentiation in the forebrain (Shibata et al., 2011).

1.3.4.4 Other functionally important miRNAs

Several other miRNAs have recently been demonstrated to function in various processes important for normal development of the brain. These include microRNAs acting to regulate neurite outgrowth such as miR375 shown to inhibit the expression of neuronal mRNA binding protein HuD, or miR132 which was shown to be expressed in response to cAMP-response element binding protein (CREB) and promote neurite outgrowth (Vo et al., 2005).

There is a clear focus on identifying biologically important miRNA-mRNA interactions. This means that a lot of important questions remain unanswered in the miRNA field including the important question about the participation of miRNA in wider genetic networks. Several recent studies begin to identify changes in the levels of mature miRNAs not only in various disease conditions (Sayed and Abdellatif, 2011), but also in response to environmental cues. It was noted that changes to light exposure can dynamically regulate miRNA levels (Krol et al., 2010a) and a recent study demonstrated the critical role of miR132 in neuronal plasticity following molecular deprivation of P24 mice (Mellios et al., 2011). Likewise, miR128b was shown to mediate neuronal plasticity involved in the formation of fear-extinction memory by regulating the expression of CREB, Protein phosphatase 1a, Reelin and Trans-acting transcription factor Sp1 (Lin et al., 2011). Exact mechanisms of these proposed networks remain to be investigated.

1.3.5 MicroRNAs in central nervous system development – Part 3, important questions

Studies ablating functional Dicer have provided useful insights into the roles of miRNAs in the developing cortex by indicating biological processes that depend on their presence. Cell survival and neuronal differentiation have been identified as main *in vivo* biological processes for which miRNA processing is required. Chapter 3 of this Thesis describes the phenotype of $Foxg1^{cre}$ –induced ablation of functional Dicer in the developing cortex. The onset of apoptosis is earlier than in other models of Dicer –deficient neuroepithelium and coincides with an abnormal pattern of expression of three important markers of the radial glia, Nestin, Sox9 and ErbB2 with the expression of all these markers being abnormally low in Dicer- deficient tissue. Analysis of the expression of proteins such as CD133, Sox2 or Musashi, all of which are already expressed by the neuroepithelial stem cells, showed that many aspects of the neuroepithelial stem cell identity are not affected by the loss of functional miRNAs. This model provides evidence that mature miRNAs play a role in normal specification of the radial glia in the developing cortex. This phenotype has not been previously described for other models of Dicer –deficient cortex. Given the role of radial glia in guiding the radial migration of the postmitotic neurons this observation raised an attractive possibility that the migration defects of postmitotic neurons reported in this and other models could be secondary to the misspecification of the radial glia.

Chapter 4 of this Thesis describes efforts undertaken with an initial aim to investigate processes which are cell –autonomously dependent on the ability to synthesise mature miRNAs. A model of mosaic Dicer ablation in a subset of radial glia was generated by electroporating a cre –expression vector into the radial glia *in utero* at E13.5. Four key observations were made. First, the presence of wild type cells appears to rescue the apoptotic phenotype following the loss of mature miRNAs. Second, loss of functional Dicer does not compromise the ability of postmitotic cells to migrate to the cortical plate. Third, Dicer deficient radial glia continue to generate cortical cells at higher rates than expected during postnatal development. Fourth, loss of functional Dicer in the radial glia of the developing cortex results in an increased rate of generating intermediate progenitor cells. This is

followed by an identification of a miRNA targeting the Tbr2 transcription factor and the functional validation of the miRNA- mRNA interaction *in vitro* and *in vivo*.

CHAPTER 2:
Materials and Methods

Unless otherwise clearly stated, all chemicals were from Fisher. All primers were manufactured and supplied by MWG Eurofins.

2.1 Animals

2.1.1 Animal work licensing

The licence authorising this work was approved by the University of Edinburgh Ethical Review Committee of 22nd September 2008 (application number PL35-08) and by the Home Office on 6th November 2008. Animal husbandry was in accordance with the UK Animals (Scientific Procedures) Act 1986 regulations.

2.1.2 Mouse lines

Mice homozygous for *Dicer1*^{fl} allele (Harfe et al., 2005) were purchased from the Jackson's Laboratories and maintained on the C57BL/6J background. To generate mice carrying the *Rosa26RYFP* (R26RYFP) transgene (Srinivas et al., 2001) (line managed by Dr. Martine Manuel), homozygous *Dicer1*$^{fl/fl}$ mice were crossed to *Rosa26RYFP*$^{+/+}$ mice to generate double hetereozygotes. Double homozygotes were selected among the F2 offspring and maintained on the mixed background thereafter.

Genomic DNA was extracted from earclips of mice using the hot sodium hydroxide and Tris (HotSHOT) method. In short, 75µl of alkaline lysis reagent, 25mM NaOH, 0.2M EDTA, (pH=12) was added per earclip and incubated at 95^{o}C for 30min followed by cooling to 4^{o}C and adding 75µl of 20mM Tris-HCl, 0.1M EDTA (pH=8) neutralising reagent. The sample was then used directly used for genotyping using the TaqMan DNA polymerase (Promega).

Genotyping was performed as previously described (Harfe et al., 2005; Srinivas et al., 2001). In short, the conditional *Dicer1*^{fl} allele was detected using primers: DicerF1 – CCT GAC AGT GAC GGT CCA AAG and DicerR1 – CAT GAC TCT

TCA ACT CAA ACT, annealing temperature 55^{o}C for 33 cycles. The floxed and wild type allele was distinguished on 2% agarose (Sea) gel electrophoresis with 1:10000 Sybersafe (Invitrogen) to visualise bands. Images of gel electrophoresis were captured using InGenius transilluminator (Syngene) and the Genesnap imaging software (Syngene). Floxed allele produced a 420bp band and the wild type allele produced a 351bp band. The *Rosa26RYFP* line was genotyped by polymerase chain reaction using the following primers: R26WTF1 – AAA GTC GCT CTG AGT TGT TAT, R26WTR – GGA GCG GGA GAA ATG GAT ATG and R26KOF1 – GCG AAG AGT TTG TCC TCA ACC with annealing temperature of 59^{o}C for 37 cycles. Denaturation and elongation steps were performed at 94^{o}C and 72^{o}C respectively. The primer pair R26WTF1 and R26WTR produced 300bp band for $R26RYFP^{+/+}$ and $R26RYFP^{+/-}$ genotypes while the primer pair R26WTF1 and R26KOF1 produced a 550bp band for the $R26RYFP^{+/-}$ and $R26RYFP^{-/-}$ genotypes.

$Foxg1^{cre}$ line (Hebert, 2000) was managed and maintained by Dr. Vassiliki Fotaki and heterozygous males were crossed to $Dicer1^{fl/fl}$ females and F1 males were genotyped for the presence of the $Foxg1^{cre}$ allele using the following primers: FcreF – CAT TTG GGC CAG CTA AAC AT and FcreR – ATT CTC CCA CCG TCA GTA CG with annealing temperature of 55^{o}C for 31 cycles producing a 300bp band.

2.1.3 Timed matings

Heterozygous $Foxg1^{cre}Dicer^{fl/+}$ males were used in timed mating experiments with $Dicer1^{fl/fl}$ females to generate $Foxg1^{cre}Dicer1^{fl/fl}$ ($Dicer1^{-/-}$) and control $Foxg1^{cre}Dicer1^{fl/+}$ ($Dicer1^{+/-}$) embryos at desired stages of development. Females were checked daily and first day when vaginal plug was detected was designated as E0.5.

For experiments aimed at mutating *Dicer1* in E14.5-E16.5 embryos by *in utero* electroporation, males homozygous for $Dicer1^{fl}$ allele (maintained on the C57BL/6J background) or C57BL/6J were crossed to $Dicer1^{fl/fl}$ females to generate the experimental $Dicer1^{fl/fl}$ and control $Dicer1^{fl/+}$ embryos.

For studies using animals older than E16.5 (three days after electroporation) males homozygous for *Dicer1*^{fl} allele (maintained on the C57BL/6J background) or C57BL/6J were crossed to *Dicer1*$^{fl/fl}$*:R26RYFP*$^{+/+}$ double –homozygotes to generate the experimental *Dicer1*$^{fl/fl}$*:R26RYFP*$^{+/+}$ and control *Dicer1*$^{fl/+}$*:R26RYFP*$^{+/+}$ embryos.

For all *in vivo* miRNA overexpression analysis wild type C57BL/6J embryos were generated by crossing wild type C57BL/6J males and females.

2.1.4 Tissue collection

To minimise animal suffering, pregnant dams were culled by cervical dislocation under terminal anaesthesia according to the Code of Practice for Humane Killing of Animals under Schedule 1 to the Animals (Scientific Procedures) Act 1986 issued by the Home Office.

For embryos younger than E12.0, embryonic age was determined based on the number of visible somites and other morphological features in accordance with the Theiler staging criteria for mouse embryos such as retina pigmentation, auditory hillocks and nasal pits. Embryos with 30-34 somites were designated as E10.25. Embryos with 45 – 47 somites was designated as E11.5 and embryos with well defined tongue, retina pigmentation but lacking 5 rows of whiskers were designated as E12.5. The amniotic sac was retained for genotyping.

Embryos were immediately decapitated following their dissection from the uterine horns and placed either directly in cold Earle's Balanced Salt Solution, 1.8mM $CaCl_2$, 5.3mM KCl, 0.8mM $MgSO_4$, 117 mM NaCl, 26mM $NaHCO_3$, 1mM NaH_2PO_4-H_2O (for cell culture studies), or ice-cold phosphate buffered saline (PBS) pH=7.4 (pre-treated with Diethyl Polycarbonate (Sigma) overnight at 37^{o}C) for staging or further dissection.

Postnatal animals were anaesthetised by intraperitoneal injection of 50mg sodium pentobarbitone (Ceva Sante Animale) and perfused transcardially with 0.1M

phosphate buffered saline pH 7.4 (PBS) and 4% paraformaldehyde (PFA) and incubated for 12hr in PFA at 4^{o}C.

2.1.5 Electroporation

ScotPil course Surgery module 4 was completed in September 2009 and training was kindly provided by Miss Soyon Chun and Dr. Robert Hindges at King's College London. Local supervision by the named veterinary surgeon, Ms Gidona Goodman was completed in May 2010.

Surgery was performed on pregnant dams 13.5 days post coitum in principle as previously described with modifications (Saito, 2006). Anaesthesia was maintained using inhaled isoflurane (Merial). In short, anaesthesia was induced by inhalation of a 2.5-3% Isoflurane pre-mixed with medical oxygen (BOC). Involuntary reflexes to stimuli were used to confirm that the animal was anaesthetised. The animal was then placed on a heating pad to prevent heat loss during surgery. Animals received a subcutaneous injection of 0.05mg/kg Buprenorphine (Reckitt Benckiser Healthcare) dissolved in water for injections (Norbrook). Fur was shaved off around the abdomen and the skin was sterilised using Medi-scrub (MediChem) solution to minimise the risk of infection. Following medial laparotomy uterine horns were exposed and maintained well hydrated using warm 37^{o}C sterile PBS throughout the procedure. Anaesthesia was maintained in accordance with the observed breathing rates with considerable animal-to–animal variations. Plasmid solution was pre-mixed with Fastgreen dye (Sigma) and injected using pneumatic picopump (PV820, WPI)) through 4in. (100mm) 1/0.75 OD/ID filament Thin Wall Glass Capillaries (WPI, TW100F-4) pulled with the flaming/brown micropipette puller (pressure, 050; heat, ramp; pull, 30; velocity, 40; time, 1, Sutter Instrument, P87) into the lateral ventricle. The embryos were then electroporated using the forceps-type electrodes (Nepagene, CUY650P5) placed at either side of the head of the embryo with positive electrode over the injected area. Each embryo received no more than 5 square 50ms pulses generated using the edit-type CUY21 electroporator (Nepa-gene, 35V, Pon = 50ms, Poff = 950ms).

In order to compare the average numbers of the GFP/YFP expressing cells derived from the electroporated radial glia by P14.5 between genotypes (*Dicer1*$^{fl/+}$*Rosa26YFP*$^{+}$ and *Dicer1*$^{fl/fl}$*Rosa26YFP*$^{+}$), cre expression vector was injected at the constant concentration of 1.35mg/ml in double -distilled water. For miRNA overexpression studies and co-electroporation, plasmids were injected at the concentration of 2.5 mg/ml in double distilled water.

At the end of the surgery, the uterine horns were then replaced into the abdominal cavity and smooth muscle layer was sutured using 4-0 vicryl sutures with cutting needle (Ethicon, W9825). Skin was stapled using 7mm Reflex Clips (WPI, 500344) applied with Reflex Clip Applier (WPI, 500343). Mice were placed back in the cage and health status was monitored daily. Buprenorphine was administered orally at 0.5mg/kg after the surgery.

2.1.6 BrdU analysis

Stock 10 mg/ml 5'-bromo-2'-deoxyuridine (BrdU, Sigma) was prepared in normal saline (0.9% NaCl) at 55^{o}C and stored at -20^{o}C. Pregnant females received an intraperitoneal (IP) injection of 0.2ml. For postnatal P3-P14 BrdU analysis, pups received IP injections of 50µg/g body weight using a 30G insulin needle (BD) before midday.

2.2 Tissue fixation, preservation, histology

2.2.1 Fixation

Tissue was fixed either in 4% PFA in PBS (pH=9), Bouin's fixative (Sigma, 75% saturated aqueous picric acid, 10% paraformaldehyde and 5% glacial acetic acid) or the Fekete's fixative (4% paraformaldehyde, 70% Ethanol, 5% glacial acetic acid). Fixation was performed at room temperature for 4hr or at 4^{o}C for 24hr with constant agitation.

Young, E9-E11 embryos were pre-embedded in 2% agarose. Tissue was then processed through a gradient of alcohol solutions and embedded in paraffin. Paraffin blocks were sectioned at 6µm using microtome and floated on the surface of 37°C waterbath before mounting on glass slides pre-coated with 100µg/ml of poly-L-lysine (Sigma) for 6min.

For cryostat sections, tissue was cryoprotected in 15% sucrose (Fisher) in PBS until sinking, equilibrated in 15% sucrose in PBS / optimal cutting temperature medium OCT (Fisher/ Raymond Lamb) for 1 hour with constant agitation before freezing on dry ice. Tissue was stored at -20°C or at -70°C for *in situ* hybridisation. Cryosections were cut at 14µm (E9-E12) or at 20µm (>E12.5) using the cryostat (Leica, CM3050S) and collected on Superfrost Plus slides (Fisher), dried at room temperature for no longer than 1hr and stored at -20°C or at -70°C for *in situ* hybridisation.

For thick sections, tissue was embedded in 4% agarose before sectioning in cold PBS at 100-300µm using the Leica vibratome. Sections were collected on Superfrost Plus slides (Fisher).

2.2.2 Cell dissociation

Cortical areas containing GFP – positive cells visualised using a Leica microscope were dissected from at least three embryos per litter in ice cold EBSS and placed in 1x Trypsin (Gibco) for 18-20min at 37°C. Trypsin was neutralized by washing the tissue in 20% Foetal Calf Serum (Gibco) in EBSS. Tissue was then washed once with EBSS and triturated in serum free culture medium at 37°C until single-cell suspension was achieved. Cells were plated at 10^3 – 10^4 cells per glass coverslip (9mm diameter, VWR) pre-coated with 100µg/ml of poly-L-lysine (Sigma) and were allowed to adhere for 1 hour at 37°C before fixation in ice-cold PFA for 20min.

2.3 Expression plasmids

2.3.1 Cre expression vector

The cre-recombinase expression plasmid (pCAG-cre-IRES-EGFP) contains ubiquitous mammalian CMV promoter with Chicken β-actin enhancer (CAG) as well as internal ribosomal entry site (IRES) followed by enhanced green fluorescent protein (EGFP) (Woodhead et al., 2006). The plasmid was kindly provided by Drs Christopher Mutch and Anjen Chenn, Northwestern University.

2.3.2 MicroRNA expression plasmid

Mature miR-92b expression plasmid GFP-miR92b was generated by cloning the genomic pre-miR92b sequence, as annotated in mirBase16 (Griffiths-Jones, 2010), into a myristolated, destablilised enhanced GFP (myr-DEGFP) expression plasmid downstream of the myr-DEGFP coding sequence, just before synthetic polyadenylation signal (Wu et al., 2002). Genomic pre-miR92b hairpin sequence was amplified from the genomic DNA by PCR using Expand High Fidelity Plus PCR system (Roche) following the manufacturer's instructions using the following primers: forward – ATA CTC CCC AGA GCA CTC CA and reverse – GCT CGG TAG AGA TCG AAA GC. Genomic clone was first cloned using blunt-end T0 cloning into pGEM-T Easy (Promega), amplified by PCR to introduce PstI restriction sites using the following primers: forward – GCA CTG CAG GCT CGG TAG AGA TCG AAA GC and reverse – CAG CTG CAG ATA CTC CCC AGA GCA CTC CA. Subsequently, the pre-miR92b was subcloned using into the myr-DEGFP expression plasmid. Cloning was confirmed by sequencing. The resulting miR92b overexpression plasmid will hereafter be referred to as GFP-miR92b.

2.3.3 Luciferase plasmid WT 3'UTR

The 3' untranslated region (3'UTR) of the mouse *Eomes* coding the Tbr2 transcription factor (hereafter referred to as the Tbr2 mRNA) was amplified from the genomic DNA by nested PCR using Expand High Fidelity Plus PCR system (Roche) following the manufacturer's instructions for the following two pairs of primers: forward1 – GTG GCG CTT ATC AGA GGA AG and reverse1 – GGA TTA AGC CTG CAG AGC AC and subsequently forward2 – AAG ATC AGC TTG CCA AGG AA and reverse2 – GAA AGG GGG CAG AAA GAA AC. The clone was then subloned into the NotI site in the multiple cloning site of the psiCHECK-2 (Promega) dual luciferase vector and is hereafter referred to as WT 3'UTR.

2.3.4 Luciferase plasmid MT 3'UTR

To delete nucleotides 2707- 2714 (GUGCAAU) of the *Eomes* mRNA coding sequence, site directed mutagenesis was performed on the 3'UTR clone of the using the QuickChangeII XL kit (Agilent) according to manufacturer's instructions with the following primers: sense – CCT TCC ACC TTT GAT GTA TCC TGT TTT TCT CTG AGA GAA GG and antisense – CCT TCT CTC AGA GAA AAA CAG GAT ACA TCA AAG GTG GAA GG. The mutagenesis was confirmed by sequencing and HpyCH4V (NEB) restriction digest (blunt-end cutting at TG/CA) and the 3'UTR was subcloned into the dual luciferase vector psiCHECK-2 (Promega) and is hereafter referred to as MT 3'UTR.

2.4 Luciferase assay

To test the ability of miR-92b to interact with the Tbr2 3'UTR, dual luciferase reporter assay was performed. HEK-293 cells were cultured in Dulbecco's DMEM (Invitrogen) supplemented with 10% Foetal Bovine Serum (Gibco) and were co-transfected with dual luciferase expression plasmid, WT 3'UTR or MT 3'UTR and GFP or GFP-miR92b using Lipofectamine 2000 (Invitrogen) according to

manufacturer's instructions in 96 well plates before passage number reached 27 (100ng luciferase plasmid and 300ng GFP or GFP-miR92b plasmid were used per well with 1µg:2.5µl ratio of plasmid: lipofectamine). Luciferase activity was assayed 48hours later using the dual luciferase reporter system (Promega) using the GloMax Luminometer (Promega).

2.5 Immunohistochemistry

Immunohistochemistry was performed using standard protocols. Paraffin sections were deparaffinised in xylene and rehydrated through a gradient of alcohol solutions before washing with PBS. Cryosections were allowed to thaw at room temperature before washing in PBS. Sections for diaminobenzidine (DAB, Sigma) staining were incubated in 0.3% hydrogen peroxidase with 10% methanol for 15min in dark. Heat induced antigen retrieval performed by microwaving the slides in 10mM sodium citrate, pH = 6.0 for 20 minutes at full power with intervals. The 96-well plates were microwaved in a 2L beaker for 5min at full power, 5min at medium power and then 10min at low power. Slides were allowed to cool for 20min and sections were washed with PBS/ 0.1%TritonX-100. Sections were blocked in the blocking solution containing 10% serum of the same species as the secondary antibody, 0.2% gelatine, PBS, 0.1% Triton X-100 for at least 1 hr at room temperature. All antibodies were delivered in the blocking solution overnight at 4^{o}C. Primary antibodies included in this study were against: β-catenin (mouse, 1:400, BD Biosciences), β-tubulin type III (TuJ1, mouse, 1:400, Sigma), BrdU (rat, 1:50, Abcam ab6326), calretinin (rabbit, 1:1000, Swant), CD133 (rat clone 13A4, 1:100, Millipore), cleaved caspase 3 (rabbit, 1:50, Cell Signalling), Cux1 (rabbit, 1:50, Santa Cruz), Ctip2 (rat, 1:250, Abcam, ab18465), Dcx (rabbit, 1:1000, Abcam, ab18723), GFAP (rabbit, 1:500, Dako), GFP (goat, 1:400, Abcam, ab6673), HuC/D (mouse IgG2b 16A11, 1:150, Invitrogen, A-21271), Ki67 (rabbit, 1:1000, Leica, NCL-Ki67p), Musashi (rabbit, 1:10, Cell Signaling, 2154S), Nestin Rat-401 (mouse, 1:100, Developmental Studies Hybridoma Bank (DSHB), University of Iowa, Iowa City, IA), NeuN (mouse, 1:500, Chemicon), Numb (rabbit, 1:100, Abcam, ab14140), Olig2 (rabbit 1:500, DSHB, University of Iowa, Iowa City, IA), Pax6 (mouse, 1:50, DSHB, University of Iowa,

Iowa City, IA), phosphorylated histone 3 pHH_3 (ser10) (rabbit, 1:100, Cell Signaling), RC2 (mouse IgM, 1:100, DSHB, University of Iowa, Iowa City, IA), Reelin (mouse G10, 1:1000, Milipore/ Chemicon), Satb2 (mouse, 1:250, Abcam, ab51502), Sox2 (rabbit, 1:3000, Millipore, AB5603), Sox9 (rabbit, 1:1500, Millipore, AB5535), Tbr1 (rabbit, 1:1000, kind gift from R.Hevner, University of Washington, WA), Tbr2 (rabbit, 1:100, Abcam, ab23345). Binding was revealed either using an appropriate Alexa-488, Alexa-564 conjugated secondary antibodies (1:400, Invitrogen), or using an appropriate biotinylated secondary antibody (1:200, Dako) with the avidin– biotin- peroxidise system (Vector Laboratories). Nuclear counterstained 4'-6-Diamino-2-phenylindole (DAPI) (Vector) was applied in PBS at 1:10000. Slides with fluorescent staining were mounted in Vectashield hard-set (Vector) while sections developed with DAB were mounted in DPX (Raymond/Lamb).

All antibodies which had not been optimised previously were initially used at a series of concentrations (1:10, 1:20, 1:50, 1:100, 1:200, 1:500 and if further dilution was needed, 1:1000, 1:2000, 1:4000 were used) with and without antigen retrieval, with DAB and fluorescence as a method of detection.

2.6 *In situ* hybridisation

2.6.1 Probes for *in situ* hybridisation

All probes used in this study were DIG-labelled and were stored at -70^{o}C in aliquots to avoid degradation. All locked nucleic acid (LNA) probes for mature miRNAs were purchased from commercial supplier (Exiqon). The following RNA probes were used for *in situ* hybridisations: Dlx2 (generous gift from John Rubenstein), Emx2 (generous gift from Antonio Simeone), Erbb2 (generous gift from Carmen Birchmeier), Foxg1 ((Tao and Lai, 1992), generous gift from Thomas Theil), Ngn2 (generous gift from Thomas Theil). Standard methods for DIG-labelling of probes were used. In short, 5µg plasmid was digested at 37^{o}C for 3hr in the presence of BSA and an 50U of an appropriate restriction enzyme (Promega or NEB). The

linearised plasmid was then purified using phenol: chloroform extraction. In short, digested plasmid was mixed 1:1 (V:V) with phenol: chloroform (Sigma), centrifuged for 5min keeping the supernatant. The DNA was mixed with 0.1 V or 3M sodium acetate, and 2V of ice cold ethanol and precipitated at -70^{o}C. Following centrifugation and washing of the pellet with 70% ethanol, the pellet was air-dried and resuspended in diethylpolycarbonate treated double –distilled water. Probes were generated using an appropriate SP6, T3 or T7 RNA polymerase (Roche) by incubating at 37^{o}C overnight in the presence of DIG-RNA labelling mix (Roche). The RNA transcripts were then ethanol precipitated in the presence of LiCl for 1 hour at -70^{o}C and reconstituted in diethylpolycarbonate treated double –distilled water.

2.6.2 RNA *in situ* hybridisation staining

In situ hybridisation was performed as described before (Wallace and Raff, 1999) and the full protocol was kindly provided by Drs Enrique Domingos and Valerie Wallace, Ottawa Hospital Research Institute.

All *in situ* hybridisation stainings were performed overnight. Optimal dilution of each probe was determined with a series of concentrations. Cryostat sections were warmed for 30min at room temperature prior to use and for cells in 96 well plates, PBS was aspirated off after washing the fixative. Probes were diluted in pre- warmed hybridisation buffer (50% formamide, 10% dextran sulfate, 1 mg/ml yeast RNA (Roche), 1x Denhart's (Invitrogen), 200mM NaCl, 10mM Tris-HCl (pH=7.5), 1mM Tris base, 5mM $NaH_2PO_4 \cdot 2H_2O$, 4mM Na_2HPO_4, 5mM EDTA (pH=8)). All probes apart from the LNA probes were denatured for 10 min at 70^{o}C. The hybridisation mix was then applied to the sections and a 22x64mm glass coverslip (VWR 631-0142) was placed on top. The slides were placed in a pre-warmed container humidified with 50% formamide, 150mM NaCl, 15mM tri-sodium citrate, pH=4.5 and incubated overnight. Incubation temperature was 65^{o}C for all protein coding genes and RNA melting temperature -30^{o}C or DNA melting temperature -21^{o}C for LNA probes as outlined by the manufacturer. After hybridisation, slides were decoverslipped and washed in 50% formamide, 150mM NaCl, 15mM tri-sodium

citrate, pH=4.5, 0.1% Tween-20 at hybridisation temperature. Slides were then washed with maleic acid buffer (100mM Maleic acid, 150mM NaCl, 0.1% Tween-20) at room temperature. Sections were incubated in a blocking solution containing 20% sheep serum, 2% blocking reagent (Roche) in maleic acid buffer for 1-2 hr at room temperature in a chamber humidified with PBS. Subsequently, sections were incubated with an alkaline phosphatase -tagged anti-DIG antibody (Roche) diluted 1:1500 in the blocking solution for 4 hours at room temperature or overnight at 4^{o}C. Sections were then washed in maleic acid buffer and the colorimetric detection of alkaline phosphatase was performed with nitro blue tetrazolium chloride and 5-bromo-4-chloro-3-indolyl phosphate (Roche) in the alkaline phosphatase staining solution containing 100mM NaCl, $MgCl_2$, 100mM Tris HCl pH=9-9.5, 10% polyvinyl alcohol (Sigma) and 0.1% Tween-20. When the reaction was complete, sections were washed with PBS and either mounted with Aquatex mounting medium (Merck) or processed through the immunohistochemical staining protocol. For dissociated cells *in situ,* all of the above steps were reproduced in the culture wells and the detection of alkaline phosphatase was performed for 7 days for all plates before proceeding with immunostaining.

2.7 Haematoxylin and Eosin staining

Wax sections were deparaffinised in Xylene and rehydrated through a descending ethanol gradient and finally in tap water. Tissue was immersed in Haematoxylin (BDH Chemicals) for 3 min following washing in tap water and alkaline tap water (400ml water with a few drops of ammonia). Sections were then washed in 70% ethanol and immersed for 30 seconds in the alcoholic Eosin Y (Sigma). Following a short wash in tap water sections were dehydrated through ethanol solutions of ascending concentrations before mounting in DPX and coverslipping.

2.8 Electrophysiology

All electrophysiological recordings were obtained by Dr. Timothy O'Leary. 300 μm thick coronal slices were prepared from P14 *Dicer1$^{fl/fl}$:R26RYFP^{+}* and control *Dicer1$^{fl/+}$:R26RYFP^{+}* -electroporated pups. Brains were removed and placed in pre-oxygenated ice-cold dissection buffer containing 86mM NaCl, 1.2mM NaH_2PO_4, 25mM KCl, 25mM $NaHCO_3$, 20mM glucose, 75mM sucrose, 0.5mM $CaCl_2$, 7mM $MgCl_2$ and cut using a Leica VT1200S vibratome. Slices recovered for 30 minutes at 35 ºC in artificial cerebrospinal fluid (aCSF) containing 124mM NaCl, 1.2mM NaH_2PO_4, 25mM KCL, 25mM $NaHCO_3$, 20mM glucose, 2mM $CaCl_2$, 1mM $MgCl_2$ continuously bubbled with 95% O_2/ 5% CO_2. For recording, slices were visualized using infra-red DIC/epifluorescence optics using an Olympus BX51WI upright microscope and continuously perfused with oxygenated aCSF containing picrotoxin (50 μM) at 33-35 ºC.

Whole-cell recordings were obtained using an Axon Multiclamp 700B amplifier and a custom National Instruments data acquisition/analysis system. Patch-pipettes (resistance 3-5 MOhm) were filled with an internal recording solution containing 130mM K-methylsulphonate, 10mM KCl, 10mM HEPES, 0.1mM EGTA, 10mM glucose, 10mM Na-phosphocreatine, 4mM Mg-ATP, 0.5mM Mg-GTP, 5mM Alexa-555 disodium salt, (pH 7.3 with KOH; 290-300 mOsm). Neuron-like YFP-positive cells in layer II/III of the cortex were visually identified and once patched their identity was confirmed by dialysis with Alexa-555. Series resistance was monitored throughout each experiment; only experiments where series resistance was <25 MOhm and varied <15% were included for analysis.

2.9 DiI labelling

Use of the lipophilic dye 1,1'-dioctadecyl-3,3,3',3'-tetramethylindocarbocyanine (DiI) (Molecular Probes) has been described before (Voigt, 1989). I followed the procedure as described for labelling radial glia (Gotz et al., 1998) and deposited DiI crystals onto the pial surface of E11.5 embryos. The embryos were then incubated at 37^{o}C in PFA for 2 weeks before sectioning at 150μm.

2.10 Imaging

Images of *in situ* hybridisation and DAB staining were taken using a Leica microscope connected to a Leica DFC480 digital camera. Immunofluorescent sections were imaged either using a Leica microscope connected to a Leica DFC 360 FX digital camera or using Zeiss LSM 150 confocal system. Image processing and analysis was performed either in ImageJ (NIH), Adobe Photoshop (Adobe) or in MatlabR2009a (Mathworks).

2.11 Quantification

2.11.1 Analysis of *Foxg1^{cre}*-induced *Dicer1* mutants

To quantify the proportions of cleaved caspase-3 and phosphorylated histone 3 (pHH3) (Guo et al., 1995) immunopositive cells, 6µm paraffin sections from 3 *Dicer1$^{-/-}$* and 3 *Dicer1$^{+/-}$* E11.5 embryos were immunostained as described above. One section from rostral and one from central telencephalon were analysed in each brain for each antigen, along with an additional DAPI counterstained section. For every section a series of images was taken covering the entire dorso-ventral extent of the telencephalon at 40x magnification for each antigen and for DAPI-counterstained cell nuclei. Counting boxes (100µm wide, running through the entire depth of the telencephalic wall) were positioned along the dorso-ventral extent of the telencephalon at constant separation of 100µm and were aligned with their base along the ventricular edge. Tissue thickness was estimated to the nearest 12.5µm along the side of each counting box. For caspase-3, numbers of positive cells were counted through the depth of the telencephalic wall. To determine overall cell densities, counts of cell nuclei were averaged over three adjacent sections from either central or rostral telencephalon and divided by the average area of the counting boxes. For pHH3 immunopositive cells, I recorded the proportions of cells that were positive for pHH3 along the ventricular edge for each counting area.

To quantify the proportions of cells in *Dicer1*$^{+/-}$ and *Dicer1*$^{-/-}$ telencephalon that were double-positive for TuJ1 and either Tbr1, Reelin or Calretinin, or that were positive for Tbr2, a similar approach was taken to the quantification described above except that counting boxes of 50µm width were placed along the dorso-ventral extent of the tissue at constant 75µm separation.

2.11.2 Analysis of mosaic *Dicer1* mutants

2.11.2.1 Enumeration of dissociated cells

For dissociated cells, 50 images were taken of fields containing GFP –expressing cells from 5 coverslips. Areas were selected based only on the GFP staining so as to image as many cells as possible. Cells were then counted manually.

2.11.2.1 Quantification of embryonic brain sections

For embryonic sections, three non-adjacent coronal sections through central telencephalon were selected for quantification. Optical sections through the dorso-lateral telencephalon containing electroporated cells were acquired at constant separation and 3-4 optical sections through the centre of the section were summed using image processing software ImageJ. Counting ladders consisting of 200µm x 40µm boxes, 10 for E14.5 and 12 for E15.5 were positioned in Adobe Photoshop with the base along ventricular edge. The exceptions included counting cleaved caspase-3 positive cells, where only a single 300 µm box was used, spanning the thickness of dorsal telencephalic wall (E15.5) or of the cortical plate (E18.5). Between 7 and 12 embryos from three surgeries were analysed per genotype for each quantification.

2.11.2.2 Quantification of postnatal brain sections

For postnatal sections, brains of all surviving mice were sectioned and analysed for GFP expression. Only brains with GFP+ cells in the ventral auditory area were considered. Counting ladders consisting of 500µm x 100µm boxes were positioned with the base along the pial edge. Exception included the quantification of Sox9 positive cells where 300µm x 100µm boxes were used, Doublecortin (Dcx) positive cells where a single 400µm box was placed spanning the thickness of the cortical wall. Borders between cortical layers were established based on nuclear counterstaining with DAPI (Vector). Identification of the subventricular zone (SVZ) at P14 was based on density of cell nuclei and position of the lateral ventricle.

2.11.3 Image analysis

Image analysis including image intensity, area, cortical thickness or distance measurements were performed either in ImageJ or in MatlabR2009a (Mathworks).

2.10.4 Statistical analysis

Student's t-tests were performed using Microsoft Office Excel (Microsoft), Tukey's tests and three-way ANOVA were performed using either Sigmastat (Systat Software) or MatlabR2009a (Mathworks).

2.12 Support

In situ hybridisation staining for miR-124 of coronal sections through the *Foxg1^{cre}Dicer1$^{fl/fl}$* and *Foxg1^{cre}Dicer1$^{fl/+}$* mice was performed by an undergraduate student, Karolina Mysiak. In addition, Karolina sectioned some of the P14

electroporated cortices, performed immunohistochemical staining for cleaved-caspase 3, Cux1, Tbr1, Satb2 and Ctip2, took images and performed initial cell counts of marker expression. All electrophysiological recordings have been obtained by Timothy O'Leary.

CHAPTER 3:

Functional Dicer is necessary for appropriate specification of radial glia during early development of mouse telencephalon.

3.1 Introduction

The embryonic forebrain (prosencephalon) comprises the telencephalon, which generates the cerebral cortex and the basal ganglia, and the diencephalon, which generates the prethalamus and the thalamus. Just after closure of the neural tube, the telencephalon is a thin neuroepithelium surrounding the ventricles. Proliferation of neuroepithelial stem cells adjacent to the ventricles leads to the thickening of the telencephalon. Between embryonic day 9.5 (E9.5) and E10.5 in mouse, the neuroepithelial stem cells mature and elaborate their radial processes to become radial glia (Misson et al., 1988), which are the progenitor cells during subsequent neurogenesis. Radial glial cells generate neurons and intermediate (basal) progenitors (Guillemot, 2005); the latter divide away from the ventricular surface to generate neurons. Newly generated neurons migrate towards the pial surface along the processes of radial glia to form the postmitotic cell layer (Gotz, 1995; Hartfuss, 2001; Kriegstein, 2003; Malatesta et al., 2000).

Mouse Dicer is a type III endoribonuclease encoded by the *Dicer1* gene (Nicholson, 2002), which catalyzes the cleavage of double stranded RNA molecules (Du, 2008). Mature microRNAs (miRNAs) are 21-27nt products of Dicer activity (Filipowicz, 2005; Gan, 2006). They interact with complementary sequences on protein coding messenger RNA molecules (mRNAs), mainly in the 3' untranslated regions (Lewis, 2005; Xie, 2005). This interaction is recognised and sustained in the RNA-induced silencing complex (RISC) (Gregory, 2005; Gregory et al., 2004; Hutvagner, 2002) and regulates expression via transcript degradation by endoribonucleolytic cleavage, deadenylation and decapping, or translational inhibition (Hammond, 2000; Martinez et al., 2002). This process takes place in the processing (P-) bodies (Ding et al., 2005), which require RNA for assembly and can maintain mRNA in an untranslated state (Teixeira et al., 2005).

Mice null for *Dicer1* are not viable past E7.5 (Bernstein et al., 2003), indicating that the endogenous RNA interference pathway is critical for mammalian development. To bypass early embryonic lethality and investigate the role of miRNAs in

telencephalic development, three mouse mutant lines carrying conditional deletions of *Dicer1* in the forebrain have been thoroughly analysed. In these lines, expression of cre-recombinase is driven by *Emx1*, *Nes* or *Camk2* promoters (Davis et al., 2008; De Pietri Tonelli, 2008; Kawase-Koga et al., 2009). The overall conclusion from these studies is that cells primarily affected by loss of Dicer are postmitotic neurons. Migration of neuronal precursors to the postmitotic layers as well as their subsequent survival are compromised in the mutant tissue, whereas apical and basal progenitor cell populations are not affected detectably until later, after E14.5, when abnormally large proportions of them undergo apoptosis (De Pietri Tonelli, 2008; Kawase-Koga et al., 2009).

A number of studies have shown that miRNAs are involved in mouse embryonic stem cell proliferation and differentiation (Kanellopoulou, 2005; Murchison et al., 2005; Rybak et al., 2008). It remains possible that Dicer is required in the early telencephalic progenitor population *in vivo* and that previous experiments did not address this. One possibility is that Dicer is required by this population earlier than previously addressed; another is that it might be required in aspects of their biology, such as cell identity, that have not been examined before. To generate a very early deletion of *Dicer1* restricted mainly to the telencephalon I used a $Foxg1^{cre}$ allele (Figure 3.01 A). Foxg1 is expressed by all cells in the telencephalic anlage at the anterior end of the neural tube from before neural plate closure. $Foxg1^{cre}$ expresses cre in the telencephalic progenitors from around E8.0 (Hebert, 2000). I found that $Foxg1^{cre}$-induced ablation of *Dicer1* (Figure 3.01 B, C) results in abnormal protein expression by neural progenitor cells (radial glia) at E11.5 coinciding with the generation of the first postmitotic neurons. Both basal progenitors and postmitotic neurons, which are normally produced by the radial glia at E11.5, are misplaced through the depth of the telencephalic wall, yet their proportional contribution to the total number of cells in the tissue is not reduced.

Figure 3.01: Conditional ablation of Dicer using constitutive *Foxg1^{cre}* line. Mice expressing cre-recombinase under the regulation of the endogenous *Foxg1* promoter (A) were crossed to mice carrying the *Dicer1^{fl}* allele where exon 23 of the *Dicer1* coding sequence was flanked by two *LoxP* sites (B). Exon 23 encodes approximately 90 residues of the RNase IIIb domain of the Dicer protein (C) which are required for normal assembly of the active site. Although the catalytic Lysine K1790 is not encoded by exon 23, cre-LoxP mediated recombination is predicted to result in a truncated protein being produced.

FIGURE 3.01

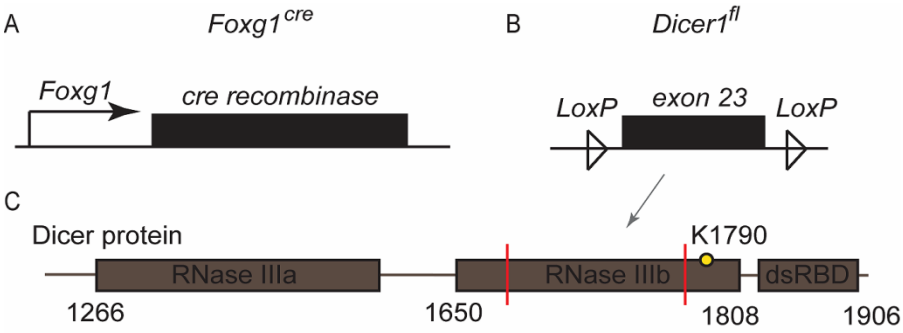
A
Foxg1cre
Foxg1
cre recombinase
B
Dicer1fl
LoxP
exon 23
LoxP
C
Dicer protein
K1790
RNase IIIa
RNase IIIb
dsRBD
1266
1650
1808
1906

3.2 Results

3.2.1 Effects of Dicer1-mutation on telencephalic miRNA levels

To confirm the anticipated effects of *Dicer1* deletion on mature miRNA production, I examined the expression of the two most abundant miRNAs in the E11.5 brain (Kloosterman, 2006; Landgraf, 2007): miR-124, whose expression is restricted to the post-mitotic neuronal population (De Pietri Tonelli, 2008; Maiorano, 2009) and miR-9, which is expressed in both the progenitor and postmitotic cells (Shibata et al., 2008). Whereas in the forebrain of control *Dicer1*$^{+/-}$ embryos mature miR-124 is detectable in the post-mitotic cell layer (Figure 3.02 A, B, C), in *Dicer1*$^{-/-}$embryos miR-124 expression is absent from the telencephalon and retained only in postmitotic cells in the hypothalamus, which expresses low levels of *Foxg1* (Figure 3.02 A', B').

In the forebrain of control embryos, mature miR-9 is present throughout the thickness of the dorsal telencephalic wall (Figure 3.02 C, G) and in the spinal cord at E11.5 (Figure 3.02 D - E) but was undetectable in the diencephalon (Figure 3.02 C, F). In the dorsal telencephalon of embryos with *Foxg1*-driven *Dicer1* deletion the level of mature miR-9 was depleted by E11.5 and was undetectable both in the cortex and in the diencephalon (Figure 3.02 C', F', G'). Mature miR-9 expression in spinal cord, where Foxg1 is not normally expressed, was unaffected in the *Dicer1*$^{-/-}$ embryos (Figure 3.02 D', E').

These results indicate that *Dicer1*$^{-/-}$ embryos show a telencephalon-specific depletion of miRNAs by E11.5.

3.2.2 Dicer-deficient neuroepithelial stem cells maintain their cell identity

To analyse the molecular identities of early telencephalic progenitors, the expression of markers of neuroepithelial stem cells as well as the expression of markers of radial glia was examined. Coronal E11.5 telencephalic sections were immunostained to detect the presence of four proteins normally expressed in the most undifferentiated neuroepithelial progenitors: stem cell marker CD133 (Prominin1); Notch signalling inhibitor Numb; Numb inhibitor Musashi; and Sox2 (sex determining region Y box 2) (Collignon, 1996; Sakakibara, 1996; Uchida, 2000; Wegner, 1999; Zhong, 2000). The vast majority of cells in the E11.5 control telencephalon are immunoreactive for CD133, Musashi, Sox2, and Numb. In *Dicer1*$^{-/-}$ telencephalon, expression of CD133, Musashi, Sox2 and Numb appeared similar to that in controls (Figure 3.03 A-D, A'-D'). To assess the mitotic activity of the progenitor cells, the average proportion of phosphorylated histone-3 (pHH_3) immunoreactive cells directly lining the ventricular surface at E11.5 was quantified. In control embryos, an average of 25.7±6.7 (mean ± s.e.m.) % of cells in the dorsal telencephalon and 25.6±5.5 % of cells in the ventral telencephalon were pHH_3 immunopositive. In *Dicer1*$^{-/-}$ embryos these values were not significantly different with 28.3±2.8 % of cells in the dorsal telencephalon ($p>0.05$, $n=3$) and 26.2±2.1 % of cells in the ventral telencephalon ($p>0.05$, $n=3$) immunopositive for pHH_3 (Figure 3.04). Furthermore, expression of genes involved in forebrain patterning was investigated and no alterations were detected in the dorso-ventral extent of the expression domains of the following transcription factors at E11.5: the pan-telencephalic marker Foxg1 (Figure 3.03 G, G') (Tao, 1992), dorsal telencephalic markers Pax6 (Figure 3.03 H, H') (Stoykova et al., 1996), Emx2 (Figure 3.03 I, I') (Yoshida et al., 1997) and Ngn2 (Figure 3.03 J, J') (Hartfuss et al., 2001) or ventral telencephalic markers Olig2 (Figure 3.03 K, K') (Gotz et al., 1998; Rubenstein and Puelles, 1994) and Dlx2 (Figure 3.03 L, L') (Rubenstein and Puelles, 1994). Overall, these results indicate that many aspects of neuroepithelial stem cell identity are not affected by the loss of Dicer.

Figure 3.02: Loss of mature miR-124 and miR-9 in the telencephalon of *Dicer1*$^{-/-}$ embryos. Two most abundant brain miRNAs, miR-124 and miR-9 were detected using LNA *in situ* hybridisation. At E11.5, mature miR-124 is expressed in the postmitotic layers (A, B). Mature miR-124 was not detected in *Dicer1*$^{-/-}$ telencephalon but its expression was maintained in hypothalamus (A', B'). In control embryos at E11.5, miR-9 is strongly expressed throughout the thickness of the dorsal telencephalon (C) and the spinal cord (D). High power images of the staining in the spinal cord (E), the diencephalon, which is devoid of mature miR-9 (F) and the dorsal telencephalon (G). Mature miR-9 was depleted from the dorsal telencephalon by E11.5 (C', G'). Expression of mature miR-9 in the spinal cord of the *Dicer1*$^{-/-}$ embryos was not altered (D', E'). High magnification image of the diencephalon (F') is included as a negative control. Abbreviations: dTel: dorsal telencephalon, vTel: ventral telencephalon, hTh: hypothalamus. Scale bar: (A, A') - 200µm, (B, B', E, E', F, F', G, G') - 50µm, (C, C', D, D') - 100 µm.

FIGURE 3.02

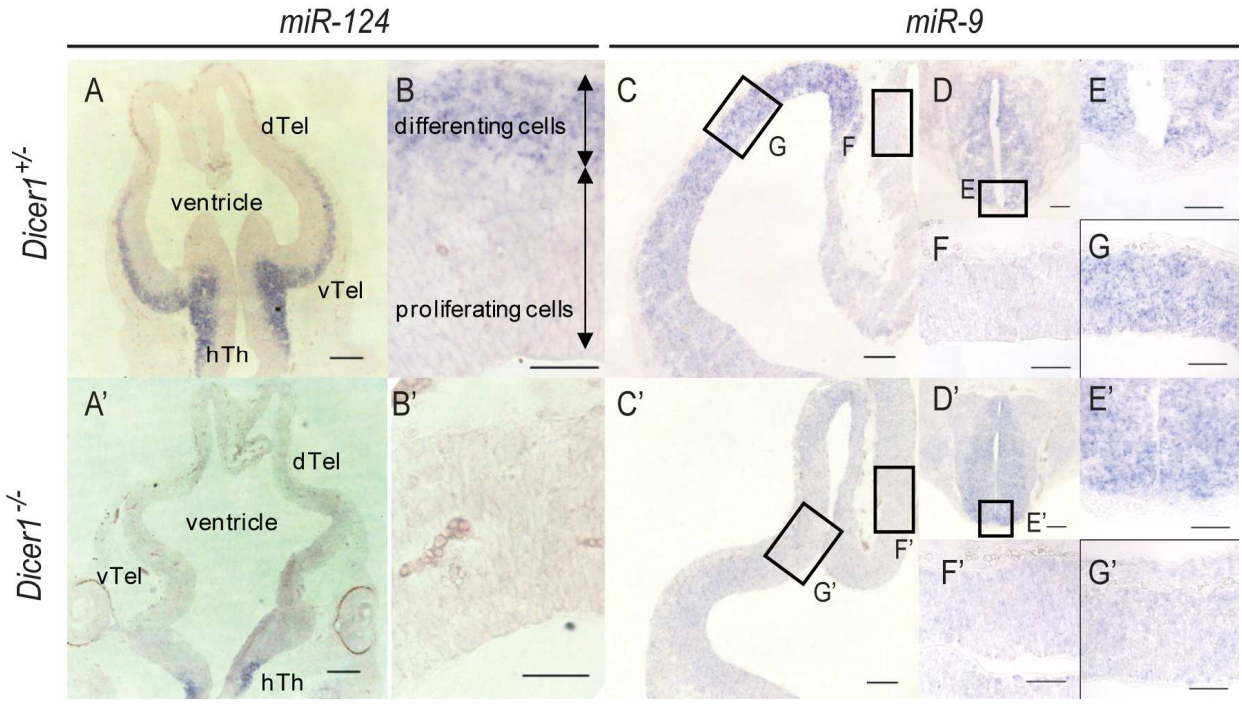
miR-124
miR-9
Dicer1+/-
Dicer1-/-
A
dTel
ventricle
vTel
hTh
B
differenting cells
proliferating cells
C
G
F
D
E
F
G
A'
dTel
ventricle
vTel
hTh
B'
C'
G'
F'
D'
E'
F'
G'

Figure 3.03: Expression of markers of neuroepithelial stem cells is normal in *Dicer1*$^{-/-}$ telencephalon. In panels A-E and A'-E' tissue orientation is ventricular surface: bottom, pia: top of the image. CD133/Prominin1 is expressed by the neuroepithelial stem cells of control (A) and *Dicer1*$^{-/-}$ telencephalon (A'). Expression of Numb inhibitor Musashi required to maintain proliferation is unchanged in *Dicer1*$^{-/-}$ telencephalon (B') compared to control (B). Sox B group member Sox2 is expressed by the proliferative neuroepithelium (C) and its expression appears normal following the loss of functional Dicer (C'). Numb protein is expressed both in the proliferative and differentiated cells layer (D) and its expression is maintained in *Dicer1*$^{-/-}$ telencephalon (D'). Radial processes were labelled using the lipophilic dye DiI to show gross morphology of the radial glia in control (E) and *Dicer1*$^{-/-}$ dorsal telencephalon (E') and that it is unchanged following the mutation. Enriched β-catenin immunostaining at the ventricular surface of the control telencephalon (F) was also unaffected by the loss of functional Dicer (F'). A normal pattern of *Foxg1* expression was obtained using RNA *in situ* hybridisation in control telencephalon (G) and *Dicer1*$^{-/-}$ telencephalon (G'). Pax6 is commonly used as a marker of dorsal telencephalon, expressed in a dorso-medial (low) to lateral (high) gradient and the protein expression was detected using immunohistochemical staining of control tissue (H) and its expression was not different in *Dicer1*$^{-/-}$ telencephalon (H'). Emx2 is expressed in a gradient complementary to Pax6 and *Emx2* mRNA expression was analysed using RNA *in situ* hybridisation in control (I) and *Dicer1*$^{-/-}$ telencephalon (I'). Analysis of Ngn2 mRNA revealed the normal salt-and-pepper expression in the dorsal telencephalon as well as eminentia thalami in both control (J) and *Dicer1*$^{-/-}$ tissue (J'). Doso-ventral extent of ventral telencephalic marker Olig2 expression was similar in control (K) and *Dicer1*$^{-/-}$ tissue (K'). A normal pattern of expression of another ventral telencephalic marker, Dlx2, was observed both in control (L) and *Dicer1*$^{-/-}$ tissue (L'). Abbreviations: Di: Diencephalon, ne: nasal epithelium. Scale bar: (A) – (F') - 50µm, (G) – (L') - 100 µm.

FIGURE 3.03

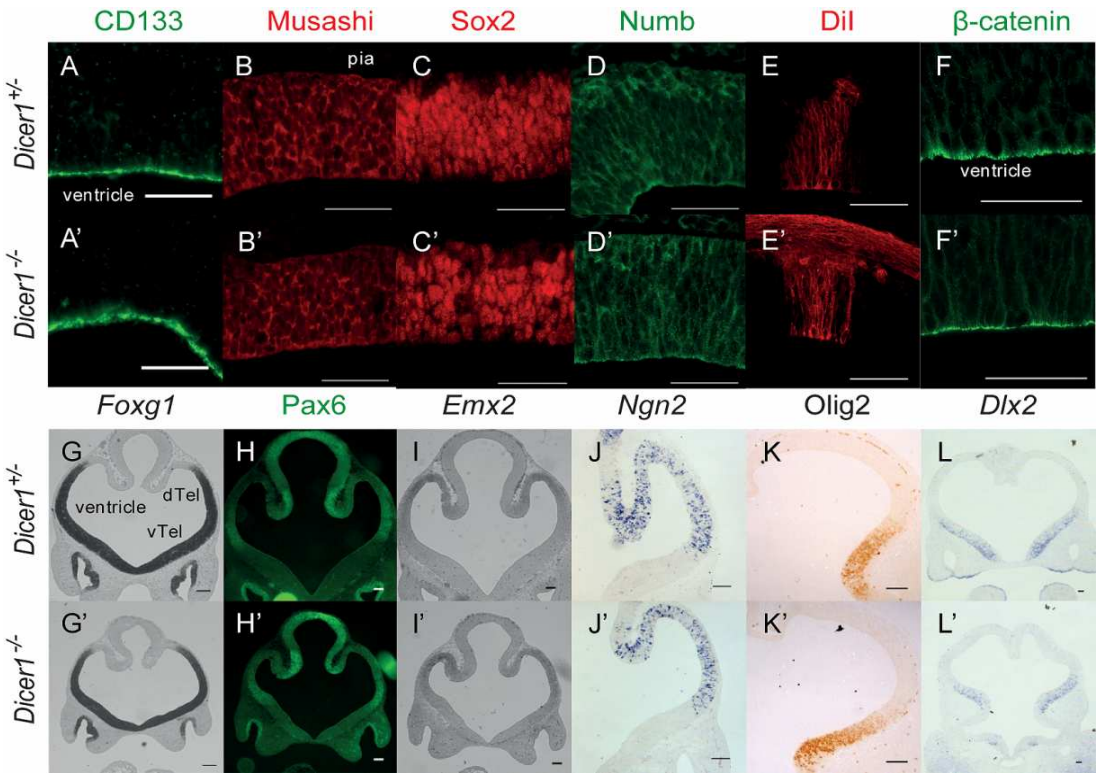
CD133
Musashi
Sox2
Numb
Dil
β-catenin
Dicer1+/-
Dicer1-/-
A
B
pia
C
D
E
F
ventricle
A'
B'
C'
D'
E'
F'
Foxg1
Pax6
Emx2
Ngn2
Olig2
Dlx2
G
H
I
J
K
L
ventricle
dTel
vTel
G'
H'
I'
J'
K'
L'

Figure 3.04: Proportion of mitotic cells remains unaltered after the loss of functional Dicer. Immunohistochemical staining using an antibody against phosphorylated (ser10) Histone 3 (pHH3) reveals that at E11.5 most immunoreactive cells are located directly at the ventricular surface (A) and loss of functional Dicer did not cause this pattern to be disrupted (A'). Quantification did not reveal any changes in the proportion of mitotic cells in either dorsal or ventral telencephalon (B). Scale bar: 50μm, error bars indicate s.e.m.

FIGURE 3.04

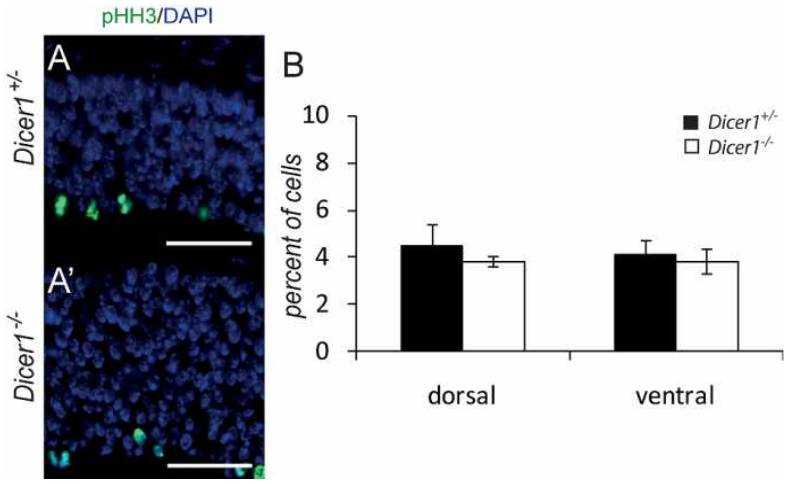
pHH3/DAPI
A
A'
Dicer1+/-
Dicer1-/-
B
percent of cells
10
8
6
4
2
0
Dicer1+/-
Dicer1-/-
dorsal
ventral

3.2.3 Radial progenitors are defective in the expression of Nestin

Around E10, the neuroepithelial stem cells generate the neurogenic progenitors, radial glia. This transformation includes elaboration of the radial processes that run between the pial and ventricular surfaces of the telencephalic wall (Misson et al., 1988). The radial processes were labelled using DiI placed on the pial surface at E11.5 and no difference was found between radial processes in *Dicer1*$^{-/-}$ and in control (*Dicer1*$^{+/-}$) tissue (Figure 3.03 E, E'). Previous experiments in which the radial processes of the telencephalic progenitor cells were disrupted showed alterations in the expression pattern of proteins which play a role in cell adhesion at the apical surface of the telencephalon, such as β-catenin (Weimer, 2009). I performed immunostaining for β-catenin and found no difference between *Dicer1*$^{-/-}$ and control tissue (Figure 3.03 F, F').

Nestin is a type IV intermediate filament protein expressed in neural progenitor cells. Two commonly used antibodies against Nestin, the Rat-401 and RC2 clones, recognise its two different isoforms whose expression is largely, but not entirely identical (Lendahl et al., 1990; Park et al., 2009). Staining using the RC2 antibody was used as the defining criterion of radial glial identity (Misson et al., 1988). Progenitors at the neuroepithelial stem cell stage (E10.25) express Nestin mainly at the pial end-feet of the radial processes both in control (Figure 3.05 A, D, arrows) and *Dicer1*$^{-/-}$ telencephalon (Figure 3.05 A', D'). By E11.5 the expression of Nestin is strongly enhanced throughout the radial processes of the progenitor cells (Figure 3.05 B, E). In the *Dicer1*$^{-/-}$ telencephalon, expression of both isoforms is lower compared to control levels (Figure 3.05 B', E').

To quantify the abnormality at E11.5, sections from 4 control and 3 *Dicer1*$^{-/-}$ embryos were immunofluorescently labelled simultaneously using identical conditions with Rat-401 or RC2 antibodies. Fluorescence image intensity was recorded from 50µm x 50µm areas ('boxes') placed at 300µm separation along the dorso-ventral extent of the telencephalon. The boxes were positioned adjacent to the

ventricular edge (Figure 3.05 C, F, box '1') as well as adjacent to the pial membrane (Figure 3.05 C, F, box '2'). Intensity recorded from an identical box was placed on an image of the spinal cord from the same section (150µm ventral to the roof plate, adjacent to the central canal) was used for normalisation. For each control and *Dicer1*$^{-/-}$ section analysed, average intensities per pixel from the series of boxes '1' and boxes '2' along the dorso-ventral extent of the telencephalon were normalised to those from the spinal cord in the same section since, as described above, the spinal cord was unaffected by the mutation (this corrects for any residual variation in staining for technical reasons between different sections). Both RC2 and Rat-401 immunostaining intensities were significantly lower in the *Dicer1*$^{-/-}$ than in the control telencephalon; in the pial region the differences were not significant (Figure 3.05 C, F). In controls, immunofluorescence intensities for both Nestin isofoms became significantly higher in the ventricular region than in the pial region (Figure 3.05 C,F), which was a reversal of the pattern in both control and *Dicer*$^{-/-}$ telencephalon at E10.25; this did not occur in *Dicer*$^{-/-}$ telencephalon. Taken together, my results indicate that loss of Dicer from the telencephalon inhibits the normal enrichment of Nestin protein in the ventricular region by E11.5.

To test if this difference could be caused by different overall cell density in *Dicer1*$^{-/-}$ tissue compared to control, densities of DAPI-stained cells in dorsal and ventral telencephalic regions were quantified. I found that in control embryos average density in the dorsal telencephalon is $22\pm4*10^3$ cells/mm^2 and $29\pm6*10^3$ cells/mm^2 in the ventral telencephalon. These values are not significantly different in *Dicer1*$^{-/-}$ embryos with $20\pm5*10^3$ cells/mm^2 in the dorsal telencephalon ($p>0.05$, $n=3$) and $24\pm6*10^3$ cells/mm^2 in the ventral telencephalon ($p>0.05$, $n=3$).

Figure 3.05: Expression of Nestin, Sox9 and ErbB2 is compromised in Dicer deficient telencephalon. The RC2 antigen is encoded by the *Nes* gene and is expressed in the basal end-feet of the radial processes of the neuroepithelial progenitor cells at E10.25 (A). In mutant tissue this pattern of expression was maintained (A'). Around the onset of neurogenesis when neuroepithelial stem cells give rise to radial glia, RC2 expression becomes elaborated by E11.5 (B). This expansion was compromised in the *Dicer1*$^{-/-}$ telencephalon (B'). Quantification of immunofluorescence intensity for RC2 antigen in ventricular and pial regions of the control (open bars) and *Dicer1*$^{-/-}$ telencephalon (filled bars) revealed significant reduction of the immunostaining in the ventricular region. Similarly to RC2, the Rat-401 is also encoded by the *Nes* gene and its expression follows the pattern of RC2 expression in the radial processes end feet at E10.25 (D) and its expression also becomes expanded by E11.5 (E). In the *Dicer1*$^{-/-}$ telencephalon, the Rat-401 expression is present in the end feet of the radial processes (D') but is reduced compared to control at E11.5 (E'). Quantification of immunofluorescence intensity revealed a significant reduction in the *Dicer1*$^{-/-}$ telencephalon in the ventricular region (F). Sox9 transcription factor expression is present in the vast majority of proliferative cells in the dorsal telencephalon at E10.25 (G) and E11.5 (H). In *Dicer1*$^{-/-}$ dorsal telencephalon only few cells are immunoreactive for Sox9 (H'). ErbB2 is a receptor for Neuregulin1 and expressed strongly in proliferative cells in control telencephalon as well as the pia (I). In *Dicer1*$^{-/-}$ telencephalon the ErbB2 mRNA *in situ* hybridisation staining was strong in the pia, but faint in the proliferative cells (I'). Expression levels of ErbB2 mRNA were quantified as described in Results standardising the levels staining both in pial and ventricular regions to the level of staining in the pia to show a significant reduction of staining in the ventricular region (J). Scale bar: 50µm, *$p<0.05$, **$p<0.01$, ***$p<0.001$, error bars indicate s.e.m.

FIGURE 3.05

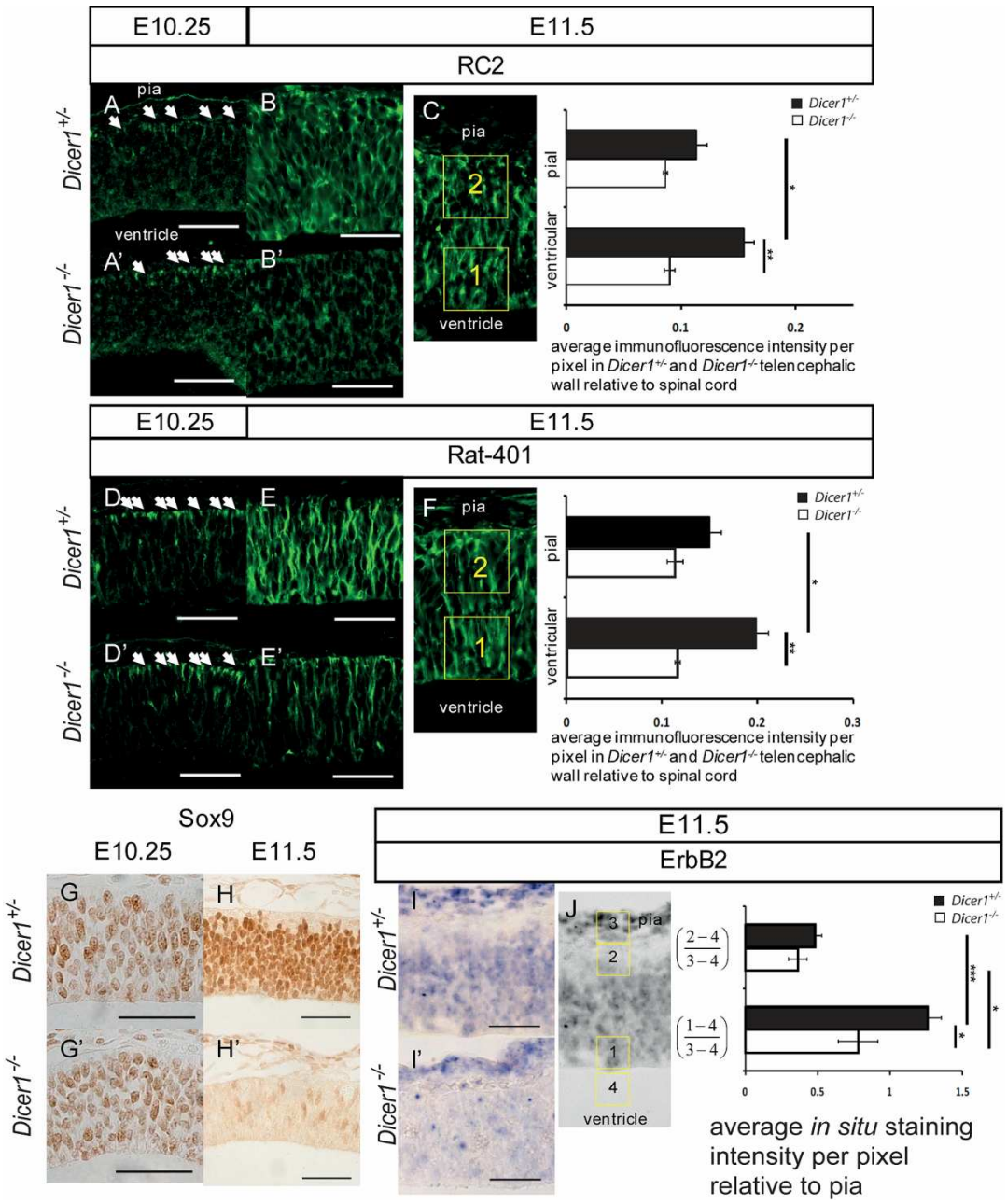
E10.25
E11.5
RC2
pia
ventricle
Dicer1+/-
Dicer1-/-
pial
ventricular
average immunofluorescence intensity per pixel in Dicer1+/- and Dicer1-/- telencephalic wall relative to spinal cord
Rat-401
Sox9
E10.25
E11.5
ErbB2
average in situ staining intensity per pixel relative to pia

3.2.4 Dicer deficient progenitors lose expression of transcription factor Sox9 and the ErbB2 receptor

Previous studies using non-neural tissues identified the transcription factor Sox9 as a co-enhancer for the expression of *Nes* gene (Flammiger et al., 2009). Immunohistochemical staining of the telencephalon around E10.25 and E11.5 reveals that while in control tissue virtually all progenitor cells are stained using the antibody against Sox9 transcription factor at both ages (Figure 3.05 G, H), in *Dicer1*$^{-/-}$ dorsal telencephalon the expression is present at E10.25 (Figure 3.05 G') and almost completely absent at E11.5 (Figure 3.05 H').

The ErbB2 receptor has been implicated in radial glia formation by mediating Neuregulin1 signalling that leads to RC2 expression (Schmid et al., 2003). *In situ* hybridisation for ErbB2 mRNA in control dorsal and ventral telencephalon shows ErbB2 is normally expressed throughout the progenitor layer and in the pia overlying the neuroepithelium (Figure 3.05 I). In *Dicer1*$^{-/-}$ tissue the ErbB2 mRNA is present in the pia but strongly reduced in the progenitor layer (Figure 3.05 I'). To quantify this observation for control (n=4) and *Dicer1*$^{-/-}$ (n=3) sections, I used a densitometric method as described above with minor modifications. A series of 30µm x 30µm boxes were placed over the telencephalic tissue adjacent to the ventricular edge (Figure 3.05 J, box '1'), adjacent to the pial edge in the differentiating preplate (Figure 3.05 J, box '2') and over the pia for normalisation (Figure 3.05 J, box '3'). A reading from a box placed over the ventricle was used to measure background (Figure 3 J, box '4') which was subtracted from values in the boxes above it. Values from box '1' (ventricular region) and box '2' (preplate region) were normalised against the corresponding value for the pia (box '3'). In both control tissue and *Dicer1*$^{-/-}$ tissue, average intensity in the ventricular region is significantly higher than that in the preplate region. The average intensity in the ventricular region is, however, significantly lower in the *Dicer1*$^{-/-}$ than in control telencephalon (Figure

3.05 J). This indicates that ErbB2 expression is significantly reduced in the ventricular zone in *Dicer1*$^{-/-}$ telencephalon.

I also examined expression of some of these markers at a later age. At E12.5 in control telencephalon, the expression pattern of Sox9 largely overlaps that of Sox2 in the progenitor cell layer (Figure 3.06 A-F). In *Dicer1*$^{-/-}$ tissue the size of the Sox2 expression domain is markedly reduced, yet the remaining cells retain intense immunofluorescent labelling (Figure 3.06 A'-C') while the expression of Sox9 is largely absent (Figure 3.06 D'-F'). The size of the TuJ1-marked population of postmitotic cells is also greatly reduced in the E12.5 *Dicer1*$^{-/-}$ telencephalon (Figure 3.06 A'-C') compared to control telencephalon (Figure 3.06 A-C). The radial glial fibre expression of Nestin (Rat-401) is also greatly reduced in the E12.5 *Dicer1*$^{-/-}$ telencephalon (Figure 3.06 D'-F') in comparison with abundant labelling in control tissue (Figure 3.06 D-F). These data are consistent with the observations from E11.5 embryos, showing a selective reduction in the expression of radial glial markers, including Sox9 and Rat-401. Together, these findings indicate that the loss of functional Dicer causes persistent incorrect specification of radial glia.

Figure 3.06: Dicer deficient telencephalon is severely disrupted by E12.5. Immunohistochemical staining for TuJ1 marks the postmitotic neurons in the telencephalon (A, C). This population is greatly reduced in *Dicer1*$^{-/-}$ telencephalon (A', C'). Sox2 marks the proliferative population (B, C), which is also diminished in the *Dicer1*$^{-/-}$ tissue (Figure S2 B', C'). At E12.5 radial glia express Rat-401 (D, F) as well as Sox9 (E, F) and in the *Dicer1*$^{-/-}$ telencephalon only a small fraction of radial processes can be detected (D', F') and the expression of Sox9 is greatly reduced (E', F'). Scale bar: 100µm.

FIGURE 3.06

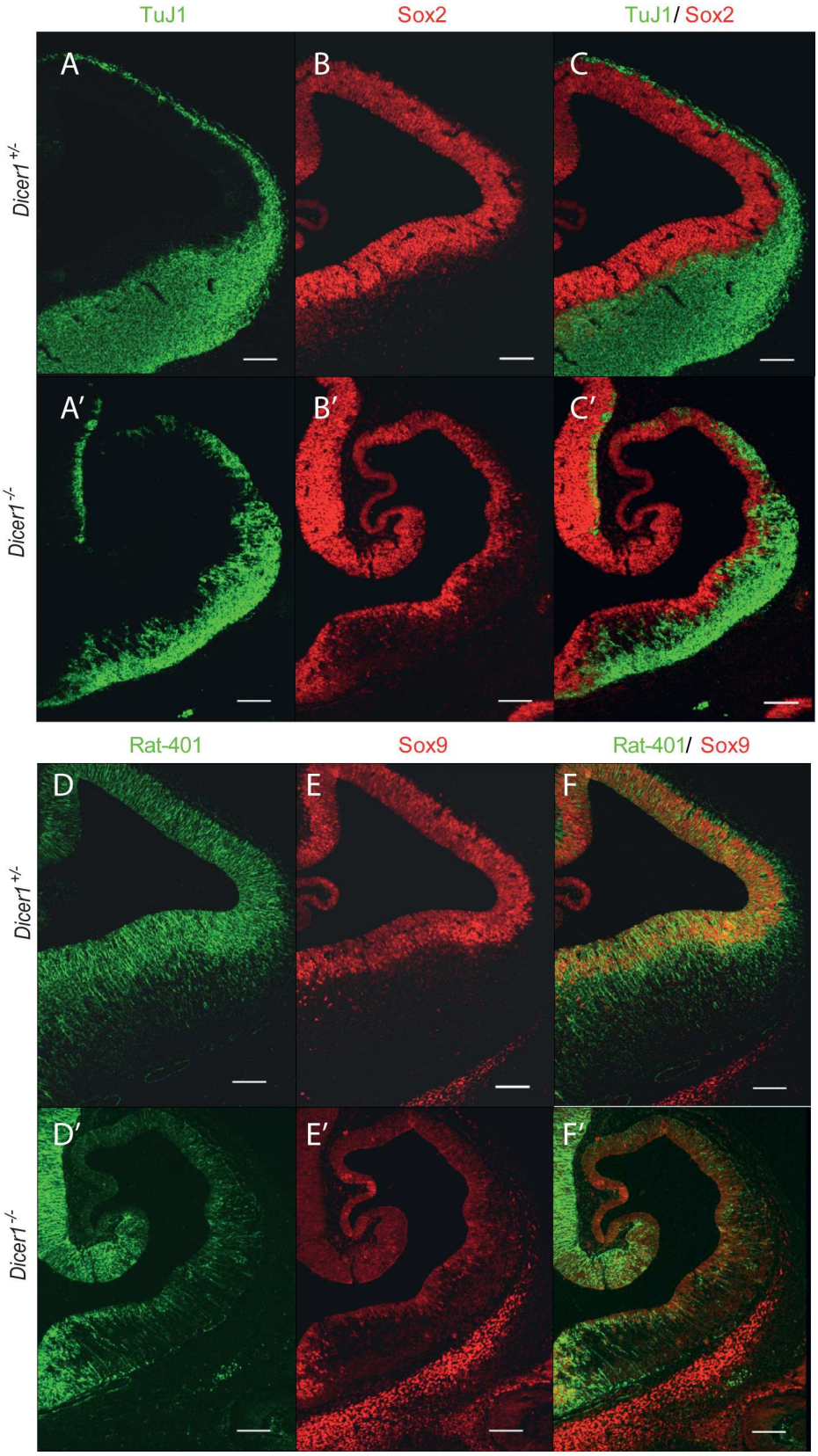
TuJ1
Sox2
TuJ1/ Sox2
A
B
C
Dicer1 +/-
A′
B′
C′
Dicer1 -/-
Rat-401
Sox9
Rat-401/ Sox9
D
E
F
Dicer1 +/-
D′
E′
F′
Dicer1 -/-

3.2.5 Loss of functional Dicer results in the expansion of basal progenitor population and misplacement of postmitotic neurons

Radial glia are progenitor cells and during normal development begin to generate postmitotic neurons as well as intermediate (basal) progenitor cells around E11.5. They also guide the radial migration of neuronal progeny to generate cortical layers (Malatesta et al., 2000; Noctor et al., 2001) and disruption of radial glia results in mislocalised neurons (Hasling et al., 2003). Previous studies identified defects in the capacity of Dicer deficient stem cells to differentiate (Kanellopoulou, 2005; Murchison et al., 2005). I anticipated that disruption of radial glia at E11.5 in *Dicer1*$^{-/-}$ telencephalon could cause defects in the capacity of these progenitors to generate postmitotic neurons and/or guide migration normally.

To address this hypothesis I looked at the pattern of expression of markers of early-born neurons, mRNA binding protein HuC/D and type III beta tubulin (TuJ1). In control telencephalon at E11.5 cells immunoreactive for HuC/D (Figure 3.07 A) or TuJ1 (Figure 3.07 B) were located beneath the pial membrane forming a coherent layer. In *Dicer1*$^{-/-}$ tissue the TuJ1 and HuC/D immunostaining revealed a pattern that was discontinuous with numerous gaps of staining beneath the pial membrane (Figure 3.07 A', B', arrows). In addition, a number of neurons were misplaced through the depth of the telencephalic wall. The overall proportions of TuJ1^{+} cells in the *Dicer1*$^{-/-}$ telencephalon (15.6±1.7%) and the control telencephalon (19.1±1.5%), irrespective of their location, were not significantly altered (Student's t-test, $p>0.05$, embryos n=9). These findings indicate that early telencephalic progenitors generate correct proportions of neurons after Dicer deletion, but many of those neurons migrate abnormally.

To test if loss of functional Dicer compromises the ability of early postmitotic neurons to complete differentiation, I quantified the proportion of TuJ1 neurons that also express a marker of more mature postmitotic neurons, Tbr1 (Englund et al., 2005). I found that about half of the TuJ1 immunopositive cells express Tbr1 both in control and *Dicer1*$^{-/-}$ telencephalon (Figure 3.07 C). In addition, I counted the proportions of cells (visualised with DAPI) that were Tbr1 positive along the dorso-ventral extent of the telencephalon (for counting strategy see Materials and Methods

as well as Figure 3.07 D). I found no difference between control and *Dicer1*$^{-/-}$ telencephalon (Figure 3.07 D, two way ANOVA, $p>0.05$, n=9).

One possible explanation for misplacement of postmitotic neurons could be a loss of Cajal Retzius cells (Schaefer, 2008). During forebrain development the Cajal-Retzius neurons in the telencephalon have been shown to originate from progenitors located in the ventricular zone of the telencephalon as well as other regions of the brain (Bielle et al., 2005). The misplacement of neurons in *Dicer1*$^{-/-}$ telencephalon might result from an absence of Cajal-Retzius cells. To test this, I quantified the proportion of TuJ1- positive cells double-positive for either Reelin or Calretinin, both of which mark the Cajal-Retzius neurons at E11.5 (Alcantara, 1998; Hevner et al., 2003). I found no difference in the proportion of TuJ1 positive cells that expressed Reelin between genotypes; the proportion of TuJ1 positive cells that co-expressed Calretinin was actually significantly increased in *Dicer1*$^{-/-}$ telencephalon compared to control (Figure 3.07 E, $p<10^{-5}$, n=9). I conclude that there is no evidence to suggest that misplaced neurons could be accounted for by a depletion of Cajal-Retzius cells from *Dicer1*$^{-/-}$ telencephalon.

Using double immunohistochemistry for Reelin and Calretinin (Figure 3.07 F, F') I found that the proportion of Reelin positive neurons that co-expressed Calretinin in *Dicer1*$^{-/-}$ telencephalon (58.6±5.3%) and control tissue (53±4.2%) were not significantly altered (Student's t-test $p>0.05$, n=9). This indicates that the subpopulation of TuJ1 neurons that is expanded in *Dicer1*$^{-/-}$ tissue expresses Calretinin but not Reelin.

Figure 3.07: Neurons and basal progenitors generated by radial precursors are affected by the loss of Dicer. HuC/D is normally expressed in early postmitotic neurons and immunostaining for HuC/D is enriched in the postmitotic layer forming a coherent staining beneath the pia (A). In *Dicer1*$^{-/-}$ telencephalon HuC/D expressing cells are misplaced through the thickness of the telencephalic wall and the staining in the layer beneath the pia is discontinuous with numerous gaps lacking staining beneath the pial membrane (A', arrows). Similarly, TuJ1 is expressed by early postmitotic neurons (B). In Dicer deficient telencephalon, TuJ1 immunoreactive cells are scattered through the depth of the neuroepithelium (B'). Tbr1 is expressed by differentiated neurons at E11.5 and labels about half of the TuJ1 positive cells in control and *Dicer1*$^{-/-}$ telencephalon (C). Quantification of the distribution of Tbr1 immunopositive cells as a proportion of total number of cells along the dorso-ventral extent of its expression domain revealed that differentiation of postmitotic neurons was not affected anywhere in the telencephalon by E11.5 following the loss of Dicer (D). Calretinin and Reelin are markers of Cajal-Retzius cells, which are involved in the regulation of radial migration of postmitotic neurons to the postmitotic layer. Quantification revealed a significant increase in the proportion of TuJ1 cells that were Calretinin double-positive in *Dicer1*$^{-/-}$ telencephalon compared to control whilst the proportion of TuJ1 cells that were Reelin double-positive was unaltered by the loss of functional Dicer (E). Expression of Reelin and Calretinin is not overlapping in all cells (F, F'). Tbr2 is expressed by the basal progenitors in control telencephalon (G). In *Dicer1*$^{-/-}$ telencephalon Tbr2 immunoreactive cells are misplaced through the depth of the telencephalic wall (G') and their proportion was increased compared to control tissue (H). Dashed lines outline the ventricular and pial edges of the telencephalic wall. Scale bar: 50μm. *$p<0.05$, ****$p<10^{-5}$ error bars indicate s.e.m.

FIGURE 3.07

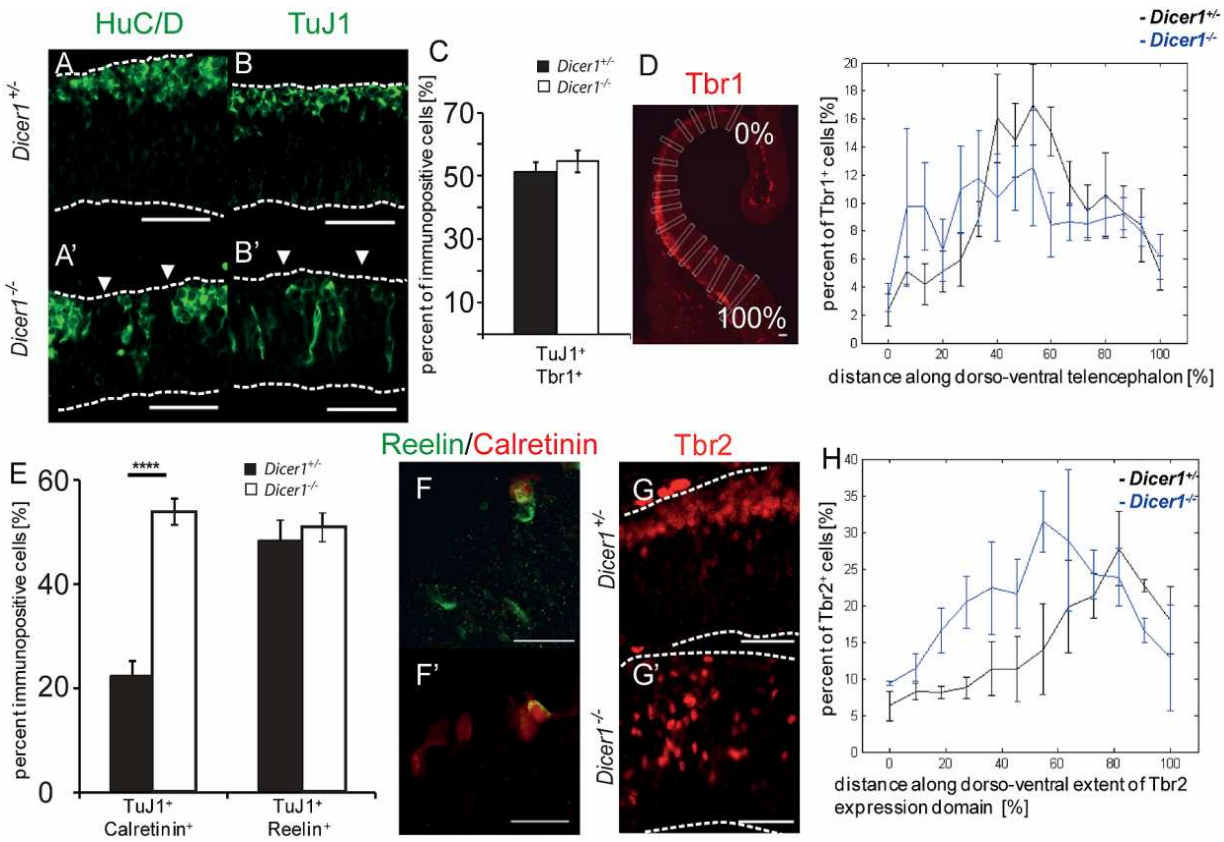
HuC/D
TuJ1
A
B
A'
B'
Dicer1+/-
Dicer1-/-
C
Dicer1+/-
Dicer1-/-
percent of immunopositive cells [%]
70
50
30
10
TuJ1+
Tbr1+
D
Tbr1
0%
100%
- Dicer1+/-
- Dicer1-/-
percent of Tbr1+ cells [%]
distance along dorso-ventral telencephalon [%]
E
****
percent immunopositive cells [%]
60
40
20
0
TuJ1+
Calretinin+
TuJ1+
Reelin+
Reelin/Calretinin
F
F'
Tbr2
G
G'
H
percent of Tbr2+ cells [%]
distance along dorso-ventral extent of Tbr2 expression domain [%]

Beside neurons, radial glia generate basal progenitors. During early telencephalic development, around E11.5 – E12.5 the transcription factor Tbr2 (Eomesodermin) is expressed by the basal progenitors and a small subset of Tbr1 positive postmitotic neurons in the dorsal telencephalon (Englund et al., 2005) (Figure 3.07 G). In *Dicer1*$^{-/-}$ tissue Tbr2 positive cells are scattered through the depth of telencephalic wall (Figure 3.07 G'), reflecting the migration defect described above. The proportion of telencephalic cells expressing Tbr2 along the dorso-ventral extent of its expression domain was quantified (see Materials and Methods) and it was found that the proportion was increased above control levels in all but the most ventral part of the *Dicer1*$^{-/-}$ dorsal telencephalon (Figure 3.07 H, two way ANOVA, $p<0.01$, n=3).

3.2.6 The proportion of apoptotic cells is increased at E11.5

Several studies have indicated that cell survival is compromised following the loss of Dicer in the telencephalon (Davis et al., 2008; De Pietri Tonelli, 2008; Kawase-Koga et al., 2010; Kawase-Koga et al., 2009; Makeyev et al., 2007). I immunostained control and *Dicer1*$^{-/-}$ telencephalon at E10.25 and at E11.5 with an antibody against cleaved caspase 3 and quantified the proportion of apoptotic cells in the telencephalon (Figure 3.08 A). While the proportion of cleaved caspase 3 positive cells is not significantly different between genotypes (n=3) at E10.25 (Figure 3.08 B, B'), at E11.5 it is significantly increased ($p<0.01$, n=3) in *Dicer1*$^{-/-}$ telencephalon compared to control tissue with immunoreactive cells scattered throughout the depth of the telencephalic wall (Figure 3.08 C, C').

I then investigated whether apoptosis could have influenced tissue development by E11.5. The average thickness of the dorsal telencephalic wall in control embryos is 90±5 (s.e.m.) µm and in ventral telencephalon 145±15 µm. These values are not significantly different in the *Dicer1*$^{-/-}$ embryos where average thicknesses of the dorsal and ventral telencephalic wall are 80±5 µm ($p>0.05$, n=3) and 130±20 µm ($p>0.05$, n=3). As described above, cell density is not different between genotypes. These data indicate that E11.5 is the first stage when apoptosis becomes significant and that prior to E11.5 cell death has not significantly affected the development of the telencephalon.

By E12.5, the proportion of apoptotic cells increased in the *Dicer1*$^{-/-}$ telencephalon (Figure 3.08 A, D'). The average thicknesses of the dorsal and ventral telencephalic wall in *Dicer1*$^{-/-}$ embryos were 85±4 µm and 136±12 µm respectively, significantly lower than in control tissue, which had corresponding values of 170±8 µm ($p<0.001$, $n=3$) and 286±32 µm ($p<0.01$, $n=3$). By E14.5, the size of the telencephalon is greatly reduced (Figure 3.09 B) compared to controls (Figure 3.09 A), presumably resulting from escalating cell death after E12.5.

Figure 3.08: E11.5 is the first embryonic day when apoptosis becomes significant. (A) Percent of cells in the telencephalon of control (open bars) and *Dicer1*$^{-/-}$ telencephalon was quantified at E10.25, E11.5 and E12.5 to show that E11.5 is the first stage at which a significantly higher number of cleaved caspase-3 immunopositive cells due to the loss of functional Dicer is detectable. Immunohistochemical staining of control tissue reveals only a small proportion of cells stain for cleaved caspase-3 in either E10.25 (B), E11.5 (C) or E12.5 (D) control telencephalon, as well as E10.25 *Dicer1*$^{-/-}$ telencephalon (B'). E11.5 is the first stage when significant levels of apoptosis are observed (C') and they are further exacerbated by E12.5 (D'). Scale bar: 50μm, **p<0.01, ***p<0.001 error bars indicate s.e.m.

FIGURE 3.08

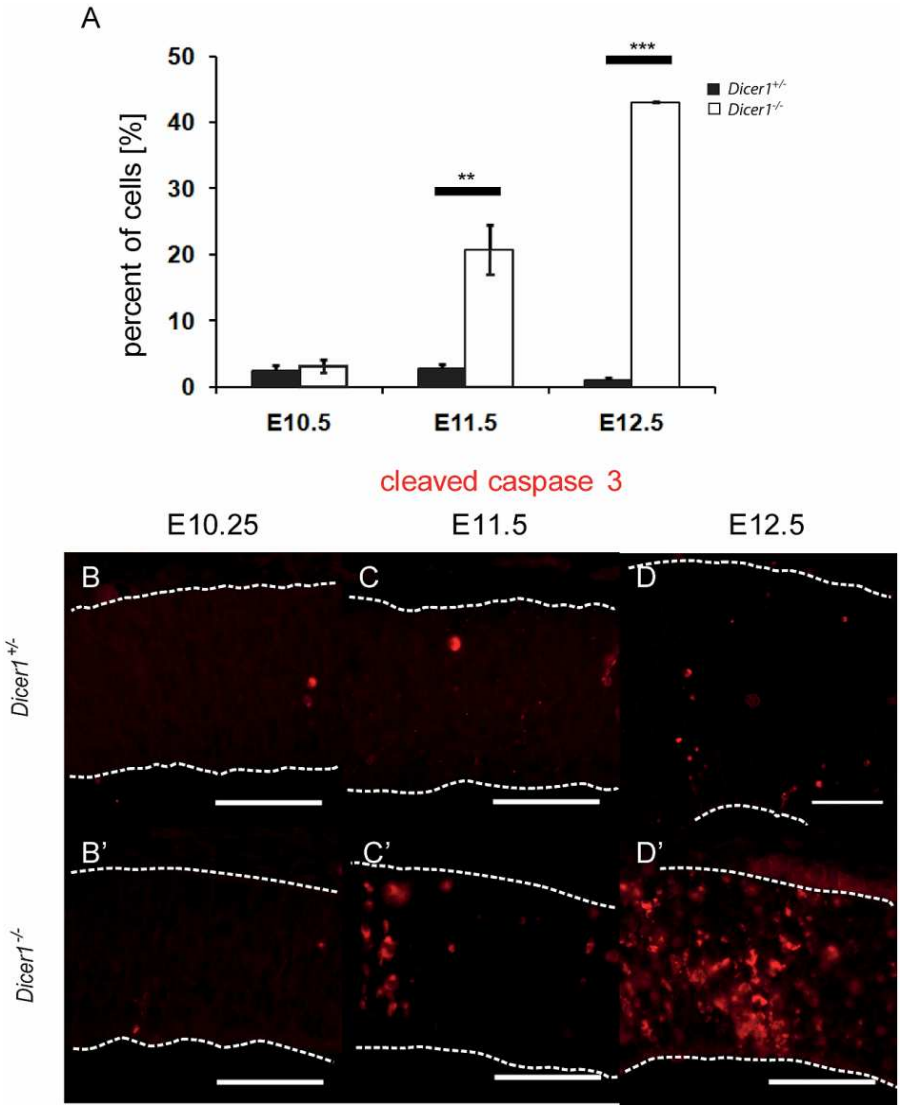
A
50
40
30
20
10
0
percent of cells [%]
***
**
Dicer1+/-
Dicer1-/-
E10.5
E11.5
E12.5
cleaved caspase 3
E10.25
E11.5
E12.5
B
C
D
B'
C'
D'
Dicer1+/-
Dicer1-/-

Figure 3.09: Volume of the *Dicer1*$^{-/-}$ telencephalic tissue is greatly reduced by E14.5. Hematoxylin and eosin staining of coronal sections through the brain at E14.5 (A) reveals a hugely abnormal telencephalon in the *Dicer1*$^{-/-}$ telencephalon (B). Scale bar: 100µm.

FIGURE 3.09

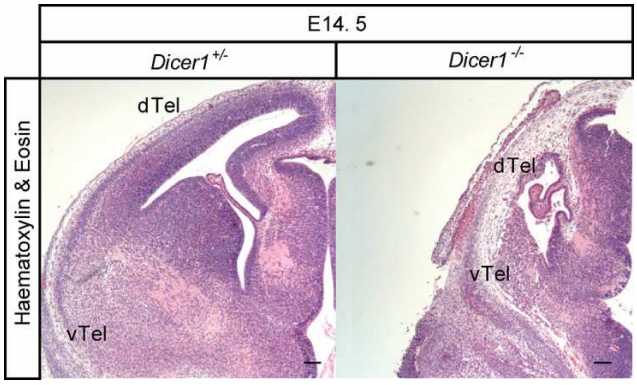

3.3 Discussion

Here I describe an analysis of early telencephalic development in mature miRNA deficiency using *Foxg1^{cre}Dicer1$^{fl/fl}$* mice. I analysed the expression of markers of neuroepithelial stem cells as well as more restricted neural progenitor cells (radial glia) and found strong evidence that around the time of development when radial glia (Misson et al., 1988) are normally generated, expression of Sox9, ErbB2 and Nestin proteins is compromised. I also found that in the absence of functional Dicer protein, radial progenitors generate normal proportions of postmitotic neurons and an increased proportion of basal progenitor cells. Both of these cell types are misplaced through the depth of the telencephalic wall in *Dicer1$^{-/-}$* telencephalon.

In previous work investigating which processes during early telencephalic development depend on miRNA maturation, three conditional mouse mutant models of *Dicer1* gene mutation have been studied. First, the *Emx1^{cre}* line leads to early recombination in the dorsal telencephalon and results in a reduction of the postmitotic cell layer through apoptosis. The newborn neurons that are generated fail to migrate to the post-mitotic layer. In this line, apical and basal progenitor cell populations are unaffected by the loss of mature miRNAs until well after the onset of apoptosis (De Pietri Tonelli, 2008). In the second model using *Nes^{cre}*, cre-recombinase is expressed later than in the *Emx1^{cre}* model. The deletion results in deficits of number and migration of postmitotic neurons while the proliferative properties of the progenitor population are completely unaffected by the loss of miRNAs. Cell survival is not affected until perinatal stages of development when a significant number of apoptotic cells is observed in the ventricular and subventricular zones (Kawase-Koga et al., 2009). The third model utilized *Camk2^{cre}* which expresses active cre from E15.5, and the primary defect was postnatal apoptotic cell death. Anterior commissure pathfinding defects and a reduction in dendritic branching in the hippocampus have also been reported (Davis et al., 2008).

My data using a cre strain that deletes earlier than in previous models that have been studied in detail indicate that in the absence of functional Dicer protein, the neuroepithelial stem cells show defects in generating radial glial progenitors around

the onset of neurogenesis. Neural progenitor cell identity is an aspect of neural development that has not, to my knowledge, been addressed in previous models of *Dicer1*$^{-/-}$ dorsal telencephalon. I found that the expression of radial glia markers RC2 and Rat-401 is severely diminished at E11.5, soon after the tissue begins to generate the first postmitotic neurons. Both antigens are encoded by the *Nes* gene. Their expression is present mainly in the basal end-feet of neuroepithelial stem cells and normally extends more widely when these generate radial glia (Gotz, 1995; Malatesta et al., 2000; Misson et al., 1988). This does not occur normally after loss of Dicer. Multiple pathways have been suggested to promote Nestin expression including Neuregulin-1 signalling through the ErbB2 receptor to promote RC2 expression in the telencephalon (Schmid et al., 2003). Null mutation of Nestin results in embryonic lethality, but no evidence has so far been found for alteration of cytoarchitecture and the exact role of Nestin remains to be unravelled. Here I propose that the level of Nestin expression is dependent upon the presence of mature miRNA processing enzyme Dicer. The effect of loss of miRNAs on Nestin might be a secondary consequence of loss of ErbB2 and/or Sox9. Importantly, Nestin is a commonly used marker for neuroepithelial malignancies (Tohyama et al., 1992) and further understanding of mechanisms regulating its expression may provide therapeutic targets of neuroepithelial tumours.

The expression of Sox9 protein is reduced between E10.25 and E11.5. According to recent reports, except for a few cases, most miRNAs control target mRNA stability by recruiting deadenylases such as CAF1 thereby reducing their stability (Fabian et al., 2009; Guo et al., 2010). Therefore, loss of mature miRNAs is predicted to result in the stabilization of their direct targets and increased protein output. Recent study found that Sox9 mRNA is targeted by miR-124 during postnatal neurogenesis (Cheng et al., 2009). I found that the Sox9 protein is lost throughout the dorsal telencephalic progenitors while miR-124 is lost from the postmitotic layer by E11.5 (Maiorano, 2009). It is plausible that the loss of Sox9 reflects the altered radial progenitor identity and that the effect is indirect. Nonetheless, direct targeting of Sox9 mRNA by miRNAs other than miR-124, such as miR-9, remains a formal possibility as miRNAs have been shown to have the capacity to promote protein expression through non-canonical pathways, although very few examples have so far

been reported (Grandjean, 2009; Vasudevan, 2007). Thus, it is conceivable that loss of miRNAs might cause direct loss of Sox9 protein.

I found that the loss of Nestin coincides with the loss of Sox9 protein. In human melanoma cells Sox9 has also been identified as an important regulator of Nestin expression (Flammiger et al., 2009). The reduction of Sox9 protein in the cortex is consistent with the reduction in the proportion of Sox9 positive cells in *Dicer1*$^{-/-}$ mutant retina (Georgi and Reh, 2010), where Sox9 normally mediates the switch between neurogenesis and gliogenesis (Stolt and Wegner, 2010) and promotes generation of the Müller glia (Poche et al., 2008). In the telencephalon, Sox9 is known to promote the establishment and maintenance of neural stem cells and promote their potential to generate neurospheres (Scott et al., 2010). Many signalling pathways have been implicated in the regulation of Sox9 expression in various tissues. Notably, these include molecules involved in forebrain development such as the Fibroblast Growth Factor (Murakami et al., 2000) Sonic hedgehog (Scott et al., 2010) and Notch1 (Meier-Stiegen et al., 2010). Dicer protein catalyses the maturation of most mature miRNAs and it is possible that at least several key developmental pathways regulating telencephalic organogenesis would be disrupted. These signalling pathways have previously been shown to be disregulated in various Dicer deficient tissues as well as through a direct regulation by specific miRNAs (Andersson et al., 2010; Davis et al., 2011; Harfe et al., 2005; Hornstein et al., 2005). Additionally, Sox9 expression is also known to be regulated by pathways directly involved in cytoskeletal remodelling, such as RhoA (Woods et al., 2005), or Vimentin (Bobick et al., 2010) and miRNAs have also been shown to play a role in regulating neuronal cytoarchitecture (Vo et al., 2005).

Apoptosis is the most widely reported phenotype of all *Dicer1*$^{-/-}$ tissues. Several mechanisms have been proposed including miR-24 regulation of caspase-3 (Walker and Harland, 2009) as well as regulation of PDCD4 or SOD1 in neurospheres (Kawase-Koga et al., 2010). It is possible that apoptosis is a secondary effect of Dicer loss. In *Nes*$^{-/-}$ mouse telencephalon a high proportion of cells undergoes apoptosis around E10.5 (Park, 2010) making the loss of Nestin a novel candidate mechanism for the induction of apoptosis at early developmental stages of neural development. In addition, activated caspase-3 has been shown to cleave Dicer in a

way that it gains an activity of a deoxyribonuclease, exacerbating cell death (Nakagawa et al., 2010).

Given the misspecification of the radial glia, it is remarkable that the progenitors do not show an inability to generate the two classes of cells that they normally generate by E11.5; postmitotic Tbr1 positive neurons and the Tbr2 positive intermediate progenitor cells (Englund et al., 2005; Guillemot, 2005; Sessa et al., 2008). The increased proportion of cells expressing Tbr2 is in line with a previous prediction based on miRNA profiling of neural progenitor cells in rat dorsal telencephalon which proposed that the expression of miR-92 is down-regulated around the onset of neurogenesis and that it could be directly targeting Tbr2 for post-transcriptional repression (Nielsen et al., 2009).

The observation that the proportion of either TuJ1 or Tbr1 expressing cells is not altered in the *Dicer1*$^{-/-}$ telencephalon generated using the *Foxg1*^{cre} line seems to contrast with other studies looking at *in vivo* neurogenesis of cortical *Dicer1*$^{-/-}$ neuroepithelium (De Pietri Tonelli, 2008; Kawase-Koga et al., 2009) as well as *Dicer1*$^{-/-}$ neural stem cells *in vitro* (Andersson et al., 2010) which have established that the ability of Dicer deficient progenitor cells to generate postmitotic neurons is compromised. It is possible that the direct neurogenesis from the radial progenitors might be compromised also in my model of *Dicer1* mutation where the radial glial identity is incorrectly specified around the time when the progenitor cells begin to generate postmitotic neurons, but that the increased proportion of the intermediate progenitors could compensate for this and, in turn, normal proportions of TuJ1-expressing cells could be generated in the mutant cortex by E11.5.

During normal corticogenesis, neurons generated prior to E11.5 contribute to the preplate. This is composed of several subpopulations including the Cajal-Retzius neurons, subplate and early projection neurons. Three commonly used markers of the very early-born neurons are Reelin, Tbr1 and Calretinin, with Reelin and Calretinin being expressed predominantly in Cajal-Retzius cells. The expression domains of these proteins are partially, but not completely overlapping at E11.5 (Hevner et al., 2003). Disruption of the Cajal Retzius cell population has been shown to lead to disrupted organisation of the telencephalon (Caviness, 1976). While it was possible

that the misplacement of neurons and basal progenitors following the loss of functional Dicer might have been caused by a loss of Cajal-Retzius cells, I found this was not the case. Failure to correctly specify radial glia cell identity is a possible explanation for the phenotype given that ablation of radial glia has been shown previously to cause defects in tissue organisation (Hasling et al., 2003).

I found that the proportion of Calretinin-expressing but not Reelin-expressing TuJ1 cells is increased in *Dicer1*$^{-/-}$ telencephalon. It is interesting that the proportion of Tbr1 did not show a significant increase given that previous studies in the wild type have shown that all Cajal-Retzius cells express Tbr1 (Hevner et al., 2003). It is possible that this relationship does not hold in the *Dicer1*$^{-/-}$ telencephalon and that some Cajal-Retzius cells fail to express Tbr1. This would need further work to investigate the nature of Cajal-Retzius cells following the loss of functional Dicer.

Taken together, my results provide a systematic description of phenotype following the loss of functional Dicer protein early during telencephalic organogenesis. I propose that during the very early development of the neuroepithelium, the progenitor cells do not develop the appropriate molecular signature of the radial glia. I found that the basal progenitor population is expanded while the proportion of postmitotic neurons is not changed (Figure 3.10). Additionally, I found that the postmitotic neurons are misplaced through the depth of the telencephalic wall and that the Cajal Retzius population, which is involved in regulating the appropriate migration of postmitotic neurons, is not reduced.

Figure 3.10: Changes to radial progenitors and their progeny in *Dicer1*$^{-/-}$ telencephalon. At E10.25 the telencephalon comprises the neuroepithelial stem cells (1) which express stem cell markers Sox2, Musashi, CD133. Expression of these proteins is maintained throughout their undifferentiated state. Dicer deficient neuroepithelium (1) does not establish appropriate molecular signature of radial glia (2) at E11.5 which express strongly Nestin and Sox9 proteins. Basal progenitors (3) and neurons (4, 5) are two classes of progeny generated by radial glia around E11.5. The proportion of Tbr2 positive basal progenitors is increased in *Dicer1*$^{-/-}$ telencephalon while the proportions of early postmitotic neurons labelled with TuJ1 and HuC/D (4) or differentiated Tbr1 positive neurons (5) are unchanged. Laminar organisation of both basal progenitors (3) and neurons (4, 5) is disrupted following the loss of functional Dicer.

FIGURE 3.10

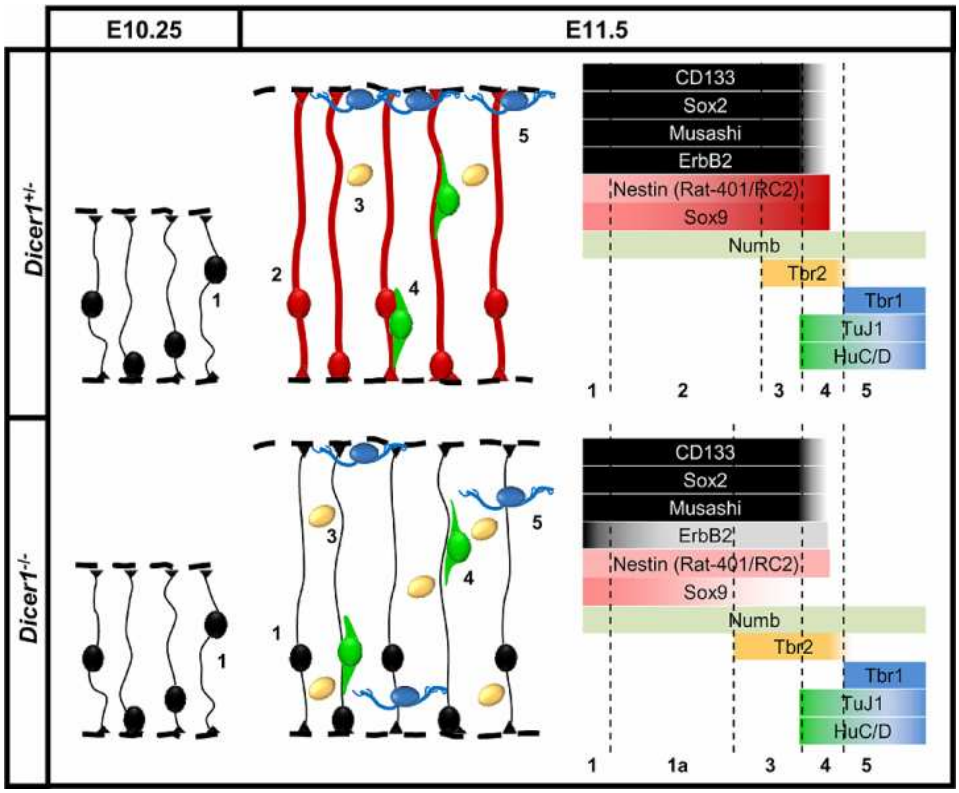
E10.25
E11.5
Dicer1+/-
Dicer1-/-
1
2
3
4
5
CD133
Sox2
Musashi
ErbB2
Nestin (Rat-401/RC2)
Sox9
Numb
Tbr2
Tbr1
TuJ1
HuC/D
1
2
3
4
5
1a

CHAPTER 4:

MicroRNA-92b controls the development of intermediate cortical progenitor cells by regulating T-box transcription factor 2.

4.1 Introduction

The excitatory neurons of the cerebral cortex are generated from radial glia that form early in corticogenesis and whose cell bodies populate the ventricular zone around the inner surface of the developing anterior end of the neural tube(Alvarez-Buylla et al., 1990; Malatesta et al., 2000; Miyata et al., 2001; Noctor et al., 2001; Voigt, 1989). Radial glial cells divide either symmetrically, producing two new radial glial cells and expanding the proliferative population, or asymmetrically to generate a new radial glial cell and either a postmitotic neuron (direct neurogenesis) or a secondary (intermediate) progenitor. Whereas postmitotic neurons migrate to the outer surface of the neural tube to contribute to the cortex, intermediate progenitors move into the subventricular zone (Haubensak et al., 2004; Hevner, 2006; Noctor et al., 2004; Smart, 1976; Takahashi et al., 1995b) where they amplify the production of neurons by undergoing a further usually symmetric division to generate a pair of postmitotic cortical neurons (indirect neurogenesis) (Haubensak et al., 2004; Hevner, 2006; Lui et al., 2011; Miyata et al., 2001; Noctor et al., 2008). In the mouse, these events occur between embryonic days 11 (E11) and E17 (Caviness, 1982; Gillies and Price, 1993; Takahashi et al., 1995a). The transition from radial glia to intermediate progenitors is controlled by a number of proteins; of these, only the T-box transcription factor Tbr2 (also known as Eomesodermin) has been shown to have a direct effect on the specification of the intermediate progenitors (Arnold et al., 2008; Pontious et al., 2008; Sessa et al., 2008).

MicroRNAs (miRNAs) are a class of short non-coding RNA molecules involved in post-transcriptional regulation of protein expression. A range of messenger RNAs (mRNAs) have been identified as direct targets of specific miRNAs in the developing brain (Makeyev et al., 2007; Packer et al., 2008; Shibata et al., 2008; Shibata et al., 2011). To determine which of the processes that occur during corticogenesis depend on the presence of mature miRNAs, several studies used cre-*loxP* technology to induce widespread ablation of the key enzyme involved in the biosynthesis of most miRNAs, Dicer, throughout the developing cortex (Davis et al., 2008; De Pietri Tonelli, 2008; Kawase-Koga et al., 2009; Nowakowski et al., 2011). One common finding was a large increase in rates of apoptotic cell death, making it

hard to deduce the extent to which loss of miRNA activity affects neuronal cell production and limiting the period over which the consequences of loss-of-function could be studied.

I generated a mosaic cortical ablation of Dicer in a relatively small subset of radial glia by electroporating a cre-recombinase expression vector into mouse embryos (Saito, 2006) that were homozygous for the *Dicer1*^{fl} allele (Harfe et al., 2005). Under these conditions *Dicer1*$^{-/-}$ cells survived well into postnatal life and, to my surprise, I found increased numbers of *Dicer1*$^{-/-}$ neurons in the cortex. I traced the cause of this to a change in the development of intermediate progenitor cells. I then used a gain-of-function and a loss-of-function approach to show that miR92b regulates the development of intermediate progenitor cells, most likely by modulating levels of their key molecular determinant, Tbr2.

4.2 Results

4.2.1 Rapid loss of mature miRNAs following mosaic ablation of functional Dicer.

I first tested the efficiency of the electroporated cre-recombinase expression vector (CAG-cre-IRES-EGFP) in reducing mature miRNA levels in *Dicer1*$^{fl/fl}$ cortical cells (Figure 4.01 A). One day after electroporation *of Dicer1*$^{fl/fl}$ or *Dicer1*$^{fl/+}$ (control) embryos, dissociated cortical cells were examined by *in situ* hybridisation with locked nucleic acid (LNA) riboprobes (Kloosterman, 2006) against two miRNAs normally highly expressed in many cortical cells, miR-9 and miR-124 (Landgraf et al., 2007). GFP-positive (GFP+) cells (Figure 4.01 B and C, filled arrows) were chosen at random and paired with nearby GFP-negative (GFP-) cells (Figure 4.01 B and C, open arrows). From the images of the *in situ* hybridizations (Figure 4.01 D, E), greyscale intensity profiles were generated (Figure 4.01 F – I) and total intensities were calculated (Figure 4.01 J). For each pair, the value for the GFP+ cell was subtracted from the value for the GFP- cell (Figure 4.01 K). Estimating the proportion of *Dicer1*$^{fl/fl}$ cells that underwent depletion was done by examining the distributions of intensity differences (Figure 4.01 L – O). All normal cortical cells

express some level of miR-9 and miR-124 at E14.5 (Maiorano, 2009). Approximately 50% of dissociated *Dicer1*$^{fl/+}$ cells showed strong staining for either miR-9 or miR-124 and so, as expected, the random pairs method gave differences normally distributed around zero (Figure 4.01 L and filled bars in N, O). In *Dicer1*$^{fl/fl}$ cells, distributions were shifted such that the vast majority of pairs (85-90%) showed differences of less than zero (Figure 4.01 M and open bars in N, O). These wholesale shifts in the distributions indicate rapid and efficient depletion of these miRNAs from almost all GFP+ *Dicer1*$^{fl/fl}$ cells, as illustrated in Figure 4.01 M.

4.2.2 Dicer deficient progenitors generate more cortical neurons.

To establish if miRNAs are involved in regulating cortical cell numbers, I labelled the progeny of cells generated from electroporated control or *Dicer*$^{fl/fl}$ radial glial progenitors using the *Rosa26RYFP* reporter (Srinivas et al., 2001). Electroporated cells were identified by immunohistochemistry using an antibody that recognises both EGFP and YFP (immunopositive cells will be referred to as GFP+ hereafter, see Chapter 2).

Apoptotic cell death commonly occurs following the widespread loss of functional Dicer in mouse embryos (Davis et al., 2008; De Pietri Tonelli, 2008; Kawase-Koga et al., 2009). I analysed sections through E13.5 electroporated *Dicer*$^{fl/+}$ and *Dicer*$^{fl/fl}$ cortex at E15.5 (Figure 4.02 A, D), E18.5 (Figure 4.02 B, E) and postnatal day 14 (P14) (Figure 4.02 C, F) for double-immunolabelling for GFP and the apoptotic marker cleaved-caspase-3. There was no evidence that the incidence of apoptosis was altered when functional Dicer was lost from small subpopulations of cortical progenitors (Figure 4.02 G), suggesting that apoptosis is not always an inevitable consequence of Dicer loss. This finding offered the opportunity to examine other defects resulting from Dicer loss. As shown in Figure 4.03 A, E13.5 *Dicer1*$^{fl/fl}$*;Rosa26RYFP*$^{+}$ or *Dicer1*$^{fl/+}$*;Rosa26RYFP*$^{+}$ embryos were electroporated and coronal sections of lateral cortex were analysed at P14. Both in control (Figure 4.03 B) and in *Dicer1*$^{fl/fl}$ mice (Figure 4.03 C), GFP+ cells were found throughout the depth of the cortex, with less in progressively deeper layers since many deep layer cells are generated earlier than the age of electroporation. Greater proportions

of GFP+ cells were found in *Dicer1*$^{fl/fl}$ mice, particularly in layer I, but also in layers II/III, V and VI, than in controls (Figure 4.03 D). This increased contribution of *Dicer1*$^{-/-}$ GFP+ cells in *Dicer1*$^{fl/fl}$ mice did not increase the average thickness of the cortical layers (Figure 1 e) but did increase the average density of cells in most layers, most notably in the superficial layers I and II/III but also in layer V (Figure 4.03 F). There were no differences in the average densities of GFP- cells between *Dicer1*$^{fl/fl}$ and control mice (Figure 4.03 G).

Figure 4.01: Levels of two brain-enriched mature miRNAs, miR9 and miR124, are reduced in cells one day after electroporation. (A) Schema showing experimental approach. E13.5 *Dicer1*$^{fl/fl}$ or *Dicer1*$^{fl/+}$ embryos were electroporated with cre expression vector. On E14.5 tissue containing GFP+ cells was dissected and dissociated cells were reacted for mature miR9 or miR124. (b-e) Examples show *in situ* hybridisation staining for miR9 in dissociated cells. Electroporated *Dicer1*$^{fl/fl}$ (B) and control *Dicer1*$^{fl/+}$ (C) cells were identified based on the expression of GFP (filled arrowheads). Among *Dicer1*$^{fl/fl}$ (D) and control (e) *Dicer1*$^{fl/+}$ cells, greyscale image intensity profiles were determined for pairs of GFP+ and GFP- cells (boxes). Scale bar 10µm. (F-I) Examples of image intensity profiles for the individual cells boxed in D and E: (G) *Dicer1*$^{fl/fl}$ GFP+, (G) *Dicer1*$^{fl/fl}$ GFP-, (H) *Dicer1*$^{fl/+}$ GFP+ and (I) *Dicer1*$^{fl/+}$ GFP-; lower grayscale values corresponding to more intense *in situ* staining and hence more miRNA. (J) To evaluate the amount of miRNA staining in GFP+ cells compared to GFP- cells, values of total image intensity were calculated for each cell by integrating its image intensity profile (F – I) according to the equation in j and for each pair of GFP+ and GFP- cells the total intensity values were subtracted according to the equation in K. (L) With both miR124 and miR9 being expressed by all cells in the developing cortex (dark shading – cell expressing high level of miRNA, grey shading – cell expressing low to moderate level of miRNA) analysis of miRNA *in situ* staining using equation in k is expected to result in either a number close to zero (case 1 and 3), a positive number (case 2) or a negative number (case 4) in cells expressing Dicer. (M) If Dicer is efficiently depleted, little or no *in situ* staining is expected in GFP+ cells (bright grey shading) and so the differences will be less than zero in all cases. (N, O) Distributions of intensity differences among *Dicer1*$^{fl/+}$ (filled bars) and *Dicer1*$^{fl/fl}$ cells for *in situ* staining for (N) miR124 and (O) miR9. Data represent analysis of results pooled from 3 experiments, each analysing 40-100 pairs of cells.

FIGURE 4.01

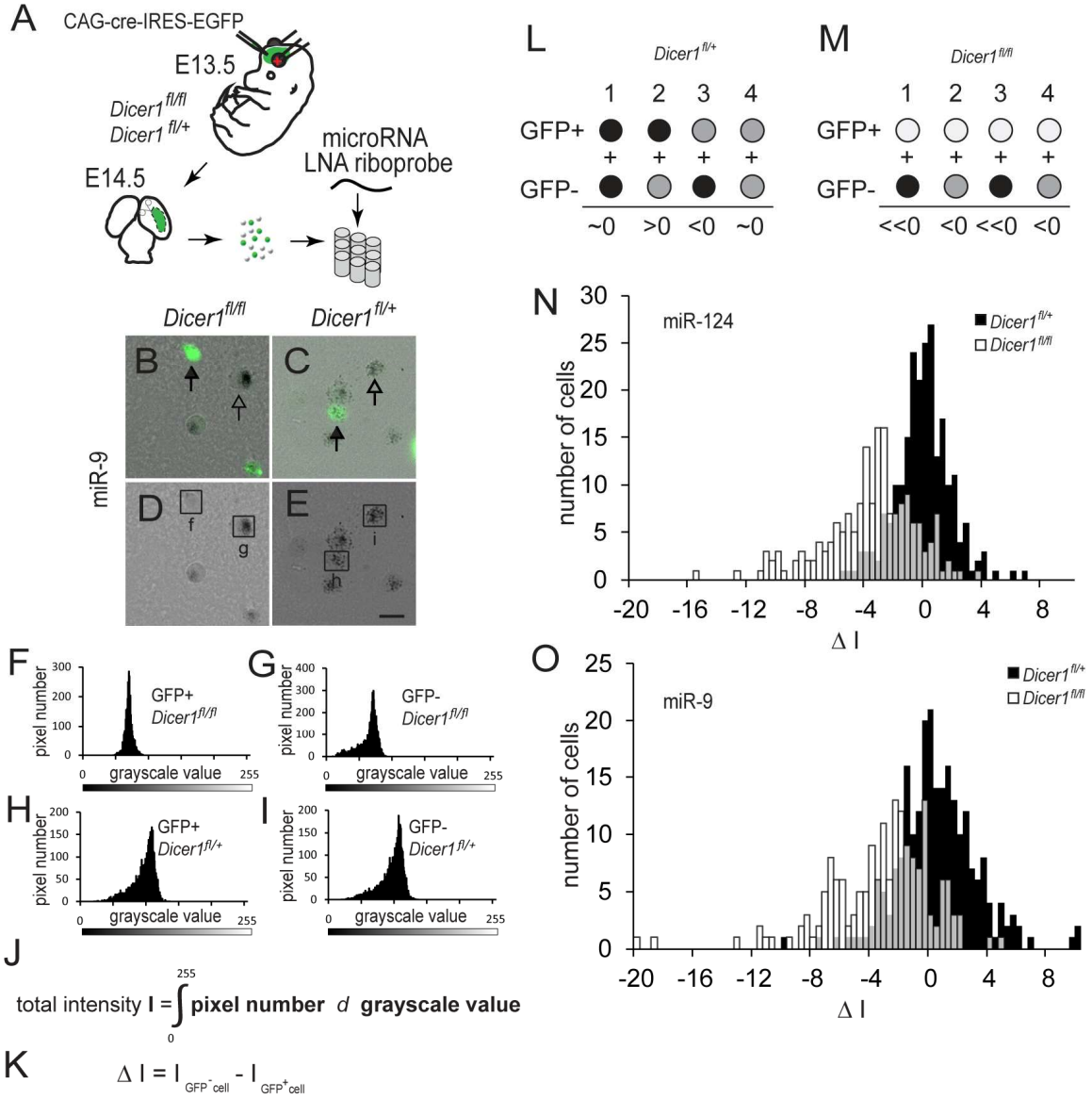
A
CAG-cre-IRES-EGFP
E13.5
Dicer1 fl/fl
Dicer1 fl/+
E14.5
microRNA
LNA riboprobe
Dicer1 fl/fl
Dicer1 fl/+
miR-9
B
C
D
E
f
g
i
j
F
GFP+
Dicer1 fl/fl
G
GFP-
Dicer1 fl/fl
H
GFP+
Dicer1 fl/+
I
GFP-
Dicer1 fl/+
pixel number
grayscale value
0
255
J
total intensity I = ∫ pixel number d grayscale value
K
Δ I = I GFP- cell - I GFP+ cell
L
Dicer1 fl/+
1 2 3 4
GFP+
GFP-
~0 >0 <0 ~0
M
Dicer1 fl/fl
1 2 3 4
GFP+
GFP-
<<0 <0 <<0 <0
N
miR-124
Dicer1 fl/+
Dicer1 fl/fl
number of cells
Δ I
O
miR-9
Dicer1 fl/+
Dicer1 fl/fl
number of cells
Δ I

Figure 4.02: No evidence of increased apoptosis following the loss of functional Dicer. (A – F) images of coronal sections containing (A – C) *Dicer1*$^{+/-}$ and (D – F) *Dicer1*$^{-/-}$ cortex at (A, D) E15.4, (B, E) E18.5 and (C, F) P14 showing immunostaining for GFP and the marker of apoptosis, cleaved caspase 3. Scale bars: A - B, D - E, 100µm; C, F, 50µm. (G) Enumeration of density of cells double-positive for GFP and cleaved caspase 3 in the dorsal telencephalon (dTel) at E15.5 or the cortical plate (CP) at E18.5 or P14 cortex (Ctx) shows no difference between genotypes. Data represent means ± s.e.m., p-values are for two-tailed unpaired Student's t test for 6 animals from 3 surgeries, 1 section analysed per animal.

FIGURE 4.02

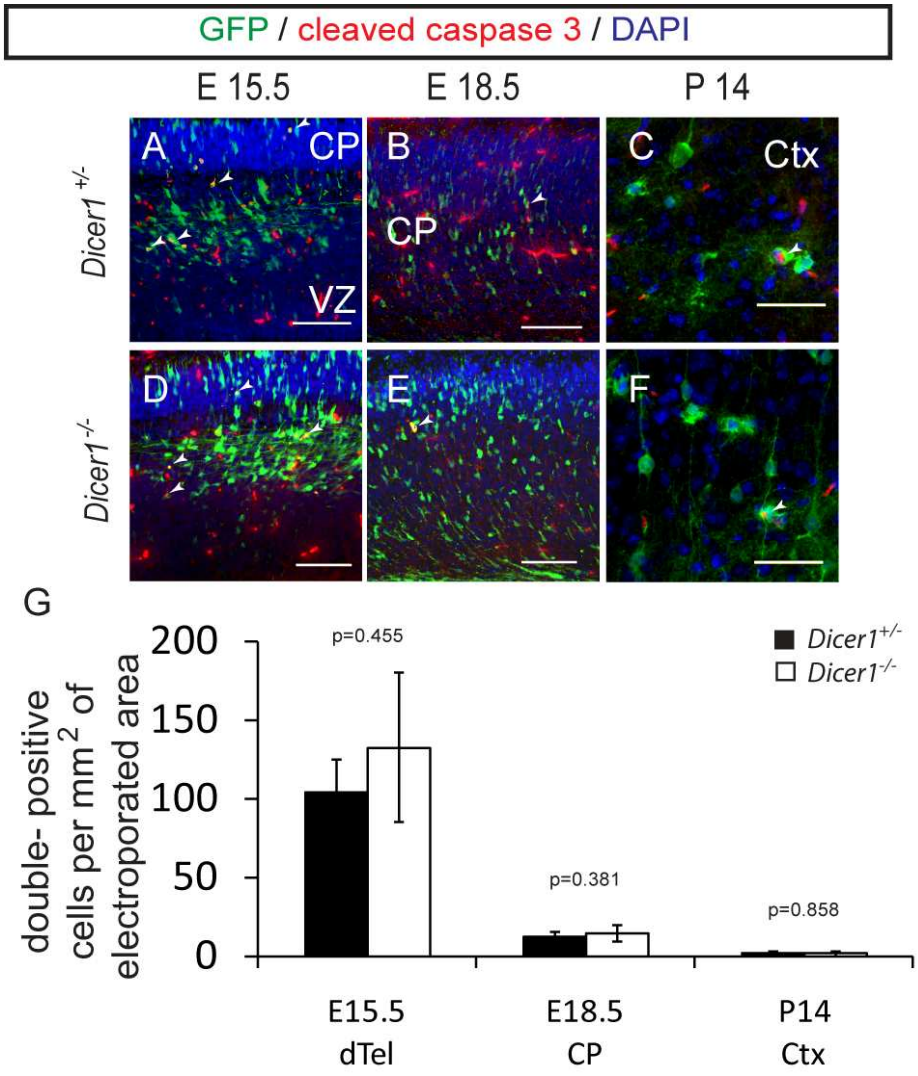
GFP / cleaved caspase 3 / DAPI
E 15.5
E 18.5
P 14
A
CP
VZ
B
CP
C
Ctx
D
E
F
Dicer1 +/-
Dicer1 -/-
G
double- positive cells per mm2 of electroporated area
200
150
100
50
0
p=0.455
p=0.381
p=0.858
Dicer1+/-
Dicer1-/-
E15.5
dTel
E18.5
CP
P14
Ctx

Figure 4.03: Dicer deficient progenitors generate abnormally many cortical cells. (A) Schema showing the experimental design. Embryonic *Dicer1*$^{fl/fl}$ and control *Dicer1*$^{fl/+}$ mice carrying the *R26RYFP* reporter allele were electroporated with cre-expression plasmid at E13.5 and allowed to develop until P14. Cells derived from electroporated radial glia were found reproducibly in the lateral cortex (red box). (A') Example of a coronal section through P14.5 cortical wall showing DAPI-stained cell nuclei. Cortical layers LI – LVI are identified based on nuclear density. Borders between layers are marked with dotted lines. Examples of coronal sections through cortices containing (B) *Dicer1*$^{+/-}$ and (C) *Dicer1*$^{-/-}$ GFP+ cells. Scale bar 50 µm. (D) The overall contribution of GFP+ cells to cortical layers I, II/III, V and VI was higher in *Dicer1*$^{fl/fl}$ than in *Dicer1*$^{fl/+}$ mice. (E) Average thicknesses of cortical layers were not different between genotypes. (F) Average densities of cell nuclei were higher in layers I, II/III and V of cortices containing *Dicer1*$^{fl/fl}$ cells. (G) Average densities of GFP- cells were not different. Data in D-G represent means ± s.e.m. from 6 animals from 3 surgeries with 5 sections analysed per animal. Borders between cortical layers were identified at low power based on DAPI nuclear counterstain. *** - $p<0.001$, * - $p<0.05$, Tukey's test.

FIGURE 4.03

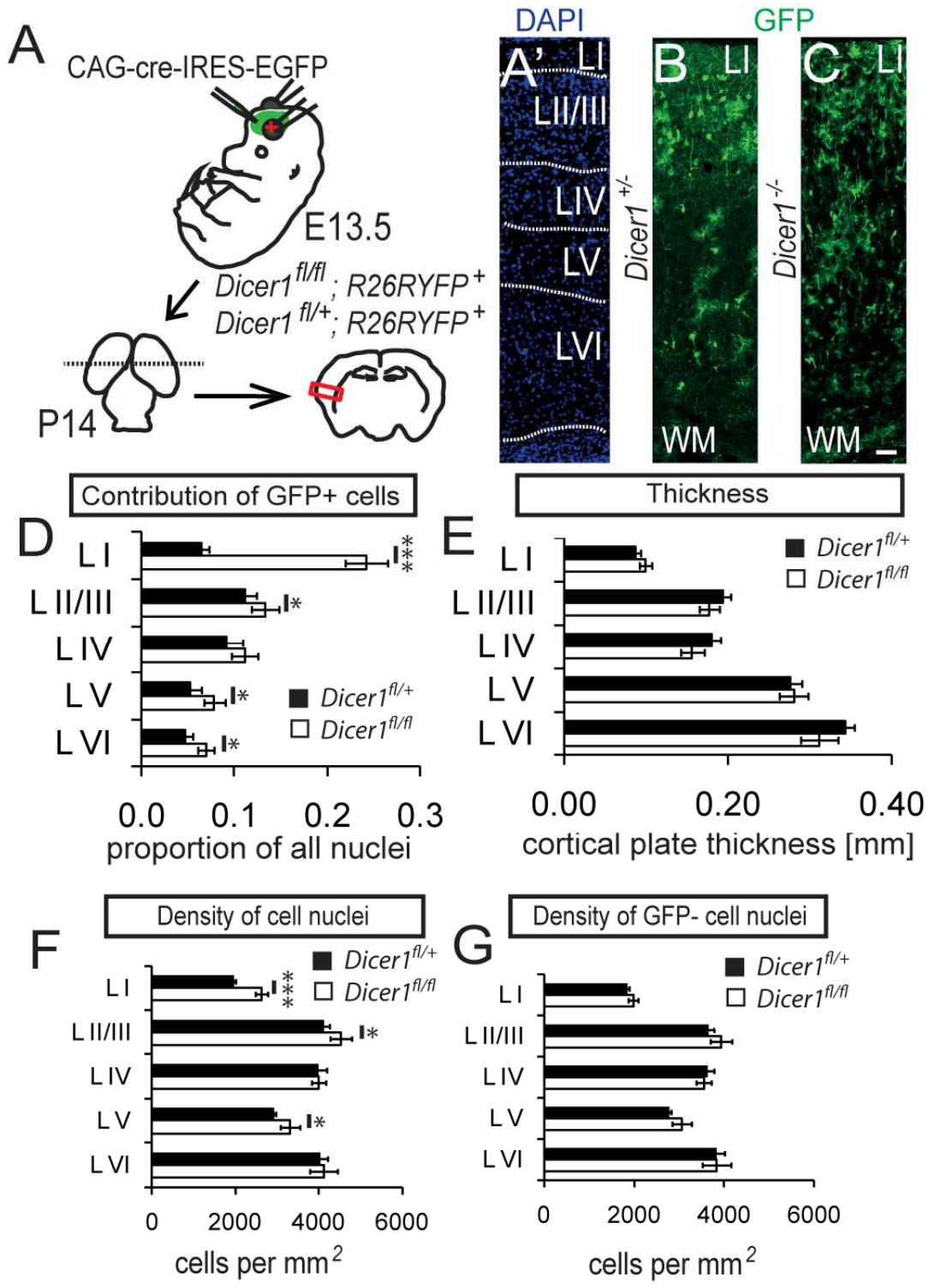
A
CAG-cre-IRES-EGFP
E13.5
Dicer1 fl/fl ; R26RYFP+
Dicer1 fl/+; R26RYFP+
P14
DAPI
GFP
A'
B
C
LI
LII/III
LIV
LV
LVI
WM
Dicer1 +/-
Dicer1 -/-
D
Contribution of GFP+ cells
L I
L II/III
L IV
L V
L VI
Dicer1 fl/+
Dicer1 fl/fl
0.0 0.1 0.2 0.3
proportion of all nuclei
E
Thickness
0.00 0.20 0.40
cortical plate thickness [mm]
F
Density of cell nuclei
0 2000 4000 6000
cells per mm 2
G
Density of GFP- cell nuclei

Closer examination of the superficially located *Dicer1*$^{-/-}$ GFP+ cells in layers II/III of P14 *Dicer1*$^{fl/fl}$ animals revealed that most cells had a neuronal morphology (Figure 4.04 B) similar to that of *Dicer1*$^{+/-}$ GFP+ cells in these layers in control animals (Figure 4.04 A). To further validate that *Dicer1*$^{-/-}$ cells were indeed neurons I obtained whole-cell patch clamp recordings from a sample of them located in layer II/III at P14 (Figure 4.04 C, D). In all cases (n = 6 cells from 4 animals from separate electroporations) cells fired fast, regenerating action potentials upon depolarization (representative recordings are shown in Fig 4.04 D) and had passive electrical properties normal for fast-spiking excitatory cortical neurons. Furthermore, these cells exhibited spontaneous excitatory postsynaptic currents (Figure 4.04 E) that were sensitive to CNQX (5 μM, n = 3 cells examined) (Figure 4.04 F). These observations indicate that *Dicer1*$^{-/-}$ cells can differentiate to form functional neurons capable of responding to synaptic input.

Next I tested the molecular properties of the abnormally large population of *Dicer1*$^{-/-}$ GFP+ cortical cells generated in the superficial layers I-III of electroporated *Dicer1*$^{fl/fl}$ mice. The molecular markers Cux1 and Satb2 are normally expressed by most neurons (Britanova et al., 2008; Nieto et al., 2004) in layers II/III and similar proportions of *Dicer1*$^{+/-}$ GFP+ and of the expanded population of *Dicer1*$^{-/-}$ GFP+ cells expressed these markers in LII/III (Figure 4.04 G, H). Normally, most neurons in layer I are generated around E11, which is before the age of electroporation. Cux1 and Satb2 are expressed by very few of them (Figure 4.04 G, H, I) and many later disappear (Price et al., 1997) to be replaced by astrocytes born during postnatal development (DeFelipe et al., 2002; Levison et al., 1993; Levison and Goldman, 1993; Voigt, 1989). In *Dicer1*$^{fl/fl}$ mice, however, about 50% of the *Dicer1*$^{-/-}$ GFP+ cells in layer I expressed superficial layer neuronal marker Cux1 (Figure 4.04 G, K). Whereas most of the relatively few GFP+ cells in layer I of control P14 *Dicer1*$^{fl/+}$ mice expressed the astrocyte marker GFAP (Figure 4.04 J), most of the more abundant *Dicer1*$^{-/-}$ GFP+ cells in layer I did not express GFAP (Figure 4.04 L), in line with their neuronal identity. From all these data I conclude that loss of Dicer from cortical progenitors between E13.5 and E14.5 results in their overproduction of superficial layer neurons with many of the Cux1-expressing neurons being displaced into layer I.

Figure 4.04: Loss of functional Dicer results in an overproduction of cortical neurons by P14. (A) Cells generated from *Dicer1*$^{+/-}$ and (B) *Dicer1*$^{-/-}$ radial glia were able to adopt neuronal morphologies (arrows). Scale bar 50 µm. (C – F) To validate that *Dicer1*$^{-/-}$ GFP+ cells can develop into functional neurons, whole-cell patch clamp recordings have been obtained from layer II/III GFP+ cells at P14. (C) Wide-field image showing the position of recording electrode. (C') A layer II/III GFP/YFP-expressing *Dicer1*$^{-/-}$ cell filled with AlexaFluor 555 dye following the recording. Scale bar is 100 µm. (D) Depolarization of a patched layer II/III *Dicer1*$^{fl/fl}$ neuron causes the neuron to fire action potentials. (E) Whole cell patch-clamp recording from a representative layer II/III *Dicer1*$^{fl/fl}$ neuron showing that the neuron is able to receive synaptic input. (F) Postsynaptic currents were sensitive to CNQX. (G) Cux1, a molecular marker of superficial layer neurons, is expressed by normal proportions of GFP+ *Dicer1*$^{-/-}$ cells in layer II/III and by an abnormally large proportion of GFP+ *Dicer1*$^{-/-}$ cells in layer I at P14. (H) The proportion of *Dicer1*$^{-/-}$ GFP+ cells expressing Satb2 is not different from the proportion of *Dicer1*$^{+/-}$ GFP+ cells expressing Satb2 in layers I and II/III. Data represent means ± s.e.m from 6 animals from 3 surgeries with 1 section analysed per animal. *** - $p<0.001$, Tukey's test. (I – L) Representative images of GFP+ cells in *Dicer1*$^{fl/+}$ animals showing that in layer I cells generally do not express neuronal marker Cux1 (I), but most cells in layer I are GFAP positive (J, arrows). In *Dicer1*$^{fl/fl}$ animals, abnormally many GFP+ cells expressed neuronal marker Cux1 (K, arrows) and most GFP+ cells do not immunoreact for GFAP (L, arrows). Scale bars 50 µm.

FIGURE 4.04

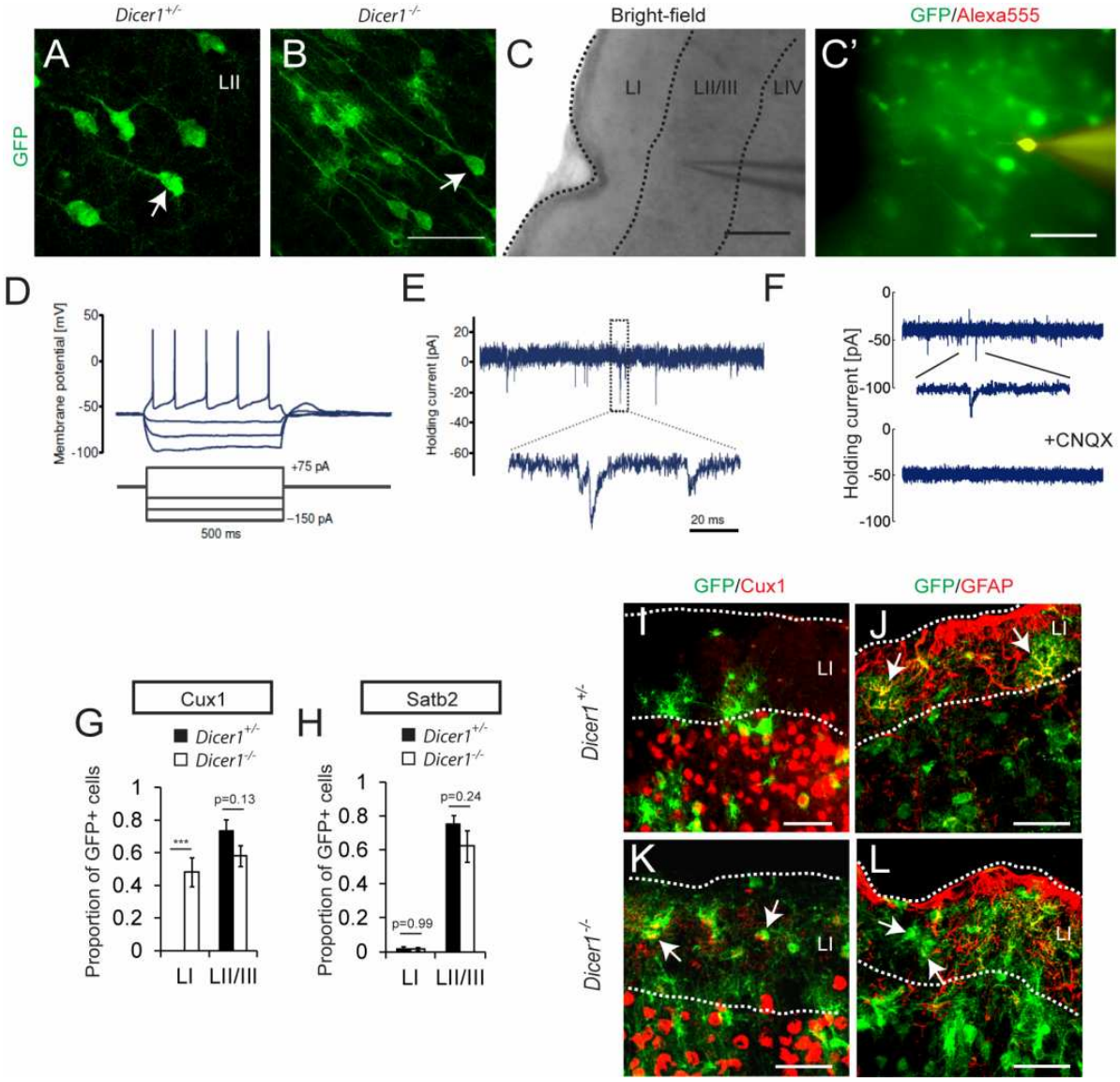
Dicer1+/-
Dicer1-/-
Bright-field
GFP/Alexa555
A
B
C
C'
GFP
LII
LI
LII/III
LIV
D
E
F
Membrane potential [mV]
+75 pA
−150 pA
500 ms
Holding current [pA]
20 ms
+CNQX
GFP/Cux1
GFP/GFAP
G
Cux1
H
Satb2
Proportion of GFP+ cells
p=0.13
p=0.24
p=0.99
I
J
K
L

Figure 4.05: Expression of deep layer neuronal markers. Images show examples of staining of P14 lateral cortex with antibodies against markers expressed by deep layer neurons, (A) Tbr1, (B) Ctip2 and (C) Satb2. Graphs to the right of each image represent quantification of the proportion of GFP+ cells expressing the respective protein among cells that are *Dicer1*$^{+/-}$ (filled bars) or *Dicer1*$^{-/-}$ (open bars). Data represent means ± s.e.m., * - $p<0.05$, p-value calculated using Student's t-test test for n = 6 animals from 3 surgeries. Abbreviation: WM – white matter. Scale bar 100 µm.

FIGURE 4.05

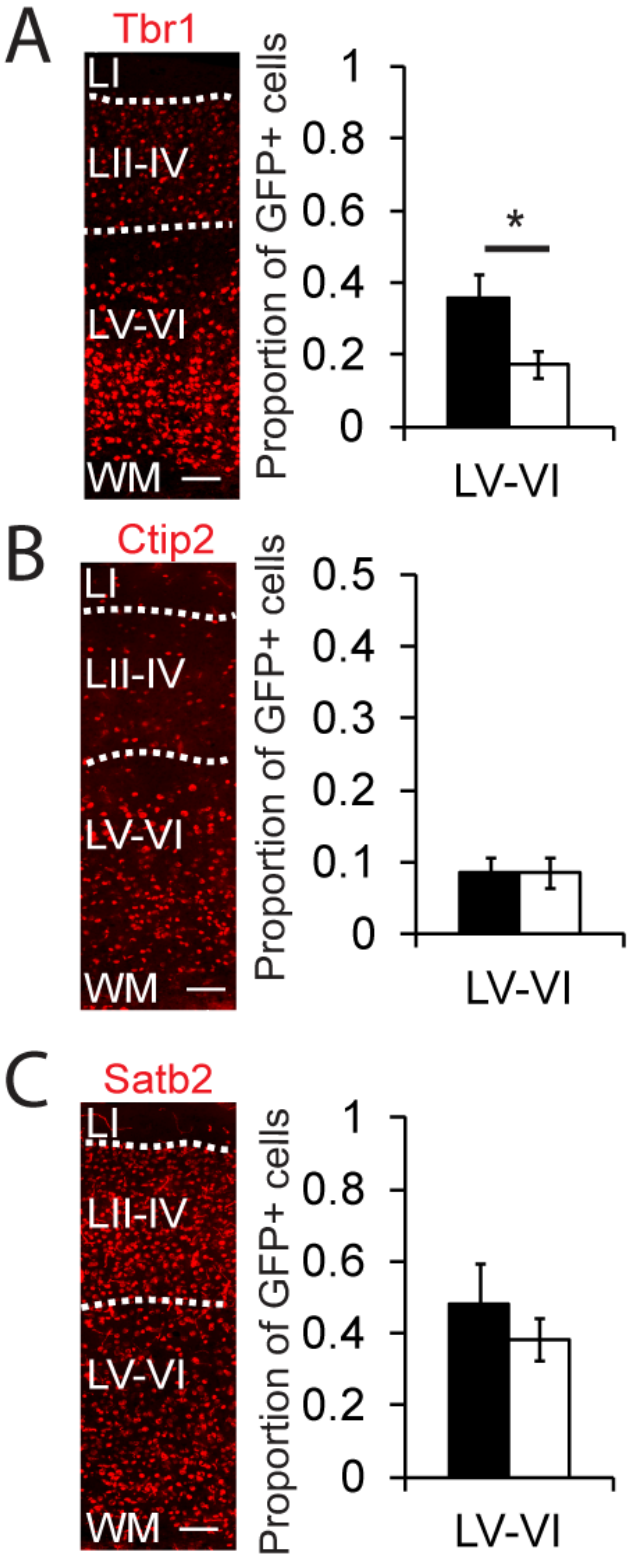
A
Tbr1
LI
LII-IV
LV-VI
WM
Proportion of GFP+ cells
1
0.8
0.6
0.4
0.2
0
*
LV-VI
B
Ctip2
LI
LII-IV
LV-VI
WM
Proportion of GFP+ cells
0.5
0.4
0.3
0.2
0.1
0
LV-VI
C
Satb2
LI
LII-IV
LV-VI
WM
Proportion of GFP+ cells
1
0.8
0.6
0.4
0.2
0
LV-VI

Normal proportions of *Dicer1*$^{-/-}$ GFP+ cells in the deep layers V and VI expressed the neuronal layer V marker Ctip2 and callosal neuronal marker Satb2. There was a significant reduction in the proportions of cells expressing layer VI neuronal marker Tbr1 (Figure 4.05). It is likely that this reduction occurred due to the dilution of a relatively normal complement of Tbr1-expressing cells, most of which would have been generated before electroporation on E13.5, by the subsequent overproduction of neurons after electroporation.

My overall conclusion is that following the loss of functional Dicer around E13.5-E14.5 progenitors generated more cortical neurons contributing particularly to the superficial layers.

4.2.3 Expansion of the Tbr2-expressing progenitor population among *Dicer1*$^{-/-}$ cells

I next examined embryonic neuronal output from *Dicer1*$^{-/-}$ progenitors in the days immediately following electroporation. Dissociated cells from cortical areas containing electroporated cells from either *Dicer1*$^{fl/fl}$ or *Dicer1*$^{fl/+}$ embryos at E14.5, E15.5 and E16.5 (Figure 4.06 A) were immunoreacted for GFP and HuC/D, a marker of early postmitotic neurons (Figure 4.06 B). Quantification showed that three days after electroporation slightly more *Dicer1*$^{-/-}$ than control GFP+ cells expressed HuC/D but this was preceded by an earlier phase during which fewer *Dicer1*$^{-/-}$ than control GFP+ cells were double-labelled for HuC/D (Figure 4.06 C). One possible explanation was that, at around E14.5, the progeny of the Sox2+ radial glia (Figure 4.06 D) enter the indirect neurogenesis pathway at an increased rate and are specified as Tbr2+ intermediate progenitors (Arnold et al., 2008; Bulfone et al., 1999; Ochiai et al., 2009; Sessa et al., 2008) (Figure 4.06 E). An early increase in the specification of intermediate progenitors at the expense of neurons could lead to a later boost in neuronal production from the larger-than-normal intermediate progenitor pool, as shown by the diagram in Figure 4.06 F.

To test this I quantified the proportions of cells that expressed Sox2 and Tbr2. Normal proportions of *Dicer1*$^{-/-}$ GFP+ cells expressed Sox2 at E14.5 and E15.5 (Figure 4.06 G) but the proportions of *Dicer1*$^{-/-}$ GFP+ cells expressing Tbr2 were

increased (Figure 4.06 H). The distributions of Tbr2-expressing *Dicer*$^{-/-}$ and control cells were compared by analysing proportions of GFP and Tbr2 double-positive cells in counting bins through the cortex (Figure 4.06 I). This showed increased Tbr2 expression among *Dicer1*$^{-/-}$ GFP+ cells in the abventricular portion of the ventricular zone and lower part of the subventricular zone at E14.5 (Figure 4.06 J) and throughout the normal Tbr2 expression domain at E15.5 (Figure 4.06 K). These results are in excellent agreement with the proposed model (Figure 4.06 F).

Figure 4.06: Increased generation of intermediate progenitor cells following the loss of miRNAs. (A) Schema showing experimental design. Electroporated tissue was dissected from *Dicer1*$^{fl/+}$ and *Dicer1*$^{fl/fl}$ brains and dissociated. (B) Dissociated cells were immunolabelled for GFP and a marker of early born neurons HuC/D (arrows). Scale bar 50µm. (C) One day after the electroporation, a reduced proportion of GFP+ *Dicer1*$^{-/-}$ cells were HuC/D-positive but over the subsequent 2 days this difference reversed. Data represent means ± s.e.m., * - $p<0.05$, ** - $p<0.01$, two tailed Student's t test; experiment was performed 4 times for E14.5 and E15.5 and 3 times for E16.5; for each dissociation tissue from at least 3 embryos was combined; a total of 23978 *Dicer1*$^{+/-}$ and 31090 *Dicer1*$^{-/-}$ cells were assessed. (D, E) Cell bodies of the Sox2 expressing radial glia are located in the ventricular zone (VZ). One day after electroporation, GFP+ cells can be found in the VZ and the subventricular zone (SVZ), where the Tbr2-expressing intermediate progenitor cells are located, and in the intermediate zone (IZ). Scale bar 100 µm. (F) Schema representing how neuronal production can be enhanced by an increased incidence of indirect neurogenesis. Radial glia (red) can produce neurons directly upon cell division in the ventricular zone (VZ) (case 1, 2) or indirectly by generating a Tbr2-positive intermediate progenitor (purple), which will further proliferate at the subventricular zone to amplify the neuronal output of the radial glia (case 3). In some cases, radial glia proliferate to expand the pool of progenitors (case 4). If more *Dicer1*$^{-/-}$ progenitors differentiate via the indirect neurogenesis pathway, the proportion of neurons will be initially reduced and later increased, consistent with the observations shown in (c). (G, H) A normal overall proportion of *Dicer1*$^{-/-}$ GFP+ cells expressed Sox2 at E14.5 and E15.5, while a higher overall proportion of *Dicer1*$^{-/-}$ GFP+ cells expressed Tbr2. Data represent means ± s.e.m.; ** - $p<0.01$, *** - $p<0.001$; two tailed unpaired Student's t test for 7-9 embryos from 3 surgeries at both E14.5 and E15.5; 3 sections were quantified for each brain. (I) Example of an image used to quantify the distribution of GFP+/Tbr2+ cells with counting ladder consisting of 10 boxes (200µm x 40 µm). (J, K) Distributions of GFP+ cells double-labelled for Tbr2 at (J) E14.5 and (K) E15.5. Expression of Tbr2 is upregulated in *Dicer1*$^{fl/fl}$ GFP+ cells in the abventricular part of the ventricular zone and in the subventricular zone at E14.5 and in the intermediate zone as well at E15.5. Data represent means ± s.e.m.; * - $p<0.05$, ** - $p<0.01$, *** - $p<0.001$, Tukey's test for 7-11 embryos from at least 3 surgeries with 3 sections analysed per brain.

FIGURE 4.06

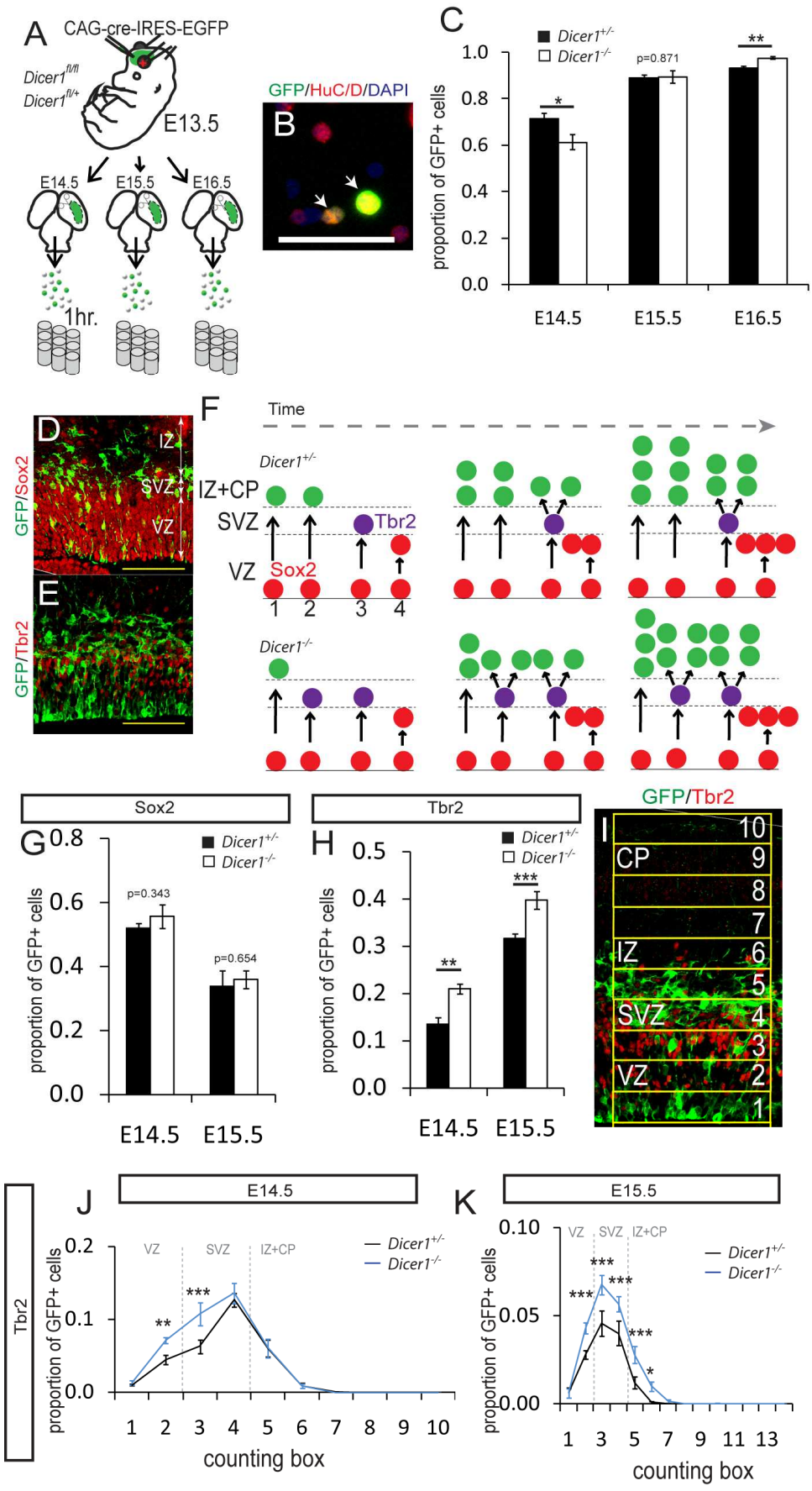
A
CAG-cre-IRES-EGFP
Dicer1fl/fl
Dicer1fl/+
E13.5
E14.5
E15.5
E16.5
1hr.
GFP/HuC/D/DAPI
B
C
Dicer1+/-
Dicer1-/-
proportion of GFP+ cells
p=0.871
*
**
E14.5
E15.5
E16.5
D
GFP/Sox2
IZ
SVZ
VZ
E
GFP/Tbr2
F
Time
Dicer1+/-
IZ+CP
SVZ
VZ
Tbr2
Sox2
1
2
3
4
Dicer1-/-
Sox2
G
p=0.343
p=0.654
E14.5
E15.5
Tbr2
H
**
***
GFP/Tbr2
I
CP
IZ
SVZ
VZ
10
9
8
7
6
5
4
3
2
1
Tbr2
J
E14.5
K
E15.5
VZ
SVZ
IZ+CP
counting box

4.2.4 *Dicer1*$^{-/-}$ cortical progenitors continue to generate increased numbers of cortical neurons postnatally

Comparison of the migration of *Dicer1*$^{-/-}$ and control postmitotic neurons using pulses of bromodeoxyuridine (BrdU) at E13.5 or E16.5 (Figure 4.07 A) revealed no differences by E18.5 (Figure 4.07 B - E). Thus, by the time of birth there was no clear explanation for the large increase in *Dicer*$^{-/-}$ neurons observed postnatally in layer I (Figures 4.03 D and 4.04 G). Therefore, I considered whether increased neurogenesis persists postnatally among *Dicer1*$^{-/-}$ cortical cells.

In P14 brains of either genotype, GFP+ cells could be found in the SVZ, along the white matter (WM) and in the cortex (Ctx) (Figure 4.08 A). During normal postnatal development of the cortex, the Tbr2-expressing population decreases in size until only a few cells can be found in the subventricular zone (SVZ) by P14 (Figure 4.08 B, B'). At P14, I found a greater proportion of GFP+ cells in the SVZ expressed Tbr2 in *Dicer1*$^{fl/fl}$ animals than in control animals (Figure 4.08 C, C', D) with no difference in the densities of surrounding GFP-/Tbr2+ cells (Figure 4.08 E). I noted that, in the P14 cortex, *Dicer1*$^{-/-}$ GFP+ cells were often arranged in chains in the superficial layers (Figure 4.08 H, outlined) whereas GFP+ cells in P14 control superficial layers were generally evenly spread out (Figure 4.08 F). These chains of *Dicer1*$^{-/-}$ cells expressed neither the mature neuronal marker NeuN (Figure 4.08 H) nor the immature astrocyte marker GFAP (Figure 4.08 G, I), suggesting that they might be recently-born and perhaps still migrating.

Both *Dicer1*$^{-/-}$ and control cells in the P14 white matter expressed the marker of migrating neuroblasts, Doublecortin (Dcx) (Figure 4.08 J). When I examined the cortex of controls at P14, I found very few cells expressing Dcx most of which were GFP- (Figure 4.08 K, K', M). Significantly more Dcx+ cells were found in *Dicer1*$^{fl/fl}$ cortex and most of these Dcx+ cells co-expressed GFP (Figure 4.08 L, L', M). There was no difference between genotypes in the average density of Dcx+/GFP– cells in the cortex (Figure 4.08 M). Overall, these data suggest abnormal persistence of cortical neurogenesis from Tbr2-expressing intermediate progenitors among *Dicer1*$^{-/-}$ cells.

To test if the output of cortical progenitors was changed postnatally in cells that had lost mature miRNAs, I administered a daily pulse of BrdU to electroporated *Dicer*$^{fl/fl}$ and control *Dicer*$^{fl/+}$ animals between P3 and P14 (Figure 4.09 A). Cells double-labelled for GFP and BrdU could be found in both *Dicer1*$^{fl/fl}$ and *Dicer1*$^{fl/+}$ cortices (Figure 4.09 B, C, arrows). Significantly more *Dicer1*$^{-/-}$ GFP+ cells than control GFP+ cells were labelled with BrdU the P14 cortex (Figure 4.09 D), particularly in layers I, II/III, V and VI (Figure 4.09 E, F), corresponding with the increased contribution of *Dicer*$^{-/-}$ GFP+ cells to these layers shown in Figure 4.03 D. The average densities of GFP- BrdU+ cells were not different between genotypes (not shown). In *Dicer1*$^{fl/fl}$ cortices (n=3), NeuN, BrdU and GFP triple-positive cells could be detected (Figure 4.09 H - H’’’, arrows). I never observed triple-labelled cells in control animals (Figure 4.09 G – G’’’). Together, these data suggest that one or more miRNAs normally restrict cell-autonomously the production and persistence of Tbr2-expressing intermediate cortical progenitor cells. The loss of these miRNAs results in an increased specification of intermediate progenitors whose activity through into postnatal life leads to the generation of increased numbers of cortical neurons. In the following experiments I tested the possible involvement of one particular miRNA in this regulation.

Figure 4.07: Loss of mature miRNAs does not affect migration of postmitotic neurons. (A) Schema showing experimental design. E13.5 *Dicer1$^{fl/fl}$;R26RYFP^{+}* or *Dicer1$^{fl/+}$;R26RYFP^{+}* embryos were electroporated with cre-expression plasmid and exposed to a pulse of BrdU on E13.5 or E16.5 and sacrificed on E18.5. (B) Representative image of a coronal section through the cortical plate of an embryo pulse-labelled with BrdU on E13.5 showing a counting ladder composed of 11 counting boxes (50µm between steps) used to quantify the relative distribution of GFP+/BrdU+ cells. Scale bar 100µm. (B') Higher magnification image showing example of a GFP+ cell which retained BrdU (arrow). Scale bar 25 µm. (C) Relative distribution of GFP+ cells at E18.5 that were labelled with BrdU given at E13.5 shows no difference between genotypes (data represent means ± s.e.m., p-value calculated using Tukey's test for 10 control and 12 experimental embryos from 3 surgeries, 5 sections analysed per brain). (D) Image of an E18.5 cortical plate immunolabelled for GFP and BrdU after a pulse given at E16.5. Scale bar 50µm. (D') High power magnification showing a GFP+ cell which retained BrdU (arrow). Scale bar 25 µm. (E) Percent depth of cortical plate migrated was calculated by measuring the distance 'd' of each cell from the white matter (WM) as indicated by arrows in d and expressed as a percent of the thickness of the cortical plate 'D' as shown by the broken line in d. There was no difference in the distribution of GFP+/BrdU+ double labelled cells between genotypes (data represent means ± s.e.m., p-value calculated using Tukey's test for 7 control and 5 experimental embryos from 3 surgeries, 8 sections analysed per brain).

FIGURE 4.07

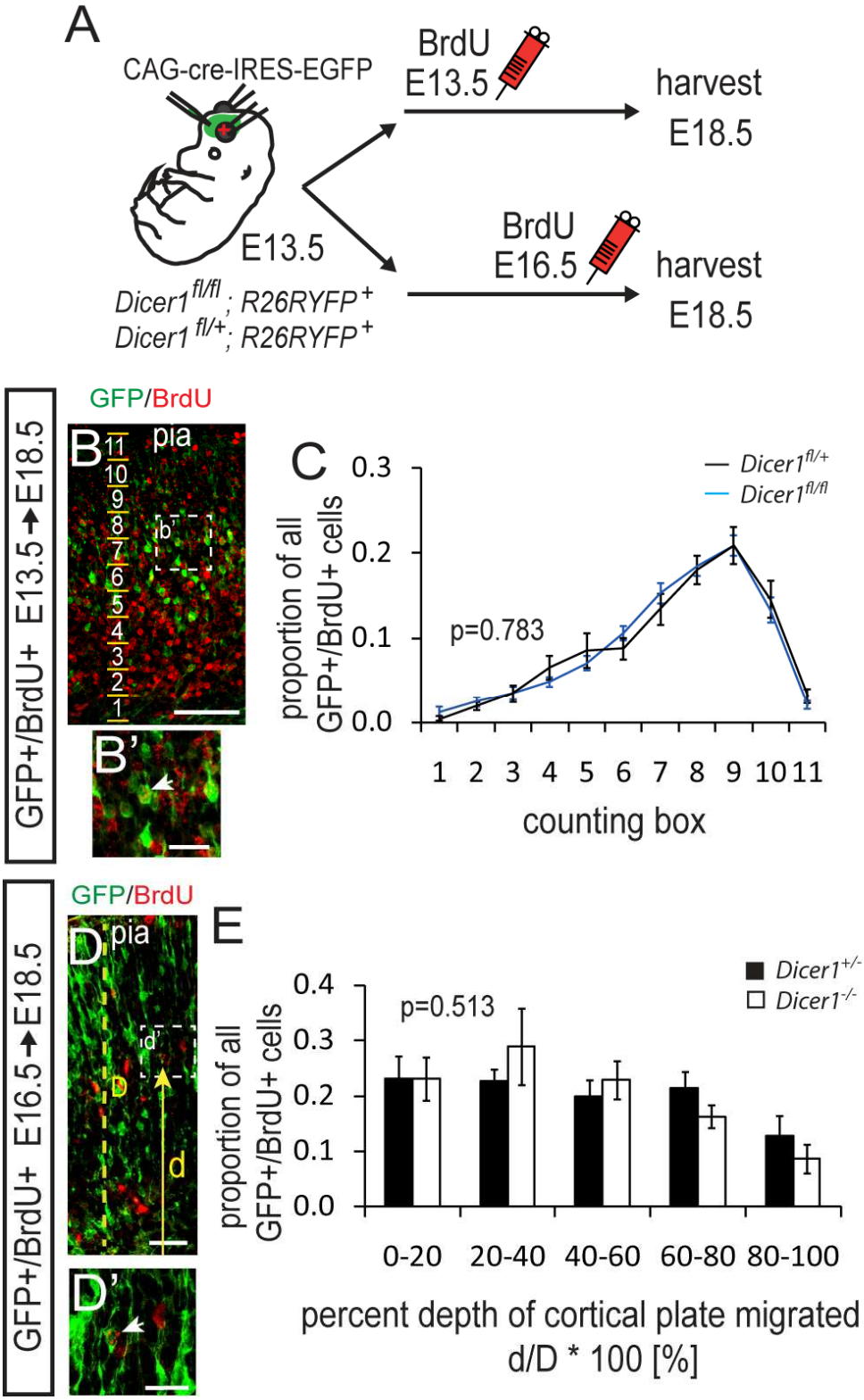
A
CAG-cre-IRES-EGFP
E13.5
Dicer1 fl/fl ; R26RYFP+
Dicer1 fl/+; R26RYFP+
BrdU
E13.5
harvest
E18.5
BrdU
E16.5
harvest
E18.5
GFP+/BrdU+ E13.5→E18.5
GFP/BrdU
B
pia
B'
C
proportion of all GFP+/BrdU+ cells
p=0.783
Dicer1 fl/+
Dicer1 fl/fl
counting box
GFP+/BrdU+ E16.5→E18.5
GFP/BrdU
D
pia
D'
E
proportion of all GFP+/BrdU+ cells
p=0.513
Dicer1 +/-
Dicer1 -/-
0-20
20-40
40-60
60-80
80-100
percent depth of cortical plate migrated
d/D * 100 [%]

Figure 4.08: Increased numbers of cortical progenitors expressing Tbr2 persist until P14 following the loss of functional Dicer. (A) Schema and example of a low power image showing the distribution of GFP+ cells typically seen in the brain of both *Dicer1*$^{fl/+}$ and *Dicer1*$^{fl/fl}$ animals in the cortex (Ctx), along the white matter (WM) and in the subventricular zone (SVZ) at P14. Scale bar 200µm. (B – B') Representative images at (B) low and (B') high magnification showing that in *Dicer1*$^{fl/+}$ SVZ at P14 GFP+ cells generally do not express Tbr2. (C – C') In *Dicer1*$^{fl/fl}$ SVZ images at (C) low and (C') high magnification GFP and Tbr2 double-labelled cells are easily detectable (arrows in C'). Scale bar b, c- 100µm, b', c'- 50 µm. (D) A higher proportion of GFP+ *Dicer1*$^{-/-}$ than *Dicer1*$^{+/-}$ cells express Tbr2 while (E) the density of GFP-/Tbr2+ cells in the SVZ was not different between genotypes. Data represent means ± s.e.m; *** - $p<0.001$, Student's t test for 8 animals from 4 surgeries, 7-8 sections counted per brain). Cells derived from the radial glia electroporated at E13.5 are expected to have reached their terminal destinations by P14 and in line with this (F) *Dicer1*$^{+/-}$ GFP+ cells are found scattered in the P14 cortex, where neurons can be labelled with NeuN and (G) astrocytes express GFAP. (H) Groups of *Dicer1*$^{-/-}$ GFP+ cells could be found arranged in chains (outlined) with most GFP+ cells negative for NeuN or (I) GFAP. Scale bar 50 µm. (J) Representative image of *Dicer1*$^{-/-}$ GFP+ cells in the WM expressing migrating neuroblast marker Doublecortin (Dcx). Scale bar 50µm. (K) Most Dcx positive cells (e.g. arrow) in the cortex at P14 did not express (K') GFP in control animals. (L) Numerous Dcx+ cells (arrows) in *Dicer1*$^{fl/fl}$ animals were double- positive for (L') GFP (arrows), primarily in deep layers of the cortex. Scale bar 50µm. (M) More Dcx expressing *Dicer1*$^{-/-}$ than *Dicer1*$^{+/-}$ cells were found per unit area of the electroporated cortex, while densities of Dcx+/GFP- cells were not different. Data represent means ± s.e.m., * - $p<0.05$, Student's t test for 6 animals from 3 surgeries, a single section was analysed per animal, counting box was 400µm wide and spanned the entire depth of the cortical wall.

FIGURE 4.08

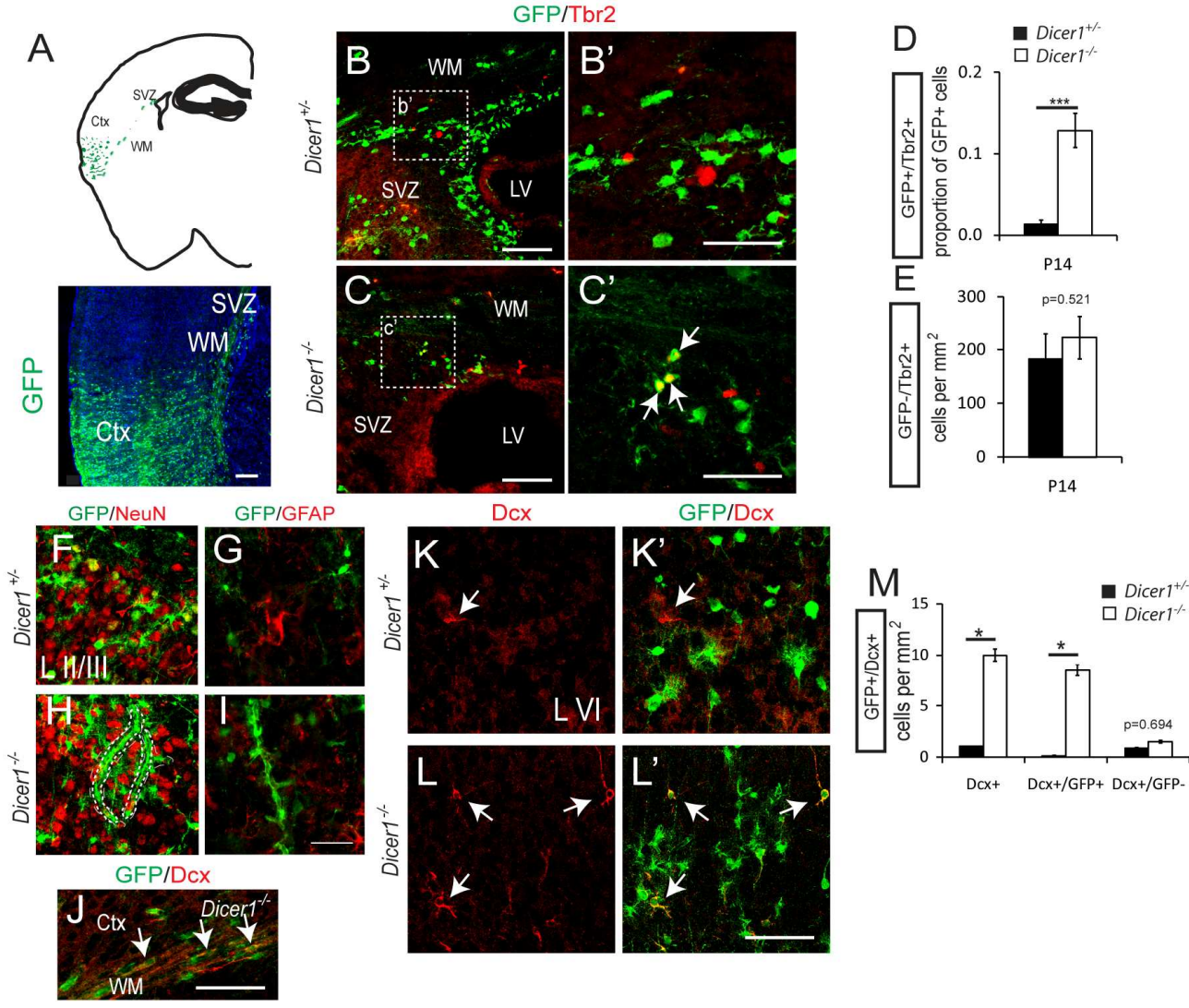
A
SVZ
Ctx
WM
GFP
SVZ
WM
Ctx
GFP/Tbr2
B
WM
b'
SVZ
LV
B'
Dicer1+/-
C
WM
c'
SVZ
LV
C'
Dicer1-/-
D
Dicer1+/-
Dicer1-/-
GFP+/Tbr2+ proportion of GFP+ cells
0.2
0.1
0.0
***
P14
E
GFP-/Tbr2+ cells per mm2
300
200
100
0
p=0.521
P14
GFP/NeuN
GFP/GFAP
F
G
Dicer1+/-
L II/III
H
I
Dicer1-/-
GFP/Dcx
J
Ctx
Dicer1-/-
WM
Dcx
GFP/Dcx
K
K'
Dicer1+/-
L VI
L
L'
Dicer1-/-
M
Dicer1+/-
Dicer1-/-
GFP+/Dcx+ cells per mm2
15
10
5
0
*
*
p=0.694
Dcx+
Dcx+/GFP+
Dcx+/GFP-

Figure 4.09: Increased postnatal neurogenesis following the loss of Dicer. (A) Schema showing the experimental design. *Dicer1*$^{fl/+}$ and *Dicer1*$^{fl/fl}$ embryos were electroporated with cre-expression vector at E13.5. Pups aged P3 - P14 received daily injections of BrdU. (B, C) Both *Dicer1*$^{+/-}$ and *Dicer1*$^{-/-}$ cells retaining BrdU were readily identifiable (arrows). Scale bar 25 µm. (D) A significantly higher proportion of *Dicer1*$^{-/-}$ cells in P14 cortices retained BrdU (data represent means ± s.e.m., **** - $p<10^{-4}$, Student's t test for 6 animals of each genotype with 2 sections counted per animal). (E, F) The distribution of GFP+/BrdU+ cells was quantified using a counting ladder consisting of 12 identical 300µm x 100µm boxes, shown in e. Significantly more GFP+ cells retaining BrdU derived from Dicer– deficient radial glia were found in layers I, II/III, V and VI retained BrdU (data represent means ± s.e.m, *** - $p<0.001$, * - $p<0.05$, Tukey's test for 6 animals from 3 surgeries of each genotype with 2 sections counted per animal). (G- G''') Representative image showing layer I of the electroporated *Dicer1*$^{fl/+}$ embryos immunolabelled for (G) GFP, (G') NeuN, (G'') BrdU showing that (G''') triple labelling was not detectable. (H- H''') In cortical layer I of electroporated *Dicer1*$^{fl/fl}$ embryos immunolabelled for (H) GFP, (H') NeuN and (H'') BrdU shows at least some *Dicer1*$^{-/-}$ cells triple- labelled (arrows). Scale bar 50µm.

FIGURE 4.09

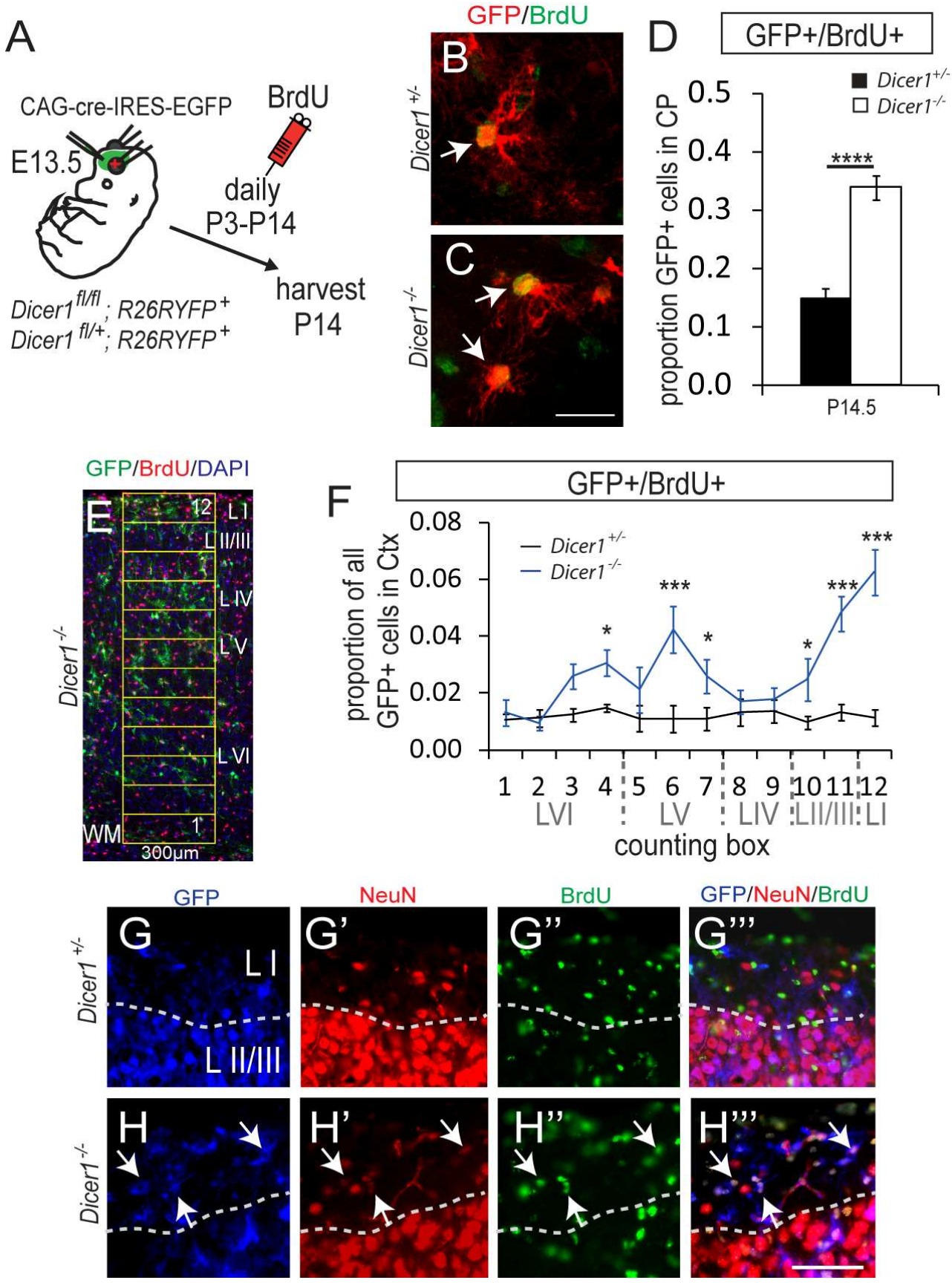
A
CAG-cre-IRES-EGFP
BrdU
E13.5
daily
P3-P14
harvest
P14
Dicer1 fl/fl ; R26RYFP+
Dicer1 fl/+ ; R26RYFP+
GFP/BrdU
B
C
Dicer1 +/-
Dicer1 -/-
D
GFP+/BrdU+
Dicer1+/-
Dicer1-/-
proportion GFP+ cells in CP
0.5
0.4
0.3
0.2
0.1
0.0
****
P14.5
GFP/BrdU/DAPI
E
12
1
L I
L II/III
L IV
L V
L VI
WM
300µm
Dicer1 -/-
F
GFP+/BrdU+
Dicer1+/-
Dicer1-/-
proportion of all GFP+ cells in Ctx
0.08
0.06
0.04
0.02
0.00
*
***
1 2 3 4 5 6 7 8 9 10 11 12
LVI
LV
LIV
LII/III
LI
counting box
GFP
NeuN
BrdU
GFP/NeuN/BrdU
G
G'
G''
G'''
L I
L II/III
Dicer1 +/-
H
H'
H''
H'''
Dicer1 -/-

4.2.5 MiR92b limits Tbr2 expression and intermediate progenitor cells

I decided to test the possible involvement of miR92b for several reasons. First, it is known to be strongly expressed in neural progenitor cells, although its physiological target is not known (Kapsimali et al., 2007; Meza-Sosa et al., 2012). Second, a single conserved site complementary to the seed region of miR92b (miRBase (Griffiths-Jones, 2004) accession: MI000521) is predicted in the 3' UTR of the mouse Tbr2 mRNA (Refseq: NM_010136.3), between nucleotides 2707 – 2714 (Figure 4.10 A) (Betel et al., 2008). Third, a previous study using microarrays to profile miRNAs and mRNAs in rat dorsal telencephalic progenitor cells proposed that miR92a and/or miR92b might regulate Tbr2 expression (Nielsen et al., 2009).

In situ hybridisation staining for mature miR92b was present throughout the developing cortex at E14.5. In the lateral cortex, which is more advanced at this age and where the SVZ is visibly formed, staining was stronger in the ventricular and intermediate zones and the cortical plate than in the SVZ, where immunostaining for Tbr2 was strong (Figure 4.11 A – B''). This suggests that high levels of miR92b could limit Tbr2 expression.

I generated a miR92b overexpression vector (GFP-miR92b) by cloning the genomic sequence containing the pre-miR92b stem loop sequence (miRBase accession: MI000521) downstream of a stop codon in a GFP expression vector (Figure 4.10 A). The GFP expression vector lacking the pre-miR92b stem loop was used as a control (Figure 4.10 B). Overexpression of miR92b in HEK-293 cells reduced *Renilla* luciferase reporter activity when the reporter sequence was joined to the full length wild-type 3'UTR of Tbr2 (construct WT 3'UTR) but not when the response element between nucleotides 2707–2714 of the full-length Tbr2 3'UTR (Refseq: NM_010136.3) was deleted using site-directed mutagenesis (construct MT 3'UTR) (Figure 4.10 B – C).

Figure 4.10: Mature miR92b interacts with the 3'UTR of Tbr2 *in vitro*. (A) MiR92b overexpression plasmid was generated by cloning the genomic sequence of the pre-miR92b hairpin downstream of a GFP coding cassette. Only one response element has been predicted for the 3'UTR of Tbr2, nt. 2707-2714 (red). (B) Vectors generated to test the ability of miR92b to interact with the 3'UTR *in vitro*. GFP expression plasmid was used as a control. The putative response site to miR92b in the 3'UTR was deleted to validate specificity. (C) Dual luciferase assay in HEK-293 cells demonstrates that miR92b can inhibit the expression of *Renilla* luciferase by interacting with the wild type 3'UTR sequence of the Tbr2 mRNA shown in a but not when nucleotides 2707-2714 are mutated. Data represent means ± s.e.m., * - $p<0.05$, ** - $p<0.01$, two tailed unpaired Student's t test for n=3 transfections.

FIGURE 4.10

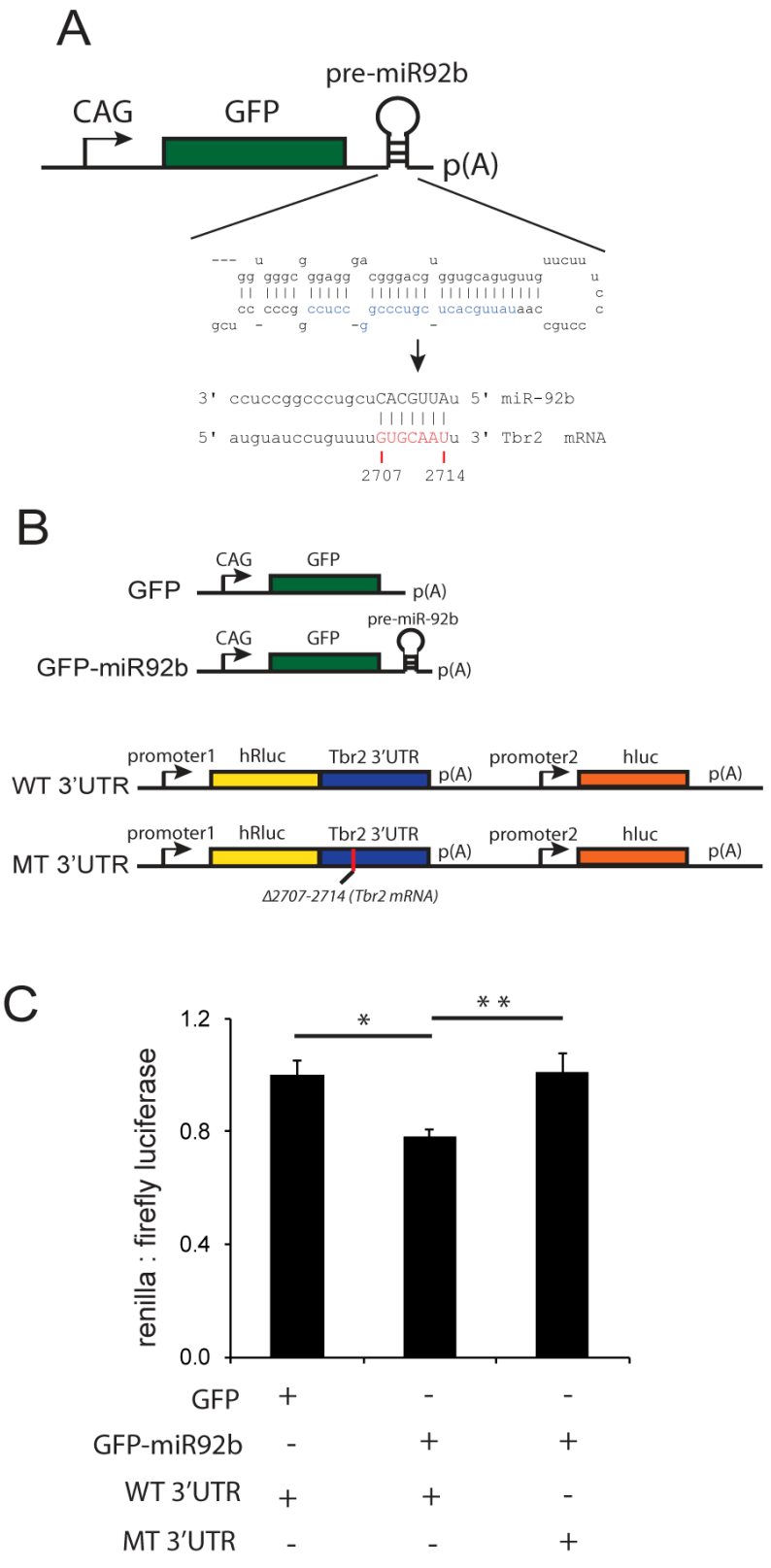
A
pre-miR92b
CAG
GFP
p(A)
3' ccuccggcccugcuCACGUUAu 5' miR-92b
5' auguauccuguuuuGUGCAAUu 3' Tbr2 mRNA
2707 2714
B
GFP
CAG
GFP
p(A)
pre-miR-92b
GFP-miR92b
WT 3'UTR
promoter1
hRluc
Tbr2 3'UTR
promoter2
hluc
MT 3'UTR
Δ2707-2714 (Tbr2 mRNA)
C
renilla : firefly luciferase
1.2
0.8
0.4
0.0
GFP + - -
GFP-miR92b - + +
WT 3'UTR + + -
MT 3'UTR - - +

Figure 4.11: Expression of miR92b at E14.5. (A – B'') Images of *in situ* hybridisation for miR92b (A, B), immunostaining for Tbr2 (A', B') and the overlays (A'', B''). Mature miR92b staining is enriched in the ventricular zone (VZ), part of the intermediate zone (IZ) and the cortical plate (CP) while in the lateral cortex it is less intense in the subventricular zone (SVZ), which has formed in this region due to its relative maturity compared to more medial cortex. There is reciprocity in the staining for Tbr2 and that for miR92b: staining for Tbr2 is strong in the SVZ, where staining for miR29b is relatively weak, and regions of the VZ that stain most strongly for miR29b do not stain for Tbr2. Scale bars 100µm. To verify the specificity of the *in situ* hybridisation probe GFP-miR92b vector was electroporated into E13.5 embryos. (C – C''') Images of control hemispheres immunostained for (C) GFP, (C') miR92b, (C'') Tbr2 and (C''') their overlay. In electroporated hemisphere containing (D) GFP+ cells stronger (D') *in situ* staining for miR29b and (D'') less staining for Tbr2 can be seen in the dorso-lateral telencephalon, (D''') coinciding with GFP+ cells. Scale bar 100µm.

FIGURE 4.11

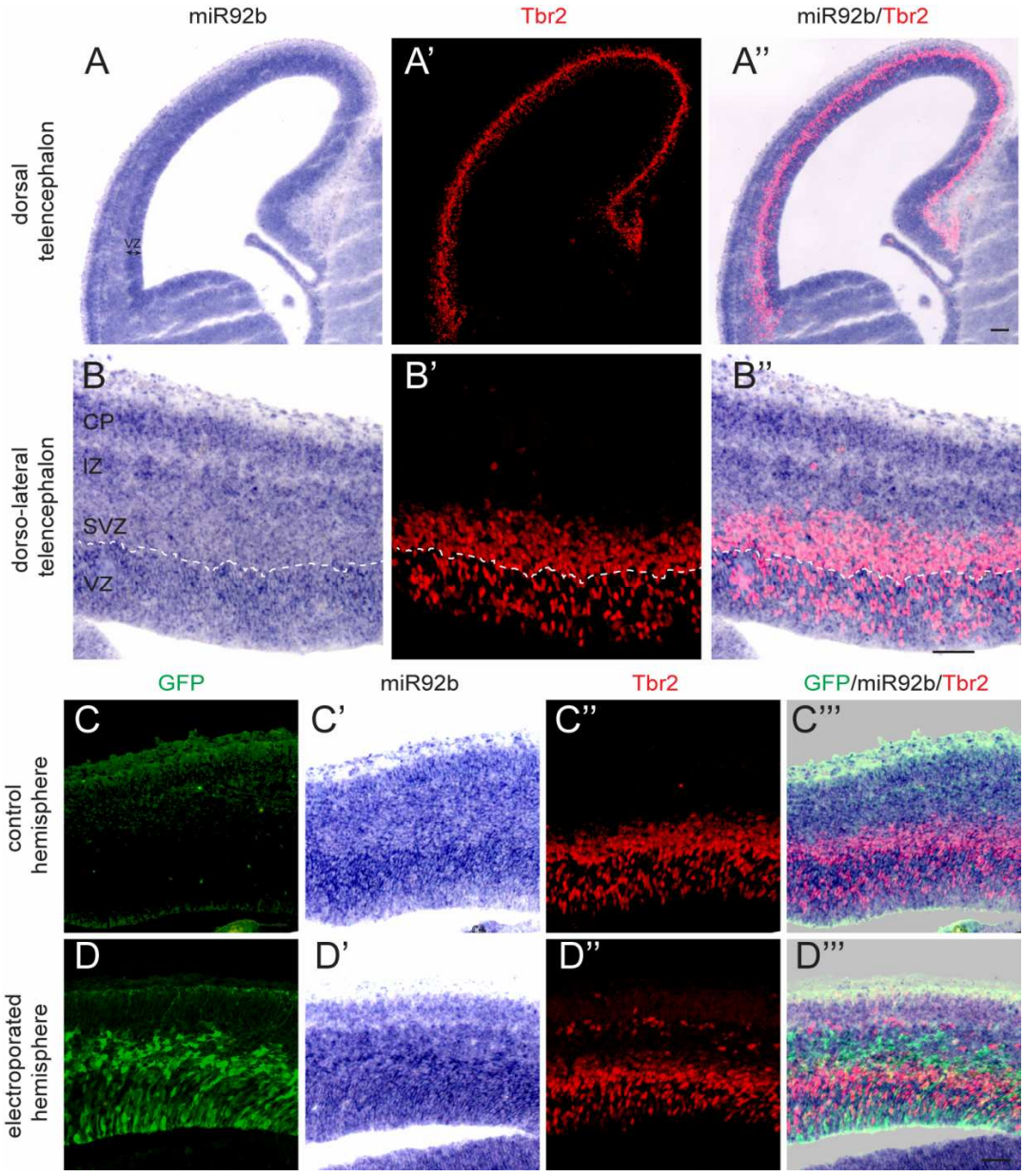
miR92b
Tbr2
miR92b/Tbr2
A
A'
A''
dorsal telencephalon
VZ
B
B'
B''
dorso-lateral telencephalon
CP
IZ
SVZ
VZ
GFP
miR92b
Tbr2
GFP/miR92b/Tbr2
C
C'
C''
C'''
control hemisphere
D
D'
D''
D'''
electroporated hemisphere

The ability of miR92b to regulate the expression of Tbr2 *in vivo* was assessed by electroporating the GFP-miR92b vector *in utero* into the cortex of wild type E13.5 embryos (Figure 4.11 C – D’’’). Overexpression was confirmed at E14.5 by comparing the pattern of miR92b *in situ* hybridisation staining between control and electroporated hemispheres; staining was increased in regions containing GFP+ cells (Figure 4.11 C, C’, D, D’). This increase was associated with a reduction in Tbr2 staining on the electroporated side (Figure 4.11 C’’, C’’’, D’’, D’’’). Electroporation of the miR92b overexpression vector resulted in fewer GFP+ cells that were double-positive for Tbr2 than electroporation of control GFP-only vector (Figure 4.12 A, B; compare black and blue bars in E). This phenotype was rescued when GFP-miR92b was co-electroporated with the WT-3’UTR vector (Figure 4.10 B) which expresses the wild type 3’UTR of Tbr2 to act as a competitor with the endogenous 3’UTR (Figure 4.12 C; orange bar in E). Conversely, the MT-3’UTR vector (Figure 4.10 B) expressing the 3’UTR of Tbr2 mRNA lacking the miR92b putative binding site failed to rescue the phenotype (Figure 4.12 D; green bar in E). Analysis of the laminar distribution of GFP+/Tbr2+ double positive cells revealed that the downregulation of Tbr2 at E14.5 after miR92b overexpression is greatest in the abventricular portion of the ventricular zone and lower SVZ (Boxes 2 and 3 in Figure 4.12 F, G), which corresponds precisely to the areas where Tbr2 was found to be upregulated at the same age following the mutation of *Dicer1* (Figure 4.06 K).

To test whether endogenous miR92b can limit Tbr2 expression *in vivo* I co-electroporated the GFP and WT-3’UTR plasmids, since the competition between WT-3’UTR and the endogenous binding site in the 3’UTR of Tbr2 mRNA would lower the levels, and hence the function, of miR92b at the endogenous site. This resulted in an increased proportion of cells expressing GFP and Tbr2 as compared with cells electroporated only with the GFP expression vector (Figure 4.12 E, G: purple bar and line). Conversely, the MT 3’UTR plasmid lacking miR92b binding site did not produce the same effect (Figure 4.12 E, G: red bar and line) demonstrating that miR-92b is an important physiological inhibitor of Tbr2 expression.

Finally, I correlated changes in the expression of Tbr2 as a result of modulation of miR92b levels with changes in cell proliferation. I predicted that soon after electroporation with the GFP-miR92b overexpression vector, as a consequence of

resulting Tbr2 downregulation, fewer proliferative GFP+ cells would be found in the SVZ but not the ventricular zone. To test this prediction, wild type E13.5 embryos were electroporated either with GFP or GFP-miR92b expression vectors. The embryos were exposed to BrdU for 1 hour on E15.5 to label cells in S-phase (Figure 4.13 A – C'). The result of overexpression of miR92b was to significantly reduce by about 30% the overall proportion of GFP+ cells that incorporated BrdU (Figure 4.13 D), as a consequence of reductions specifically in the SVZ and not in other layers (Figure 4.13 E). Overexpression also caused an increase in the relative proportion of GFP+ cells (most of which did not contain BrdU) in the intermediate zone (Figure 4.13 F), suggesting that the decrease in the proliferative population in the SVZ was accompanied by a corresponding increase in the exit of cells from the proliferative zones towards the cortical plate. My data strongly suggest that miR92b, via its significant role in regulating Tbr2, is important to control the balance between the intermediate progenitor and the postmitotic states (Figure 4.13 G).

Figure 4.12: miR92b targets Tbr2 *in vivo*. (A – D) Images show representative examples of sections through the E14.5 telencephalic wall electroporated at E13.5 with (A) control GFP expression vector, (B) miR92b overexpressing GFP-miR92b vector only or co-electroporated with (C) GFP-miR92b and a vector expressing the full 3'UTR of Tbr2 or (D) GFP-miR92b and a vector expressing the mutated 3'UTR of Tbr2 lacking nt. 2707-2714. Arrows indicate GFP and Tbr2 double-labelled cells. Scale bar 50µm. (E) Overexpression of miR92b results in downregulation of Tbr2 protein expression (blue) compared to control GFP-vector expression (black), which can be rescued by overexpressing the full length 3'UTR of Tbr2 (orange) but not when the miR92b response element was mutated (green). When the action of endogenous miRNAs was competed out with the full-length 3'UTR the Tbr2 expression increased (purple) but not when the 3'UTR lackied the miR92b response element (red) (data represent means ± s.e.m., ** - $p<0.01$, *** - $p<0.001$, two-tailed unpaired Student's t test for 8-11 embryos from 3 surgeries, 3 sections analysed per brain). (F) Example of an image used to quantify the distribution of GFP+/Tbr2+ cells at E14.5 with a counting ladder consisting of 10 boxes (200µm x 40 µm). (G) Analysis of the distribution of GFP/Tbr2 double-positive cells manipulated as in e shows that by E14.5 changes in Tbr2 expression took place mainly in the abventricular portion of the ventricular zone (VZ) and the subventricular zone (SVZ).

FIGURE 4.12

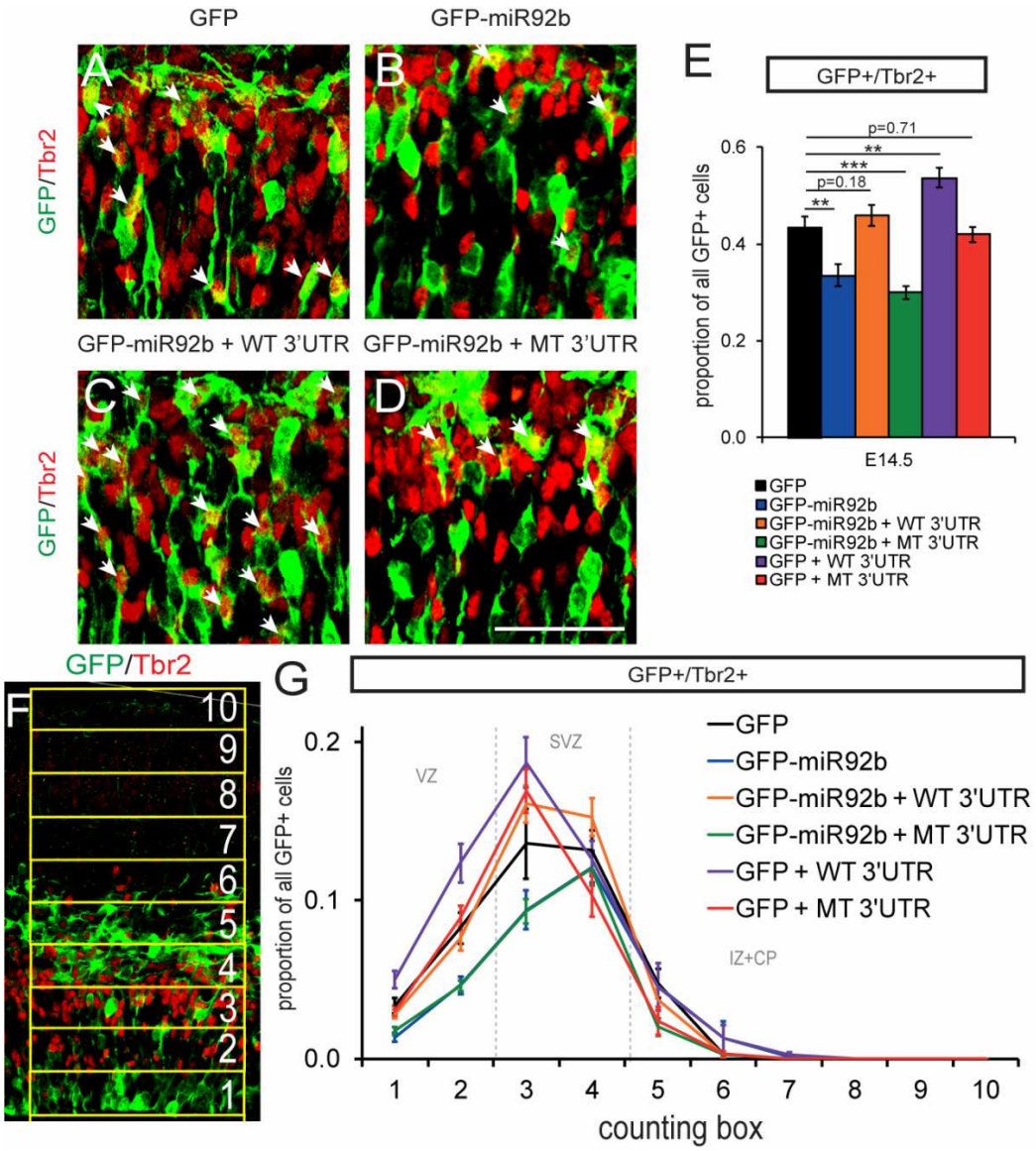
GFP
GFP-miR92b
A
B
GFP/Tbr2
GFP-miR92b + WT 3'UTR
GFP-miR92b + MT 3'UTR
C
D
GFP/Tbr2
E
GFP+/Tbr2+
p=0.71
**
***
p=0.18
**
proportion of all GFP+ cells
0.6
0.4
0.2
0.0
E14.5
GFP
GFP-miR92b
GFP-miR92b + WT 3'UTR
GFP-miR92b + MT 3'UTR
GFP + WT 3'UTR
GFP + MT 3'UTR
GFP/Tbr2
F
10
9
8
7
6
5
4
3
2
1
G
GFP+/Tbr2+
VZ
SVZ
IZ+CP
proportion of all GFP+ cells
0.2
0.1
0.0
1
2
3
4
5
6
7
8
9
10
counting box
GFP
GFP-miR92b
GFP-miR92b + WT 3'UTR
GFP-miR92b + MT 3'UTR
GFP + WT 3'UTR
GFP + MT 3'UTR

Figure 4.13: miR92b regulates intermediate progenitor cell specification. (A) Schema showing electroporation of either GFP or GFP-miR92b expression plasmid into wild type C57BL/6J mice on E13.5 followed by BrdU labelling of cells in S-phase on E15.5. (B, C) Example images of telencephalon electroporated with control GFP or miR92b expression plasmid showing GFP+ cells some of which incorporate BrdU, with high power examples shown in B' and C' (arrows). (D) Overall, fewer GFP-miR92b expressing cells incorporated BrdU and (E) the analysis of the distributions of GFP+/BrdU+ cells showed fewer GFP-miR92b cells incorporating BrdU on E15.5 in the subventricular zone. (F) Analysis of the relative distribution of GFP+ cells showed more cells in the intermediate zone following miR-92b overexpression (data in D – F represent means ± s.e.m., ** - $p<0.01$, *** - $p<0.001$, Tukey's test for 12 embryos from 3 surgeries, with 3 sections analysed per brain). (G) Schema showing my model proposing that miR92b overexpression results in fewer cells entering the indirect rather than the direct neurogenesis pathway.

FIGURE 4.13

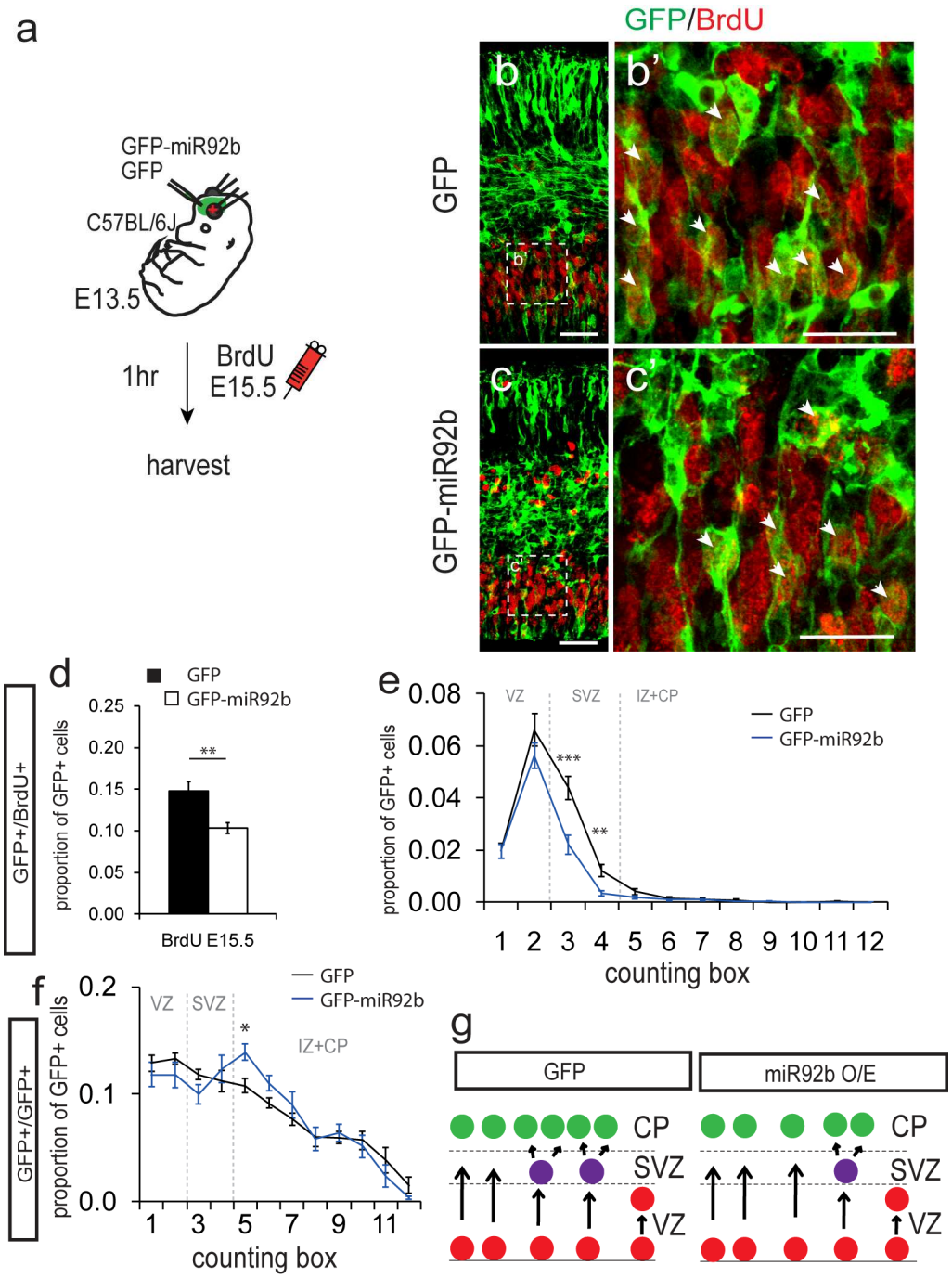
a
GFP-miR92b
GFP
C57BL/6J
E13.5
1hr
BrdU
E15.5
harvest
GFP/BrdU
GFP
GFP-miR92b
b
b'
c
c'
d
GFP+/BrdU+
proportion of GFP+ cells
GFP
GFP-miR92b
**
BrdU E15.5
e
proportion of GFP+ cells
VZ
SVZ
IZ+CP
GFP
GFP-miR92b
***
**
counting box
f
GFP+/GFP+
proportion of GFP+ cells
VZ
SVZ
IZ+CP
GFP
GFP-miR92b
*
counting box
g
GFP
miR92b O/E
CP
SVZ
VZ

4.3 Discussion

Intermediate progenitor cells are thought to be the key neuron- producing cells in the developing cortex (Kowalczyk et al., 2009). An increase in the size of the intermediate progenitor population and the prolongation of the neurogenic period are believed to have coincided with the expansion of the neocortex in mammals (Kriegstein et al., 2006). Mechanisms controlling the size of the intermediate progenitor population during development remain unclear but are of great interest for understanding the mechanisms of cortical development and evolution.

Several factors regulating the specification and maintenance of the intermediate progenitors have been described and most are thought to act both in the radial glia and in the intermediate progenitors (Pontious et al., 2008). Unlike most of these factors, Tbr2 seems to act specifically in cells from the time of their exit from the radial glial cell state, driving them towards the intermediate progenitor state. Loss of Tbr2 results in loss of intermediate progenitor cells but causes no detectable changes to the radial glial population (Arnold et al., 2008; Sessa et al., 2008). My discovery of a microRNA that regulates Tbr2 adds significantly to our understanding of how the numbers of intermediate progenitor cells, and hence of cortical neurons, are regulated.

The abnormal presence of *Dicer*$^{-/-}$ neurons in layer I was a striking result whose explanation fits well with my model of prolonged cortical neurogenesis after loss of Dicer. Cajal-Retzius neurons, which are generated around E11.5, are known to safe-guard layer I from new neurons entering it but they disappear during postnatal development(Chowdhury et al., 2010; Hashimoto-Torii et al., 2008). In layer I of the P14 *Dicer1*$^{fl/fl}$ and *Dicer1*$^{fl/+}$ cortex the densities of non-electroporated cells were not significantly different and so it can be anticipated that the disappearance of Cajal-Retzius cells takes place at a normal rate in *Dicer1*$^{fl/fl}$ electroporated areas. This might explain why *Dicer*$^{-/-}$ neurons born late during postnatal development and arriving in the cortex following the loss of Cajal-Retzius might have failed to terminate their migration before entering layer I.

It is unclear if the increased specification of intermediate progenitors and prolongation of neurogenesis following the loss of miRNAs are both caused by the increased expression of Tbr2, or whether the loss miRNAs extends the neurogenic

period by a separate mechanism. To the best of my knowledge, long term gain of Tbr2 function study has not been performed and so it is not possible to determine whether increased production of intermediate progenitor cells would be sufficient to extend the time-span of mouse cortical neurogenesis. However, it could be speculated that an abnormally large population of intermediate progenitors generated during embryonic development could result in a delayed postnatal depletion of that population. Another possibility is that due to the increased expression of Tbr2 the intermediate progenitor cells increase their rate of cell cycle re-entry. It has been recently suggested that the intermediate progenitors are instrumental to the maintenance of radial glia proliferation (Yoon et al., 2008) and so an enlarged population of subventricular progenitors could result in an extended maintenance of undifferentiated radial glia.

This study describes experimental evidence that miR92b regulates the expression of Tbr2 in the developing cortex. This miRNA has previously been described to be expressed at high levels in proliferating populations such as neural progenitors (Kapsimali et al., 2007), to target cell cycle checkpoint gene p57 in mouse embryonic stem cells (Sengupta et al., 2009) and Dickkopf-3 in neuroblastoma (Haug et al., 2011). It is believed to target a similar, if not identical, repertoire of transcripts as miR92a (Ventura et al., 2008). The response element to miR92ab in the 3'UTR of Tbr2 mRNA is conserved in mammalian species (Figure 4.14 A) and so it is likely that the interaction between miR92b and the 3'UTR of Tbr2 mRNA is also conserved.

The expansion of the neocortex has been recently proposed to be largely due on the expansion of the subventricular zone and the progenitors residing therein acting to amplify the cellular output of the radial glia by indirect neurogenesis (Lui et al., 2011). It remains to be investigated if miR92b could have contributed to this, for example due to changes in its expression. Mechanisms regulating miRNA expression at the transcriptional level are very poorly understood, although it has been appreciated that the upstream genomic sequence contains similar chromatin structure as that of protein coding genes (Ozsolak et al., 2008). In addition, several factors have been shown to regulate the processing and stability of pre-miRNA hairpin and these include the secondary structure of the hairpin itself, sequence modifications and RNA binding proteins (Krol et al., 2010b). Sequence comparison of some of the

mammalian pre-miR92b hairpins (Figure 4.14 B) shows that while most of the sequence is very highly conserved, a few discreet nucleotide differences exist between rodents and primates, particularly in the unpaired regions of the hairpin (Figure 4.14 C), and could result in changes to miRNA processing or activity. However, very little is currently known about the evolutionary conservation miRNAs and whether changes in their hairpin precursor sequence or expression levels could have contributed to the evolution of tissues, such us the cerebral cortex.

Figure 4.14: Conservation of miR92b and the response element in the 3'UTR of Tbr2. (A) Multiple sequence alignment of sections of Tbr2 mRNAs containing the response element to miR92b from 16 mammalian species (highlighted in yellow). (B) Alignment of precursor miR92b sequences from 9 mammalian species including rodents and primates (MirBase accession numbers next to miRNA name). Mature miR92b is highlighted in yellow and most of the nucleotides are identical in all species (*). Mouse miR92b differs from other species at a few residues (highlighted in green). (C) Predicted secondary structure of the mouse pre-miR92b hairpin shows that residues which are different between the mouse and other mammals are not part of the mature miRNA sequence and are not involved in base-pairing. All sequence alignments were performed using ClustalW.

FIGURE 4.14

A

```
P.troglodytes       CTTG-ATGCATCCTGTTTTGTGCAATTCTCTAAAAGAAGGTGCCAAAGCTTTTTGATTGC 5158
H.sapiens           CTTG-ATGCATCCTGTTTTGTGCAATTCTCTAAAAGAAGGTGCCAAAGCTTTTTGATTGC 5594
G.gorilla           CTTG-ATGCATCCTGTTTTGTGCAATTCTCTAAAAGAAGGTGCCAAAGCTTTTTGATTGC 5367
M.mulata            CTTG-ATGCATCCTGTTTTGTGCAATTCTCTAAAAGAAGGTGCCAAAGCTTTTTGATTGC 5026
N.leucogenys        CTTA-ATGCATCCTGTTTTGTGCAATTCTCTAAAAGAAGGTGCCAAAGCTTTTTGATTGC 5346
C.jacchus           CTTG-ATGCATCCTGTTTTGTGCAATTATCTAAAAGAAGGTGCCAAAGCTTTTTGATTGC 5371
M.murinus           CTTG-ATGCGTCCTGTTTTGTGCAATTCTCTTAAAGAAGGTGCCAAAGCTTTTTGATTGC 5384
L.africana          CTCC-CTGCATCCCGTTTTGTGCAATTCTCTAAAG-AAGGTGCCAAAGCTTTTTGATTG- 5270
O.cuniculus         CTTG-ATGCATCCTGTTTTGTGCAATTGTCTCAAAGAAGGTGCCAAAGCTTTTTGATTGC 5103
M.musculus          CTTTGATGTATCCTGTTTTGTGCAATTCTCTGAGAGAAGGCGCCAAAGCTTTGCCACGGC 6822
C.familiaris        CTCG-ATGCATCCCGTTTTGTGCAATCCTCTAAAAGAAGGTACCAAAGCTTTTTGATTGC 5416
E.caballus          CTTG-ATGCGTCCCGTTTTGTGCAATTCTCTAAAAGAAGGTGCCAAAGCTTTTTGATTGC 5292
S.scrofa            CTTG-ACGCATACTGTTTTGTGCAATTCTCTAAAAGAAGGTGCCAAAGCGTTTCGATTGC 5200
B.taurus            CCCG-ATGTGTCCTGTTTTGTGCAATTCTCTAAAAGAAGGTGCCAAAGCTTTTTGACTGC 5172
T.truncatus         CCTG-ATGCATCCCGTTTTGTGCAATTCTCTAAAAGAAGGTGCCAAAGCTTTTTGATTGC 5530
F.catus             CATG-ATGCATCCTGTTTTGTGCAATCCTCTAAAAGAAGGTGCCAAAGCTTTTTGATTGC 6138
                    *    . * .*.* ************  *** *.. **** .******* **   *  *
```

B

pre-miR-92b

```
hsa-mir-92b MI0003560  CGGGCCCCGGGCGGGCGGGAGGGACGGGACGCGGUGCAGUGUUGUUUUUUCCCCCGCCAA 60
ppy-mir-92b MI0014809  CGGGCCCCGGGCGGGCGGGAGGGACGGGACGCGGUGCAGUGUUGUUUUUUCCCCCGCCAA 60
mml-mir-92b MI0007607  CGGGCCCCGGGCGGGCGGGAGGGACGGGACGCGGUGCAGUGUUGUUCUUUCCCCCGCCAA 60
eca-mir-92b MI0012719  ------------GGGCGGGAGGGACGGGACGCGGUGCAGUGUUGUUCUUUCCCCCGCCAA 48
cfa-mir-92b MI0008119  --------------------AGGGACGGGACGCGGUGCAGUGUUGUUCUCUCCCCCGCCAA 41
ssc-mir-92b MI0013126  ----------GCGGGCGGGAGGGACGGGACGCGGUGCAGUGUUGUUCUUUCCCCUGCCAA 50
bta-mir-92b MI0009906  CGGGCCCCGGGCGGGCGGGAGGGACGGGACGCGGUGCAGUGUUGUUCUUUCCCCUGCCAA 60
rno-mir-92b MI0006167  ---------GGUGGGCAGGAGGGACGGGACGCGGUGCAGUGUUGUUCUUUCCCCUGCCAA 51
mmu-mir-92b MI0005521  ---------GGUGGGCGGGAGGGACGGGACGUGGUGCAGUGUUGUUCUUUCCCCUGCCAA 51
                                 ************ ************** * ***** *****

hsa-mir-92b MI0003560  UAUUGCACUCGUCCCGGCCUCCGGCCCCCCCGGCCC 96
ppy-mir-92b MI0014809  UAUUGCACUCGUCCCGGCCUCCGGCCCCUCCGGCCC 96
mml-mir-92b MI0007607  UAUUGCACUCGUCCCGGCCUCCGGCCCCCCCGGCCC 96
eca-mir-92b MI0012719  UAUUGCACUCGUCCCGGCCUCCGGCCC--------- 75
cfa-mir-92b MI0008119  UAUUGCACUCGUCCCGGCCUCC-------------- 63
ssc-mir-92b MI0013126  UAUUGCACUCGUCCCGGCCUCCGGCCCCC------ 80
bta-mir-92b MI0009906  UAUUGCACUCGUCCCGGCCUCCGGCCCCCUCGGCCC 96
rno-mir-92b MI0006167  UAUUGCACUCGUCCCGGCCUCCGGCCCCCUCG---- 83
mmu-mir-92b MI0005521  UAUUGCACUCGUCCCGGCCUCCGGCCCCCUCG---- 83
                       **********************
```

C

pre-mmu-miR-92b

```
---  u    g     ga       u           uucuu
   gg gggc ggagg  cgggacg ggugcaguguug     u
   || |||| |||||  |||||||  ||||||||||||     c
   cc cccg ccucc  gcccugc ucacguuauaac      c
gcu  -    g     -g       -            cguccc
```

CHAPTER 5:
General Discussion

Inspiration to pursue the research questions addressed in this thesis was driven by a paper from Gregory Wulczyn's lab which looked at the temporal variation of miRNA expression during the development of mouse brain (Smirnova et al., 2005). The data suggested that miRNA expression may be developmentally regulated. This project was focused initially on an attempt to reveal what developmental processes are crucially dependent on miRNA production. This was first addressed by ablating functional Dicer throughout the developing telencephalon using the conditional cre-LoxP system using mice expressing cre under the regulation of the endogenous *Foxg1* regulatory region. It was concluded that neuroepithelial stem cells which are unable to produce mature miRNAs fail to correctly specify the radial glia. Second, I generated a mosaic ablation of functional Dicer by delivering a cre expression vector by *in utero* electroporation into a subset of the radial glia. Analysis of the short and long term effects on the population of *Dicer1*$^{-/-}$ cells generated in this way suggested that miRNAs are important regulators of the specification of intermediate progenitor cells in the developing cortex. Third, miR92b was shown to regulate the expression of Tbr2 in the developing cortex *in vivo*. Together, the data presented in this thesis support the idea that the miRNA pathway is important for normal development of the progenitor cells of the cortex.

As a result of miRNA depletion in the early telencephalon, a large proportion of the neuroepithelial cells undergo apoptosis and this is a phenotype found in every model of Dicer deficient cortex generated using genetic cre lines described so far (De Pietri Tonelli, 2008; Kawase-Koga et al., 2009; Konopka et al., 2010). The onset of apoptosis following the *Foxg1*^{cre} induced Dicer ablation takes place earlier than in the cases of other cre drivers and this is consistent with the idea that the onset of defects following miRNA depletion correlates with the timing of cre activity (Kawase-Koga et al., 2009) (Figure 5.1). In contrast, the result showing absence of apoptosis of Dicer deficient cells following the mosaic loss of Dicer in the radial glia remains to be reconciled with the literature. This difference might be accounted for by the fact that different studies used different methods to assess cell death (immunostaining for cleaved caspase-3 versus transferase- mediated biotinylated UTP nick end labelling staining) which may have different sensitivity to recognising apoptotic cells and it is possible that I have underestimated the proportion of apoptotic cells in the absence of functional Dicer following the electroporation of

cre- expression vector. It has been suggested that the rate of clearance of apoptotic cells may be very rapid in the telencephalon (Wilkie et al., 2004) and therefore differences in the sensitivity of detection of apoptotic cells between different approaches may lead to different conclusions. Nonetheless, the fact that *Dicer1*$^{-/-}$ cells were found to contribute to a higher proportion of cells at P14 strongly suggests that if Dicer- deficient cells undergo apoptosis the loss of *Dicer1*$^{-/-}$ cells had a lesser effect than the embryonic and/or postnatal overproduction of cortical cells by the electroporated radial glia.

An alternative explanation could be that the pool of mature miRNAs is not restricted to individual cells and so the wild type cells present in the vicinity of Dicer deficient cells could rescue the apoptotic phenotype. Intercellular RNA interference is known to take place in plants (Dunoyer et al., 2007). However, this has never been successfully demonstrated in animals. Nonetheless, it is a provocative thought that miRNAs may be travelling between cells and the comparison of two models of Dicer ablation in the retina, induced with *Chx10*^{cre} and *αPax6*^{cre}, would support this idea. Both *Chx10*^{cre} and *αPax6*^{cre} lines (Marquardt et al., 2001; Rowan and Cepko, 2004) recombine the Rosa26 locus (Soriano, 1999) around E10.5, but the pattern of recombination differs in that the *Chx10*^{cre} recombines cells in a more mosaic fashion (stripes) while the *αPax6*^{cre} induces a more widespread recombination in the developing retina (Georgi and Reh, 2010; Rowan and Cepko, 2004). It is intriguing that the study which used the *Chx10*^{cre} to ablate Dicer function found a phenotype only in postnatal animals (Damiani et al., 2008), while the study using *αPax6*^{cre} found a phenotype as early as E16.5 (Georgi and Reh, 2010). Mechanism which could account for this are poorly understood, although recent demonstration that miRNAs can be found in extracellular microvesicles (Yuan et al., 2009) hints at the possibility that these molecules can indeed travel between cells. However, if this was the case, it would be difficult to explain why other phenotypes, including the increased expression of Tbr2 were not rescued.

Another important difference between my results and what could be anticipated based on the published data is the decreased abundance of miRNAs one day after the electroporation of the Cre- expression plasmid. A recent study looking at the dynamics of miRNA turnover in Dicer- deficient cells reported that it takes approximately 3 days after the wild type *Dicer1* mRNA is lost for the miRNA levels

to be affected (Gantier et al., 2011). However, other reports indicate that the rates of miRNA turnover may differ greatly between cell types (Krol et al., 2010a). It is important for the progress of the field that this is further pursued, but the dynamics of miRNA turnover has not been the key focus of this study. Instead, this study aimed to present evidence that the levels of mature miRNA are affected by the manipulation and the data obtained suggest that already one day after the electroporation the miRNA levels are detectably changed. It is possible that mature miRNA turnover rates are very tissue and context specific.

The finding that following the loss of functional Dicer corticogenesis is enhanced during postnatal development with at least a subset of cells destined to become neurons may have important implications for future research. Increasingly many studies have investigated mechanisms that could regulate the neuro- to gliogenesis switch in the developing radial glia (see Chapter 1) and this study provides a new class of candidate molecules that should be taken into account. I anticipate that the extension of neurogenesis following the loss of functional Dicer could be an indirect effect. Loss of mature miRNAs increases the proportion of cells that express Tbr2 and this is predicted to specify the differentiating cells to become intermediate progenitors. A recent study showed that intermediate progenitors are necessary to maintain stable Hes1 oscillation in the developing radial glia (Yoon et al., 2008) and so it is theoretically possible that increased size of the intermediate progenitor cell population could result in a prolonged maintenance of the radial glia. Another possibility is that following the loss of miRNAs the expression of Tbr2 is prolonged in the intermediate progenitors and that this enables them to re-enter the cell cycle more times than normal, hence prolonging their maintenance. It is known that while the mouse intermediate progenitors generally only divide once, they can also divide twice and thrice (Noctor et al., 2004), and that this could be under the control of some of the transcription factors expressed in that population, such as Cux2 (Nieto et al., 2004). The understanding of the molecular mechanisms of cell cycle re-entry is of further importance to the field in view of recent findings which have undermined the predominant belief that the quiescent stem cells in adult animals can re-enter the cell cycle, divide and then return to quiescence and that they can do so infinitely many times. Recent evidence suggested that the adult stem cells are much more like the embryonic progenitors in that they can only divide a few times before

differentiating (Encinas et al., 2011). It can be anticipated that better understanding of the molecular processes that regulate these events will help to design novel therapies to treat neurodegenerative diseases or delay or prevent age related cognitive decline.

This study identifies a new interaction between miR92b and the 3'UTR of Tbr2. The finding that the interaction is functional and that the overexpression of this miRNA causes fewer cells to express Tbr2 was surprising, because the 3'UTR of the Tbr2 mRNA contains only a single site which is complementary to the seed sequence of the miRNA. Other investigators looking for candidate miRNAs tend to focus on candidates which have multiple binding sites (Sandro Banfi, Telethon Institute of Genetics and Medicine and Stefano Piccolo, University of Padua, personal communication) and so obtaining a positive result based on minimal interaction was surprising. However, miRNA- target mRNA interactions can be highly contextual and are still very poorly understood. It is not clear, for example, if a given miRNA can control most or all of the mRNAs containing the response element or if there are additional mechanisms regulating the availability of particular mRNA transcripts for miRNA- dependent inhibition of translation or mRNA degradation. The possibility to address this question *in vivo* is further complicated by the fact that most genes contain multiple predicted binding sites in their 3'UTRs and so if one was to mutate a response element to a given miRNA, other miRNAs could have compensatory effects.

This study opens several interesting research questions requiring future work. Firstly, it needs to be assessed whether the interaction between miR-92b and Tbr2 has an impact on cortical cell generation from radial glia over a longer period of time, which would be the prediction of this study. Secondly, it would be informative to know which, if any, other transcripts are targeted by miR92b, particularly with an aim of determining if miR92b regulates only Tbr2 or a network of genes involved in the regulation of intermediate progenitors. It also remains to be established if the closely related miR92a, a member of the miR17~92 cluster, can regulate Tbr2.

Another interesting question is about the exact nature and function of the miR92b – Tbr2 mRNA interaction. Tbr2 expression has never, to the best of my knowledge, been reported in the radial glia, but Ngn2, a proneural transcription factor which has

recently been demonstrated to directly promote the expression of Tbr2 (Ochiai et al., 2009), is expressed in the radial glia (Shimojo et al., 2008). It not clear at this stage whether mRNA encoding Tbr2 is produced, but unpublished quantitative PCR data from iPS- derived neural stem cells where Tbr2 mRNA can be detected would support this hypothesis. Given that miR92b appears to be expressed throughout the ventricular zone (Figure 4.11 A – A’’’) it is conceivable to hypothesise that miR92b could be repressing the translation of Tbr2 mRNA. Another possibility is that miR92b controls the dynamics of Tbr2 production in the postmitotic cells. It has been proposed Tbr2 is expressed during both direct and indirect neurogenesis and that its prolonged expression would promote the specification of the intermediate progenitors (Hevner, 2006). It is possible that miR92b promotes direct neurogenesis by limiting Tbr2 expression (Figure 5.01).

Figure 5.01: Proposed function of miR92b in the regulation of cortical neurogenesis. It has been proposed that cortical neurogenesis is controlled by a sequential action of transcription factors, Pax6 > Ngn2 > Tbr2 > NeuroD1 (Hevner et al., 2006). It is possible that miR92b promotes indirect neurogenesis by limiting the expression of Tbr2 in the differentiating cell.

FIGURE 5.01

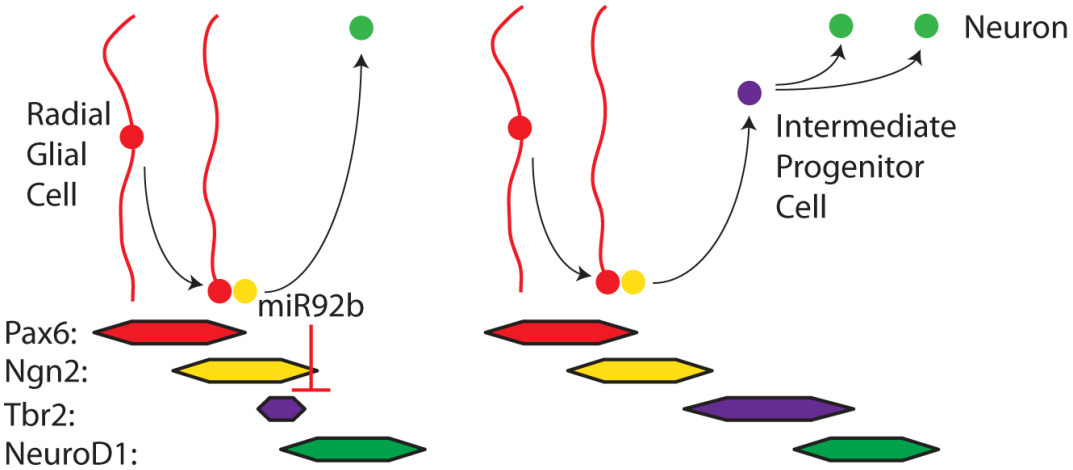
Radial
Glial
Cell
miR92b
Pax6:
Ngn2:
Tbr2:
NeuroD1:
Intermediate
Progenitor
Cell
Neuron

Additionally, it would be interesting to know if the interaction between miR92b and Tbr2 3'UTR is conserved in other species. This is interesting not only because the cross-species comparison of the miRNA:mRNA interaction network has not been investigated in great detail (Griffiths-Jones et al., 2011) but also because the expansion of the subventricular zone precursors, including the Tbr2- expressing neural progenitors, is thought to have underlain the evolutionary expansion of the neocortex (Cheung et al., 2007). It has been proposed that the action of most miRNAs can only induce moderate changes to the protein output from their target mRNAs (Guo et al., 2010), rather than acting as a binary switch. The data presented in Chapter 4 of this thesis, showing that overexpression of miR-92b resulted in about 25% (luciferase assay) – 50% (*in vivo*) changes in protein expression are in excellent agreement with this hypothesis. Changes to the expression levels of these molecules or their processing in various tissues could, in theory, be an excellent mechanism of modest evolutionary variation.

As I pointed out in the Discussion section of Chapter 4, the sequence of the precursor hairpin of miR92b differs between rodents and primates at discreet residues and it is subject to a further study whether these changes affect the efficiency of the precursor processing and whether these differences could be linked to the evolutionary expansion of the neocortex.

Finally, it remains to be determined what factors are involved in the expression of miR-92b. The molecular determinants of miRNA expression patterns are essentially unknown. Several approaches have been taken to identify the binding sites for RNA polymerase II and RNA polymerase III for intergenic and intronic miRNAs (Monteys et al., 2010; Zhou et al., 2007), but it is not clear whether the expression of miRNAs is additionally regulated by enhancers or specific transcription factors in a similar way to the protein coding genes. These would be obvious candidates explaining spatial and temporal patterns of expression of some mature miRNAs (Kloosterman, 2006; Smirnova et al., 2005). It was proposed that the expression of intronic miRNAs could correlate with the expression of their respective host genes, but this was not corroborated by the sequencing data (Monteys et al., 2010). It is clear that posttranscriptional mechanisms are also involved in regulating miRNA

expression since, at least in the few examples of miRNAs that have been more extensively studied, mature miRNAs are only present in a subset of cells expressing the pre-miRNA hairpin (Maiorano, 2009; Shibata et al., 2011). However, the molecular factors that could be involved in this are not known. One possible mechanism involves modifications of the 3' end of the miRNAs, such as adenylation, ubiquitination or RNA editing which may be important determinants of the efficiency of miRNA or target identification (Burroughs et al., 2010; Krol et al., 2010b). However, it still needs to be determined what could regulate the specificity of these modifications. The work described in this thesis indicates that even minimal interaction between the miRNA and the target mRNA via the seed region may be biologically significant, raising the possibility that all other residues could be subject to modifications.

BIBLIOGRAPHY

Acampora, D., Mazan, S., Lallemand, Y., Avantaggiato, V., Maury, M., Simeone, A. and Brulet, P. (1995). Forebrain and midbrain regions are deleted in Otx2-/- mutants due to a defective anterior neuroectoderm specification during gastrulation. *Development* **121**, 3279-90.

Alcantara, S., Ruiz, M., D'Arcangelo, G., Ezan, F., de Lecea, L., Curran, T., Sotelo, C., Soriano, E.,. (1998). Regional and cellular patterns of reelin mRNA expression in the forebrain of the developing and adult mouse. . *Journal of Neuroscience* **18**, 7779 - 7799.

Alvarez-Buylla, A., Theelen, M. and Nottebohm, F. (1990). Proliferation "hot spots" in adult avian ventricular zone reveal radial cell division. *Neuron* **5**, 101-9.

Ambros, V., Bartel, B., Bartel, D. P., Burge, C. B., Carrington, J. C., Chen, X., Dreyfuss, G., Eddy, S. R., Griffiths-Jones, S., Marshall, M. et al. (2003). A uniform system for microRNA annotation. *RNA* **9**, 277-9.

Ambros, V. and Horvitz, H. R. (1987). The lin-14 locus of Caenorhabditis elegans controls the time of expression of specific postembryonic developmental events. *Genes Dev* **1**, 398-414.

Andersson, T., Rahman, S., Sansom, S. N., Alsio, J. M., Kaneda, M., Smith, J., O'Carroll, D., Tarakhovsky, A. and Livesey, F. J. (2010). Reversible block of mouse neural stem cell differentiation in the absence of dicer and microRNAs. *PLoS One* **5**, e13453.

Angevine, J. B., Jr. and Sidman, R. L. (1961). Autoradiographic study of cell migration during histogenesis of cerebral cortex in the mouse. *Nature* **192**, 766-8.

Anthony, T. E., Klein, C., Fishell, G. and Heintz, N. (2004). Radial glia serve as neuronal progenitors in all regions of the central nervous system. *Neuron* **41**, 881-90.

Anton, E. S., Marchionni, M. A., Lee, K. F. and Rakic, P. (1997). Role of GGF/neuregulin signaling in interactions between migrating neurons and radial glia in the developing cerebral cortex. *Development* **124**, 3501-10.

Aoto, K., Nishimura, T., Eto, K. and Motoyama, J. (2002). Mouse GLI3 regulates Fgf8 expression and apoptosis in the developing neural tube, face, and limb bud. *Dev Biol* **251**, 320-32.

Aravin, A. A., Hannon, G. J. and Brennecke, J. (2007). The Piwi-piRNA pathway provides an adaptive defense in the transposon arms race. *Science* **318**, 761-4.

Arlotta, P., Molyneaux, B. J., Chen, J., Inoue, J., Kominami, R. and Macklis, J. D. (2005). Neuronal subtype-specific genes that control corticospinal motor neuron development *in vivo*. *Neuron* **45**, 207-21.

Arnold, S. J., Huang, G. J., Cheung, A. F., Era, T., Nishikawa, S., Bikoff, E. K., Molnar, Z., Robertson, E. J. and Groszer, M. (2008). The T-box transcription factor Eomes/Tbr2 regulates neurogenesis in the cortical subventricular zone. *Genes Dev* **22**, 2479-84.

Babiarz, J. E., Hsu, R., Melton, C., Thomas, M., Ullian, E. M. and Blelloch, R. (2011). A role for noncanonical microRNAs in the mammalian brain revealed by phenotypic differences in Dgcr8 versus Dicer1 knockouts and small RNA sequencing. *RNA* **17**, 1489-501.

Beck, C. R., Collier, P., Macfarlane, C., Malig, M., Kidd, J. M., Eichler, E. E., Badge, R. M. and Moran, J. V. (2010). LINE-1 retrotransposition activity in human genomes. *Cell* **141**, 1159-70.

Belgard, T. G., Marques, A. C., Oliver, P. L., Abaan, H. O., Sirey, T. M., Hoerder-Suabedissen, A., Garcia-Moreno, F., Molnar, Z., Margulies, E. H. and Ponting, C. P. (2011). A transcriptomic atlas of mouse neocortical layers. *Neuron* **71**, 605-16.

Bernstein, E., Caudy, A. A., Hammond, S. M. and Hannon, G. J. (2001). Role for a bidentate ribonuclease in the initiation step of RNA interference. *Nature* **409**, 363-6.

Bernstein, E., Kim, S. Y., Carmell, M. A., Murchison, E. P., Alcorn, H., Li, M. Z., Mills, A. A., Elledge, S. J., Anderson, K. V. and Hannon, G. J. (2003). Dicer is essential for mouse development. *Nat Genet* **35**, 215-7.

Betel, D., Wilson, M., Gabow, A., Marks, D. S. and Sander, C. (2008). The microRNA.org resource: targets and expression. *Nucleic Acids Res* **36**, D149-53.

Betschinger, J., Mechtler, K. and Knoblich, J. A. (2003). The Par complex directs asymmetric cell division by phosphorylating the cytoskeletal protein Lgl. *Nature* **422**, 326-30.

Bettenhausen, B., Hrabe de Angelis, M., Simon, D., Guenet, J. L. and Gossler, A. (1995). Transient and restricted expression during mouse embryogenesis of Dll1, a murine gene closely related to Drosophila Delta. *Development* **121**, 2407-18.

Beveridge, N. J., Gardiner, E., Carroll, A. P., Tooney, P. A. and Cairns, M. J. (2010). Schizophrenia is associated with an increase in cortical microRNA biogenesis. *Mol Psychiatry* **15**, 1176-89.

Bielle, F., Griveau, A., Narboux-Neme, N., Vigneau, S., Sigrist, M., Arber, S., Wassef, M. and Pierani, A. (2005). Multiple origins of Cajal-Retzius cells at the borders of the developing pallium. *Nat Neurosci* **8**, 1002-12.

Bishop, K. M., Goudreau, G. and O'Leary, D. D. (2000). Regulation of area identity in the mammalian neocortex by Emx2 and Pax6. *Science* **288**, 344-9.

Bobick, B. E., Tuan, R. S. and Chen, F. H. (2010). The intermediate filament vimentin regulates chondrogenesis of adult human bone marrow-derived multipotent progenitor cells. *J Cell Biochem* **109**, 265-76.

Borello, U. and Pierani, A. (2010). Patterning the cerebral cortex: traveling with morphogens. *Curr Opin Genet Dev* **20**, 408-15.

Bouwmeester, T. (2001). The Spemann-Mangold organizer: the control of fate specification and morphogenetic rearrangements during gastrulation in Xenopus. *Int J Dev Biol* **45**, 251-8.

Brennecke, J., Hipfner, D. R., Stark, A., Russell, R. B. and Cohen, S. M. (2003). bantam encodes a developmentally regulated microRNA that controls cell proliferation and regulates the proapoptotic gene hid in Drosophila. *Cell* **113**, 25-36.

Britanova, O., Akopov, S., Lukyanov, S., Gruss, P. and Tarabykin, V. (2005). Novel transcription factor Satb2 interacts with matrix attachment region DNA elements in a tissue-specific manner and demonstrates cell-type-dependent expression in the developing mouse CNS. *Eur J Neurosci* **21**, 658-68.

Britanova, O., de Juan Romero, C., Cheung, A., Kwan, K. Y., Schwark, M., Gyorgy, A., Vogel, T., Akopov, S., Mitkovski, M., Agoston, D. et al. (2008). Satb2 is a postmitotic determinant for upper-layer neuron specification in the neocortex. *Neuron* **57**, 378-92.

Bulfone, A., Martinez, S., Marigo, V., Campanella, M., Basile, A., Quaderi, N., Gattuso, C., Rubenstein, J. L. and Ballabio, A. (1999). Expression pattern of the Tbr2 (Eomesodermin) gene during mouse and chick brain development. *Mech Dev* **84**, 133-8.

Burroughs, A. M., Ando, Y., de Hoon, M. J., Tomaru, Y., Nishibu, T., Ukekawa, R., Funakoshi, T., Kurokawa, T., Suzuki, H., Hayashizaki, Y. et al. (2010). A comprehensive survey of 3' animal miRNA modification events and a possible role

for 3' adenylation in modulating miRNA targeting effectiveness. *Genome Res* **20**, 1398-410.

Campbell, K. (2003). Signaling to and from radial glia. *Glia* **43**, 44-6.

Caudy, A. A., Myers, M., Hannon, G. J. and Hammond, S. M. (2002). Fragile X-related protein and VIG associate with the RNA interference machinery. *Genes Dev* **16**, 2491-6.

Caviness, V. S., Jr. (1976). Patterns of cell and fiber distribution in the neocortex of the reeler mutant mouse. *J Comp Neurol* **170**, 435-47.

Caviness, V. S., Jr. (1982). Neocortical histogenesis in normal and reeler mice: a developmental study based upon [3H]thymidine autoradiography. *Brain Res* **256**, 293-302.

Cepko, C. L., Ryder, E., Austin, C., Golden, J., Fields-Berry, S. and Lin, J. (1998). Lineage analysis using retroviral vectors. *Methods* **14**, 393-406.

Cerutti, L., Mian, N. and Bateman, A. (2000). Domains in gene silencing and cell differentiation proteins: the novel PAZ domain and redefinition of the Piwi domain. *Trends Biochem Sci* **25**, 481-2.

Cheever, A. and Ceman, S. (2009a). Phosphorylation of FMRP inhibits association with Dicer. *RNA* **15**, 362-6.

Cheever, A. and Ceman, S. (2009b). Translation regulation of mRNAs by the fragile X family of proteins through the microRNA pathway. *RNA Biol* **6**, 175-8.

Chekulaeva, M., Parker, R. and Filipowicz, W. (2010). The GW/WG repeats of Drosophila GW182 function as effector motifs for miRNA-mediated repression. *Nucleic Acids Res* **38**, 6673-83.

Cheng, L. C., Pastrana, E., Tavazoie, M. and Doetsch, F. (2009). miR-124 regulates adult neurogenesis in the subventricular zone stem cell niche. *Nat Neurosci* **12**, 399-408.

Chenn, A. and Walsh, C. A. (2002). Regulation of cerebral cortical size by control of cell cycle exit in neural precursors. *Science* **297**, 365-9.

Cheung, A. F., Pollen, A. A., Tavare, A., DeProto, J. and Molnar, Z. (2007). Comparative aspects of cortical neurogenesis in vertebrates. *J Anat* **211**, 164-76.

Chowdhury, T. G., Jimenez, J. C., Bomar, J. M., Cruz-Martin, A., Cantle, J. P. and Portera-Cailliau, C. (2010). Fate of cajal-retzius neurons in the postnatal mouse neocortex. *Front Neuroanat* **4**, 10.

Collignon, J., Sockanathan, S., Hacker, A., Cohen-Tannoudji, M., Norris, D., Rastan, S., Stevanovic, M., Goodfellow, PN., Lovell-Badge, R., . (1996). A comparison of the properties of Sox-3 with Sry and two related genes, Sox-1 and Sox-2. . *Development* **122**, 509 - 520.

Conlon, F. L. and Smith, J. C. (1999). Interference with brachyury function inhibits convergent extension, causes apoptosis, and reveals separate requirements in the FGF and activin signalling pathways. *Dev Biol* **213**, 85-100.

Coufal, N. G., Garcia-Perez, J. L., Peng, G. E., Yeo, G. W., Mu, Y., Lovci, M. T., Morell, M., O'Shea, K. S., Moran, J. V. and Gage, F. H. (2009). L1 retrotransposition in human neural progenitor cells. *Nature* **460**, 1127-31.

Cubelos, B., Sebastian-Serrano, A., Kim, S., Moreno-Ortiz, C., Redondo, J. M., Walsh, C. A. and Nieto, M. (2008). Cux-2 controls the proliferation of neuronal intermediate precursors of the cortical subventricular zone. *Cereb Cortex* **18**, 1758-70.

Damiani, D., Alexander, J. J., O'Rourke, J. R., McManus, M., Jadhav, A. P., Cepko, C. L., Hauswirth, W. W., Harfe, B. D. and Strettoi, E. (2008). Dicer inactivation leads to progressive functional and structural degeneration of the mouse retina. *J Neurosci* **28**, 4878-87.

Davis, N., Mor, E. and Ashery-Padan, R. (2011). Roles for Dicer1 in the patterning and differentiation of the optic cup neuroepithelium. *Development* **138**, 127-38.

Davis, T. H., Cuellar, T. L., Koch, S. M., Barker, A. J., Harfe, B. D., McManus, M. T. and Ullian, E. M. (2008). Conditional loss of Dicer disrupts cellular and tissue morphogenesis in the cortex and hippocampus. *J Neurosci* **28**, 4322-30.

De Pietri Tonelli, D., Pulvers, J.N., Haffner, C., Murchison, E.P., Hannon, G.J., Huttner, W.B.,. (2008). miRNAs are essential for survival and differentiation of newborn neurons but not for expansion of neural progenitors during early neurogenesis in the mouse embryonic neocortex. . *Development* **135**, 3911 – 3921

DeFelipe, J., Alonso-Nanclares, L. and Arellano, J. I. (2002). Microstructure of the neocortex: comparative aspects. *J Neurocytol* **31**, 299-316.

Desai, A. R. and McConnell, S. K. (2000). Progressive restriction in fate potential by neural progenitors during cerebral cortical development. *Development* **127**, 2863-72.

Ding, L., Spencer, A., Morita, K. and Han, M. (2005). The developmental timing regulator AIN-1 interacts with miRISCs and may target the argonaute protein ALG-1 to cytoplasmic P bodies in C. elegans. *Mol Cell* **19**, 437-47.

Doe, C. Q., Chu-LaGraff, Q., Wright, D. M. and Scott, M. P. (1991). The prospero gene specifies cell fates in the Drosophila central nervous system. *Cell* **65**, 451-64.

Doench, J. G. and Sharp, P. A. (2004). Specificity of microRNA target selection in translational repression. *Genes Dev* **18**, 504-11.

Doetsch, F., Caille, I., Lim, D. A., Garcia-Verdugo, J. M. and Alvarez-Buylla, A. (1999). Subventricular zone astrocytes are neural stem cells in the adult mammalian brain. *Cell* **97**, 703-16.

Dragatsis, I. and Zeitlin, S. (2000). CaMKIIalpha-Cre transgene expression and recombination patterns in the mouse brain. *Genesis* **26**, 133-5.

Du, T. and Zamore, P. D. (2005). microPrimer: the biogenesis and function of microRNA. *Development* **132**, 4645-52.

Du, Z., Lee, J. K., Tjhen, R., Stroud, R. M. and James, T. L. (2008). Structural and biochemical insights into the dicing mechanism of mouse Dicer: a conserved lysine is critical for dsRNA cleavage. *Proc Natl Acad Sci U S A* **105**, 2391-6.

Dulabon, L., Olson, E. C., Taglienti, M. G., Eisenhuth, S., McGrath, B., Walsh, C. A., Kreidberg, J. A. and Anton, E. S. (2000). Reelin binds alpha3beta1 integrin and inhibits neuronal migration. *Neuron* **27**, 33-44.

Dunoyer, P., Himber, C., Ruiz-Ferrer, V., Alioua, A. and Voinnet, O. (2007). Intra- and intercellular RNA interference in Arabidopsis thaliana requires components of the microRNA and heterochromatic silencing pathways. *Nat Genet* **39**, 848-56.

Echelard, Y., Epstein, D. J., St-Jacques, B., Shen, L., Mohler, J., McMahon, J. A. and McMahon, A. P. (1993). Sonic hedgehog, a member of a family of putative signaling molecules, is implicated in the regulation of CNS polarity. *Cell* **75**, 1417-30.

Eiraku, M., Watanabe, K., Matsuo-Takasaki, M., Kawada, M., Yonemura, S., Matsumura, M., Wataya, T., Nishiyama, A., Muguruma, K. and Sasai, Y. (2008) Self-organised formation of polarized cortical tissues from ESCs and its active manipulation by extrinsic signals. *Cell Stem Cell* **3**, 519 - 532.

Encinas, J. M., Michurina, T. V., Peunova, N., Park, J. H., Tordo, J., Peterson, D. A., Fishell, G., Koulakov, A. and Enikolopov, G. (2011). Division-coupled astrocytic differentiation and age-related depletion of neural stem cells in the adult hippocampus. *Cell Stem Cell* **8**, 566-79.

Englund, C., Fink, A., Lau, C., Pham, D., Daza, R. A., Bulfone, A., Kowalczyk, T. and Hevner, R. F. (2005). Pax6, Tbr2, and Tbr1 are expressed sequentially by radial glia, intermediate progenitor cells, and postmitotic neurons in developing neocortex. *J Neurosci* **25**, 247-51.

Ericson, J., Muhr, J., Jessell, T. M. and Edlund, T. (1995). Sonic hedgehog: a common signal for ventral patterning along the rostrocaudal axis of the neural tube. *Int J Dev Biol* **39**, 809-16.

Fabian, M. R., Mathonnet, G., Sundermeier, T., Mathys, H., Zipprich, J. T., Svitkin, Y. V., Rivas, F., Jinek, M., Wohlschlegel, J., Doudna, J. A. et al. (2009). Mammalian miRNA RISC recruits CAF1 and PABP to affect PABP-dependent deadenylation. *Mol Cell* **35**, 868-80.

Fabian, M. R., Sonenberg, N. and Filipowicz, W. (2010). Regulation of mRNA translation and stability by microRNAs. *Annu Rev Biochem* **79**, 351-79.

Farazi, T. A., Juranek, S. A. and Tuschl, T. (2008). The growing catalog of small RNAs and their association with distinct Argonaute/Piwi family members. *Development* **135**, 1201-14.

Fenelon, K., Mukai, J., Xu, B., Hsu, P. K., Drew, L. J., Karayiorgou, M., Fischbach, G. D., Macdermott, A. B. and Gogos, J. A. (2011). Deficiency of Dgcr8, a gene disrupted by the 22q11.2 microdeletion, results in altered short-term plasticity in the prefrontal cortex. *Proc Natl Acad Sci U S A* **108**, 4447-52.

Feng, L., Hatten, M. E. and Heintz, N. (1994). Brain lipid-binding protein (BLBP): a novel signaling system in the developing mammalian CNS. *Neuron* **12**, 895-908.

Filipowicz, W., Jaskiewicz, L., Kolb, FA., Pillai, RS. (2005). Post-transcriptional gene silencing by siRNAs and miRNAs. . *Current Opinion in Structural Biology* **15**, 331 – 341.

Fineberg, S. K., Kosik, K. S. and Davidson, B. L. (2009). MicroRNAs potentiate neural development. *Neuron* **64**, 303-9.

Fire, A., Xu, S., Montgomery, M. K., Kostas, S. A., Driver, S. E. and Mello, C. C. (1998). Potent and specific genetic interference by double-stranded RNA in Caenorhabditis elegans. *Nature* **391**, 806-11.

Flammiger, A., Besch, R., Cook, A. L., Maier, T., Sturm, R. A. and Berking, C. (2009). SOX9 and SOX10 but not BRN2 are required for nestin expression in human melanoma cells. *J Invest Dermatol* **129**, 945-53.

Frantz, G. D. and McConnell, S. K. (1996). Restriction of late cerebral cortical progenitors to an upper-layer fate. *Neuron* **17**, 55-61.

Fujita, S. (1963). The matrix cell and cytogenesis in the developing central nervous system. *J Comp Neurol* **120**, 37-42.

Gaiano, N., Kohtz, J. D., Turnbull, D. H. and Fishell, G. (1999). A method for rapid gain-of-function studies in the mouse embryonic nervous system. *Nat Neurosci* **2**, 812-9.

Gaiano, N., Nye, J. S. and Fishell, G. (2000). Radial glial identity is promoted by Notch1 signaling in the murine forebrain. *Neuron* **26**, 395-404.

Gan, J., Tropea, JE., Austin, BP., Court, DL., Waugh, DS., Ji, X. (2006). Structural insight into the mechanism of double- stranded RNA processing by Ribonuclease III. . *Cell* **124**, 355 – 366

Gantier, M. P., McCoy, C. E., Rusinova, I., Saulep, D., Wang, D., Xu, D., Irving, A. T., Behlke, M. A., Hertzog, P. J., Mackay, F. et al. (2011). Analysis of microRNA turnover in mammalian cells following Dicer1 ablation. *Nucleic Acids Res* **39**, 5692-703.

Gaspard, N., Bouschet, T., Hourez, R., Dimidschstein, J., Naeije, G., van den Ameele, J., Espuny-Camacho, I., Herpoel, A., Passante, L., Schiffmann, S. N., Gaillard, A. and Vanderhaeghen, P. (2008) An intrinsic mechanism of corticogenesis from embryonic stem cells. *Nature* **455**, 351 - 358.

Gaughwin, P., Ciesla, M., Yang, H., Lim, B. and Brundin, P. (2011). Stage-specific modulation of cortical neuronal development by Mmu-miR-134. *Cereb Cortex* **21**, 1857-69.

Georgi, S. A. and Reh, T. A. (2010). Dicer is required for the transition from early to late progenitor state in the developing mouse retina. *J Neurosci* **30**, 4048-61.

Ghashghaei, H. T., Weimer, J. M., Schmid, R. S., Yokota, Y., McCarthy, K. D., Popko, B. and Anton, E. S. (2007). Reinduction of ErbB2 in astrocytes promotes radial glial progenitor identity in adult cerebral cortex. *Genes Dev* **21**, 3258-71.

Gillies, K. and Price, D. J. (1993). The fates of cells in the developing cerebral cortex of normal and methylazoxymethanol acetate-lesioned mice. *Eur J Neurosci* **5**, 73-84.

Gotz, M. (1995). Getting the re and being there in the cerebral cortex. . *Experientia* **51**, 301 - 316.

Gotz, M., Stoykova, A. and Gruss, P. (1998). Pax6 controls radial glia differentiation in the cerebral cortex. *Neuron* **21**, 1031-44.

Grandjean, V., Gounon, P., Wagner, N., Martin, L., Wagner, KD., Florence, Bernex., Cuzin, F., Rassoulzadegan, M. (2009). The miR-124-Sox9 paramutation: RNA-mediated epigenetic control of embryonic and adult growth. . *Development* **136**, 3647 – 3655

Gregory, R., Chendrimada, TP., Cooch, N., Shiekhattar, R.,. (2005). Human RISC couples microRNA biogenesis and posttranscriptional gene silencing. *Cell* **123**, 631 – 640

Gregory, R. I., Yan, K. P., Amuthan, G., Chendrimada, T., Doratotaj, B., Cooch, N. and Shiekhattar, R. (2004). The Microprocessor complex mediates the genesis of microRNAs. *Nature* **432**, 235-40.

Griffiths-Jones, S. (2004). The microRNA Registry. *Nucleic Acids Res* **32**, D109-11.

Griffiths-Jones, S. (2010). miRBase: microRNA sequences and annotation. *Curr Protoc Bioinformatics* **Chapter 12**, Unit 12 9 1-10.

Griffiths-Jones, S., Hui, J. H., Marco, A. and Ronshaugen, M. (2011). MicroRNA evolution by arm switching. *EMBO Rep* **12**, 172-7.

Guillemot, F. (2005). Cellular and molecular control of neurogenesis in the mammalian telencephalon. . *Current Opinion in Cell Biology* **17**, 639 – 647

Guo, H., Ingolia, N. T., Weissman, J. S. and Bartel, D. P. (2010). Mammalian microRNAs predominantly act to decrease target mRNA levels. *Nature* **466**, 835-40.

Guo, X. W., Th'ng, J. P., Swank, R. A., Anderson, H. J., Tudan, C., Bradbury, E. M. and Roberge, M. (1995). Chromosome condensation induced by fostriecin does not require p34cdc2 kinase activity and histone H1 hyperphosphorylation, but is associated with enhanced histone H2A and H3 phosphorylation. *EMBO J* **14**, 976-85.

Hamilton, B. J., Nichols, R. C., Tsukamoto, H., Boado, R. J., Pardridge, W. M. and Rigby, W. F. (1999). hnRNP A2 and hnRNP L bind the 3'UTR of glucose transporter 1 mRNA and exist as a complex *in vivo*. *Biochem Biophys Res Commun* **261**, 646-51.

Hammond, S., Bernstein, E., Beach, D., Hannon, GJ.,. (2000). An RNA-directed nuclease mediates post-transcriptional gene silencing in Drosophila cells. . *Nature* **404**, 293 – 296

Harfe, B. D., McManus, M. T., Mansfield, J. H., Hornstein, E. and Tabin, C. J. (2005). The RNaseIII enzyme Dicer is required for morphogenesis but not patterning of the vertebrate limb. *Proc Natl Acad Sci U S A* **102**, 10898-903.

Hartfuss, E., Galli, R., Heins, N. and Gotz, M. (2001). Characterization of CNS precursor subtypes and radial glia. *Dev Biol* **229**, 15-30.

Hashimoto-Torii, K., Torii, M., Sarkisian, M. R., Bartley, C. M., Shen, J., Radtke, F., Gridley, T., Sestan, N. and Rakic, P. (2008). Interaction between Reelin and Notch signaling regulates neuronal migration in the cerebral cortex. *Neuron* **60**, 273-84.

Hasling, T. A., Gierdalski, M., Jablonska, B. and Juliano, S. L. (2003). A radialization factor in normal cortical plate restores disorganized radial glia and disrupted migration in a model of cortical dysplasia. *Eur J Neurosci* **17**, 467-80.

Hatakeyama, J., Bessho, Y., Katoh, K., Ookawara, S., Fujioka, M., Guillemot, F. and Kageyama, R. (2004). Hes genes regulate size, shape and histogenesis of the nervous system by control of the timing of neural stem cell differentiation. *Development* **131**, 5539-50.

Haubensak, W., Attardo, A., Denk, W. and Huttner, W. B. (2004). Neurons arise in the basal neuroepithelium of the early mammalian telencephalon: a major site of neurogenesis. *Proc Natl Acad Sci U S A* **101**, 3196-201.

Haug, B. H., Henriksen, J. R., Buechner, J., Geerts, D., Tomte, E., Kogner, P., Martinsson, T., Flaegstad, T., Sveinbjornsson, B. and Einvik, C. (2011). MYCN-regulated miRNA-92 inhibits secretion of the tumor suppressor DICKKOPF-3 (DKK3) in neuroblastoma. *Carcinogenesis* **32**, 1005-12.

Hebert, J., McConnell, SK.,. (2000). Targeting of cre to the Foxg1 (BF-1) locus mediates loxP recombination in the telencephalon and other developing head structures. . *Developmental Biology* **222**, 296 - 306.

Hebert, J. M. and Fishell, G. (2008). The genetics of early telencephalon patterning: some assembly required. *Nat Rev Neurosci* **9**, 678-85.

Hevner, R. F. (2006). From radial glia to pyramidal-projection neuron: transcription factor cascades in cerebral cortex development. *Mol Neurobiol* **33**, 33-50.

Hevner, R. F., Hodge, R. D., Daza, R. A. and Englund, C. (2006). Transcription factors in glutamatergic neurogenesis: conserved programs in neocortex, cerebellum, and adult hippocampus. *Neurosci Res* **55**, 223-33.

Hevner, R. F., Neogi, T., Englund, C., Daza, R. A. and Fink, A. (2003). Cajal-Retzius cells in the mouse: transcription factors, neurotransmitters, and birthdays suggest a pallial origin. *Brain Res Dev Brain Res* **141**, 39-53.

Hevner, R. F., Shi, L., Justice, N., Hsueh, Y., Sheng, M., Smiga, S., Bulfone, A., Goffinet, A. M., Campagnoni, A. T. and Rubenstein, J. L. (2001). Tbr1 regulates differentiation of the preplate and layer 6. *Neuron* **29**, 353-66.

Hirabayashi, Y., Suzki, N., Tsuboi, M., Endo, T. A., Toyoda, T., Shinga, J., Koseki, H., Vidal, M. and Gotoh, Y. (2009). Polycomb limits the neurogenic competence of neural precursor cells to promote astrogenic fate transition. *Neuron* **63**, 600-13.

Hornstein, E., Mansfield, J. H., Yekta, S., Hu, J. K., Harfe, B. D., McManus, M. T., Baskerville, S., Bartel, D. P. and Tabin, C. J. (2005). The microRNA miR-196 acts upstream of Hoxb8 and Shh in limb development. *Nature* **438**, 671-4.

Huang, C. R., Schneider, A. M., Lu, Y., Niranjan, T., Shen, P., Robinson, M. A., Steranka, J. P., Valle, D., Civin, C. I., Wang, T. et al. (2010). Mobile interspersed repeats are major structural variants in the human genome. *Cell* **141**, 1171-82.

Hunter, K. E. and Hatten, M. E. (1995). Radial glial cell transformation to astrocytes is bidirectional: regulation by a diffusible factor in embryonic forebrain. *Proc Natl Acad Sci U S A* **92**, 2061-5.

Hutvagner, G. and Zamore, P. D. (2002). A microRNA in a multiple-turnover RNAi enzyme complex. *Science* **297**, 2056-60.

Ihrie, R. A. and Alvarez-Buylla, A. (2011). Lake-front property: a unique germinal niche by the lateral ventricles of the adult brain. *Neuron* **70**, 674-86.

Iskow, R. C., McCabe, M. T., Mills, R. E., Torene, S., Pittard, W. S., Neuwald, A. F., Van Meir, E. G., Vertino, P. M. and Devine, S. E. (2010). Natural mutagenesis of human genomes by endogenous retrotransposons. *Cell* **141**, 1253-61.

Johnson, D. S., Mortazavi, A., Myers, R. M. and Wold, B. (2007). Genome-wide mapping of *in vivo* protein-DNA interactions. *Science* **316**, 1497-502.

Kamakura, S., Oishi, K., Yoshimatsu, T., Nakafuku, M., Masuyama, N. and Gotoh, Y. (2004). Hes binding to STAT3 mediates crosstalk between Notch and JAK-STAT signalling. *Nat Cell Biol* **6**, 547-54.

Kaneko, H., Dridi, S., Tarallo, V., Gelfand, B. D., Fowler, B. J., Cho, W. G., Kleinman, M. E., Ponicsan, S. L., Hauswirth, W. W., Chiodo, V. A. et al. (2011). DICER1 deficit induces Alu RNA toxicity in age-related macular degeneration. *Nature* **471**, 325-30.

Kanellopoulou, C., Muljo, SA., Kung, AL., Ganesan, S., Drapkin, R., Jenuwein, T., Livingston, DM., Rajewski, K., . (2005). Dicer- deficient mouse embryonic stem cells are defective in differentiation and centromeric silencing. . *Genes and Development* **19**, 489 – 501

Kapsimali, M., Kloosterman, W. P., de Bruijn, E., Rosa, F., Plasterk, R. H. and Wilson, S. W. (2007). MicroRNAs show a wide diversity of expression profiles in the developing and mature central nervous system. *Genome Biol* **8**, R173.

Kawahara, Y., Zinshteyn, B., Sethupathy, P., Iizasa, H., Hatzigeorgiou, A. G. and Nishikura, K. (2007). Redirection of silencing targets by adenosine-to-inosine editing of miRNAs. *Science* **315**, 1137-40.

Kawase-Koga, Y., Low, R., Otaegi, G., Pollock, A., Deng, H., Eisenhaber, F., Maurer-Stroh, S. and Sun, T. (2010). RNAase-III enzyme Dicer maintains signaling pathways for differentiation and survival in mouse cortical neural stem cells. *J Cell Sci* **123**, 586-94.

Kawase-Koga, Y., Otaegi, G. and Sun, T. (2009). Different timings of Dicer deletion affect neurogenesis and gliogenesis in the developing mouse central nervous system. *Dev Dyn* **238**, 2800-12.

Kimelman, D. and Kirschner, M. (1987). Synergistic induction of mesoderm by FGF and TGF-beta and the identification of an mRNA coding for FGF in the early Xenopus embryo. *Cell* **51**, 869-77.

Kiriakidou, M., Tan, G. S., Lamprinaki, S., De Planell-Saguer, M., Nelson, P. T. and Mourelatos, Z. (2007). An mRNA m7G cap binding-like motif within human Ago2 represses translation. *Cell* **129**, 1141-51.

Kloosterman, W., Wienholds, E., de Bruijn, E., Kauppinen, S., Plasterk, R.H.A.,. (2006). *In situ* detection of miRNAs in animal embryos using LNA-modified oligonucleotide probes. *Nature Methods* **3**, 27 - 29.

Konopka, W., Kiryk, A., Novak, M., Herwerth, M., Parkitna, J. R., Wawrzyniak, M., Kowarsch, A., Michaluk, P., Dzwonek, J., Arnsperger, T. et al. (2010). MicroRNA loss enhances learning and memory in mice. *J Neurosci* **30**, 14835-42.

Koo, B. K., Lim, H. S., Song, R., Yoon, M. J., Yoon, K. J., Moon, J. S., Kim, Y. W., Kwon, M. C., Yoo, K. W., Kong, M. P. et al. (2005). Mind bomb 1 is essential for generating functional Notch ligands to activate Notch. *Development* **132**, 3459-70.

Kopan, R. and Ilagan, M. X. (2009). The canonical Notch signaling pathway: unfolding the activation mechanism. *Cell* **137**, 216-33.

Kosodo, Y., Roper, K., Haubensak, W., Marzesco, A. M., Corbeil, D. and Huttner, W. B. (2004). Asymmetric distribution of the apical plasma membrane during neurogenic divisions of mammalian neuroepithelial cells. *EMBO J* **23**, 2314-24.

Kowalczyk, T., Pontious, A., Englund, C., Daza, R. A., Bedogni, F., Hodge, R., Attardo, A., Bell, C., Huttner, W. B. and Hevner, R. F. (2009). Intermediate neuronal progenitors (basal progenitors) produce pyramidal-projection neurons for all layers of cerebral cortex. *Cereb Cortex* **19**, 2439-50.

Kriegstein, A., Gotz, M. (2003). Radial glia diversity: a matter of cell fate. . *Glia* **43**, 37- 43

Kriegstein, A., Noctor, S. and Martinez-Cerdeno, V. (2006). Patterns of neural stem and progenitor cell division may underlie evolutionary cortical expansion. *Nat Rev Neurosci* **7**, 883-90.

Krol, J., Busskamp, V., Markiewicz, I., Stadler, M. B., Ribi, S., Richter, J., Duebel, J., Bicker, S., Fehling, H. J., Schubeler, D. et al. (2010a). Characterizing light-regulated retinal microRNAs reveals rapid turnover as a common property of neuronal microRNAs. *Cell* **141**, 618-31.

Krol, J., Loedige, I. and Filipowicz, W. (2010b). The widespread regulation of microRNA biogenesis, function and decay. *Nat Rev Genet* **11**, 597-610.

Kuchinke, U., Grawe, F. and Knust, E. (1998). Control of spindle orientation in Drosophila by the Par-3-related PDZ-domain protein Bazooka. *Curr Biol* **8**, 1357-65.

Kuida, K., Haydar, T. F., Kuan, C. Y., Gu, Y., Taya, C., Karasuyama, H., Su, M. S., Rakic, P. and Flavell, R. A. (1998). Reduced apoptosis and cytochrome c-mediated caspase activation in mice lacking caspase 9. *Cell* **94**, 325-37.

Kumar, M. S., Pester, R. E., Chen, C. Y., Lane, K., Chin, C., Lu, J., Kirsch, D. G., Golub, T. R. and Jacks, T. (2009). Dicer1 functions as a haploinsufficient tumor suppressor. *Genes Dev* **23**, 2700-4.

Kuramochi-Miyagawa, S., Watanabe, T., Gotoh, K., Totoki, Y., Toyoda, A., Ikawa, M., Asada, N., Kojima, K., Yamaguchi, Y., Ijiri, T. W. et al. (2008). DNA methylation of retrotransposon genes is regulated by Piwi family members MILI and MIWI2 in murine fetal testes. *Genes Dev* **22**, 908-17.

Kuschel, S., Ruther, U. and Theil, T. (2003). A disrupted balance between Bmp/Wnt and Fgf signaling underlies the ventralization of the Gli3 mutant telencephalon. *Dev Biol* **260**, 484-95.

Lagos-Quintana, M., Rauhut, R., Yalcin, A., Meyer, J., Lendeckel, W. and Tuschl, T. (2002). Identification of tissue-specific microRNAs from mouse. *Curr Biol* **12**, 735-9.

Landgraf, P., Rusu, M., Sheridan, R., Sewer, A., Iovino, N., Aravin, A., Pfeffer, S., Rice, A., Kamphorst, AO., Landthaler, M., Lin, C., Socci, ND., Hermida, L., Fulci, V., Chiaretti, S., Foa, R., Schliwka, J., Fuchs, U., Novosel, A., Muller, RU., Schermer, B., Bissels, U., Inman, J., Phan, Q., Chien, M., Weir, DB., Choksi, R., De Vita, G., Frezzetti, D., Trompeter, HI., Hornung, V., Teng, G., Hartmann, G., Palkovits, M., Di Lauro, R., Wernet, P., Macino, G., Rogler, CE., Nagle, JW., Ju, J., Papavasiliou, F.N., Benzing, T., Lichter, P., Tam, W., Brownstein, M.J., Bosio, A., Borkhardt, A., Russo, J.J., Sander, C., Zavolan, M., Toshl, T.,. (2007). A mammalian microRNA expression atlas on small RNA library sequencing. *Cell* **129**, 1401 - 1414.

Lathia, J. D., Patton, B., Eckley, D. M., Magnus, T., Mughal, M. R., Sasaki, T., Caldwell, M. A., Rao, M. S., Mattson, M. P. and ffrench-Constant, C. (2007). Patterns of laminins and integrins in the embryonic ventricular zone of the CNS. *J Comp Neurol* **505**, 630-43.

Lawson, K. A. and Pedersen, R. A. (1992). Clonal analysis of cell fate during gastrulation and early neurulation in the mouse. *Ciba Found Symp* **165**, 3-21; discussion 21-6.

Lee, E. J., Banerjee, S., Zhou, H., Jammalamadaka, A., Arcila, M., Manjunath, B. S. and Kosik, K. S. (2011). Identification of piRNAs in the central nervous system. *RNA* **17**, 1090-9.

Lee, J. K., Cho, J. H., Hwang, W. S., Lee, Y. D., Reu, D. S. and Suh-Kim, H. (2000). Expression of neuroD/BETA2 in mitotic and postmitotic neuronal cells during the development of nervous system. *Dev Dyn* **217**, 361-7.

Lee, R. C., Feinbaum, R. L. and Ambros, V. (1993). The C. elegans heterochronic gene lin-4 encodes small RNAs with antisense complementarity to lin-14. *Cell* **75**, 843-54.

Lee, Y., Jeon, K., Lee, J. T., Kim, S. and Kim, V. N. (2002). MicroRNA maturation: stepwise processing and subcellular localization. *EMBO J* **21**, 4663-70.

Lee, Y., Kim, M., Han, J., Yeom, K. H., Lee, S., Baek, S. H. and Kim, V. N. (2004). MicroRNA genes are transcribed by RNA polymerase II. *EMBO J* **23**, 4051-60.

Lendahl, U., Zimmerman, L. B. and McKay, R. D. (1990). CNS stem cells express a new class of intermediate filament protein. *Cell* **60**, 585-95.

Leone, D. P., Srinivasan, K., Chen, B., Alcamo, E. and McConnell, S. K. (2008). The determination of projection neuron identity in the developing cerebral cortex. *Curr Opin Neurobiol* **18**, 28-35.

Lessard, J., Wu, J. I., Ranish, J. A., Wan, M., Winslow, M. M., Staahl, B. T., Wu, H., Aebersold, R., Graef, I. A. and Crabtree, G. R. (2007). An essential switch in subunit composition of a chromatin remodeling complex during neural development. *Neuron* **55**, 201-15.

Levison, S. W., Chuang, C., Abramson, B. J. and Goldman, J. E. (1993). The migrational patterns and developmental fates of glial precursors in the rat subventricular zone are temporally regulated. *Development* **119**, 611-22.

Levison, S. W. and Goldman, J. E. (1993). Both oligodendrocytes and astrocytes develop from progenitors in the subventricular zone of postnatal rat forebrain. *Neuron* **10**, 201-12.

Lewis, B. P., Burge, C. B. and Bartel, D. P. (2005). Conserved seed pairing, often flanked by adenosines, indicates that thousands of human genes are microRNA targets. *Cell* **120**, 15-20.

Lim, L. P., Lau, N. C., Garrett-Engele, P., Grimson, A., Schelter, J. M., Castle, J., Bartel, D. P., Linsley, P. S. and Johnson, J. M. (2005). Microarray analysis shows that some microRNAs downregulate large numbers of target mRNAs. *Nature* **433**, 769-73.

Lin, Q., Wei, W., Coelho, C. M., Li, X., Baker-Andresen, D., Dudley, K., Ratnu, V. S., Boskovic, Z., Kobor, M. S., Sun, Y. E. et al. (2011). The brain-specific microRNA miR-128b regulates the formation of fear-extinction memory. *Nat Neurosci* **14**, 1115-7.

Lui, J. H., Hansen, D. V. and Kriegstein, A. R. (2011). Development and evolution of the human neocortex. *Cell* **146**, 18-36.

Lund, E., Guttinger, S., Calado, A., Dahlberg, J. E. and Kutay, U. (2004). Nuclear export of microRNA precursors. *Science* **303**, 95-8.

Macrae, I. J., Zhou, K., Li, F., Repic, A., Brooks, A. N., Cande, W. Z., Adams, P. D. and Doudna, J. A. (2006). Structural basis for double-stranded RNA processing by Dicer. *Science* **311**, 195-8.

Maiorano, N. A., Mallamaci, A., . (2009). Promotion of embryonic cortico-cerebral neurogenesis by miR-124. . *Neural Development* **4**, 40.

Makeyev, E. V., Zhang, J., Carrasco, M. A. and Maniatis, T. (2007). The MicroRNA miR-124 promotes neuronal differentiation by triggering brain-specific alternative pre-mRNA splicing. *Mol Cell* **27**, 435-48.

Malatesta, P., Hartfuss, E. and Gotz, M. (2000). Isolation of radial glial cells by fluorescent-activated cell sorting reveals a neuronal lineage. *Development* **127**, 5253-63.

Marquardt, T., Ashery-Padan, R., Andrejewski, N., Scardigli, R., Guillemot, F. and Gruss, P. (2001). Pax6 is required for the multipotent state of retinal progenitor cells. *Cell* **105**, 43-55.

Martello, G., Rosato, A., Ferrari, F., Manfrin, A., Cordenonsi, M., Dupont, S., Enzo, E., Guzzardo, V., Rondina, M., Spruce, T. et al. (2010). A MicroRNA targeting dicer for metastasis control. *Cell* **141**, 1195-207.

Martinez, J., Patkaniowska, A., Urlaub, H., Luhrmann, R. and Tuschl, T. (2002). Single-stranded antisense siRNAs guide target RNA cleavage in RNAi. *Cell* **110**, 563-74.

Matsuo, I., Kuratani, S., Kimura, C., Takeda, N. and Aizawa, S. (1995). Mouse Otx2 functions in the formation and patterning of rostral head. *Genes Dev* **9**, 2646-58.

McCarthy, M., Turnbull, D. H., Walsh, C. A. and Fishell, G. (2001). Telencephalic neural progenitors appear to be restricted to regional and glial fates before the onset of neurogenesis. *J Neurosci* **21**, 6772-81.

McConnell, S. K. (1995). Constructing the cerebral cortex: neurogenesis and fate determination. *Neuron* **15**, 761-8.

McConnell, S. K. and Kaznowski, C. E. (1991). Cell cycle dependence of laminar determination in developing neocortex. *Science* **254**, 282-5.

Meier-Stiegen, F., Schwanbeck, R., Bernoth, K., Martini, S., Hieronymus, T., Ruau, D., Zenke, M. and Just, U. (2010). Activated Notch1 target genes during embryonic cell differentiation depend on the cellular context and include lineage determinants and inhibitors. *PLoS One* **5**, e11481.

Mellios, N., Sugihara, H., Castro, J., Banerjee, A., Le, C., Kumar, A., Crawford, B., Strathmann, J., Tropea, D., Levine, S. S. et al. (2011). miR-132, an experience-dependent microRNA, is essential for visual cortex plasticity. *Nat Neurosci* **14**, 1240-2.

Melton, C., Judson, R. L. and Blelloch, R. (2010). Opposing microRNA families regulate self-renewal in mouse embryonic stem cells. *Nature* **463**, 621-6.

Meza-Sosa, K. F., Valle-Garcia, D., Pedraza-Alva, G. and Perez-Martinez, L. (2012). Role of microRNAs in central nervous system development and pathology. *J Neurosci Res* **90**, 1-12.

Ming, G. L. and Song, H. (2011). Adult neurogenesis in the mammalian brain: significant answers and significant questions. *Neuron* **70**, 687-702.

Miranda, K. C., Huynh, T., Tay, Y., Ang, Y. S., Tam, W. L., Thomson, A. M., Lim, B. and Rigoutsos, I. (2006). A pattern-based method for the identification of MicroRNA binding sites and their corresponding heteroduplexes. *Cell* **126**, 1203-17.

Miska, E. A., Alvarez-Saavedra, E., Abbott, A. L., Lau, N. C., Hellman, A. B., McGonagle, S. M., Bartel, D. P., Ambros, V. R. and Horvitz, H. R. (2007). Most Caenorhabditis elegans microRNAs are individually not essential for development or viability. *PLoS Genet* **3**, e215.

Misson, J. P., Edwards, M. A., Yamamoto, M. and Caviness, V. S., Jr. (1988). Identification of radial glial cells within the developing murine central nervous system: studies based upon a new immunohistochemical marker. *Brain Res Dev Brain Res* **44**, 95-108.

Miyata, T., Kawaguchi, A., Okano, H. and Ogawa, M. (2001). Asymmetric inheritance of radial glial fibers by cortical neurons. *Neuron* **31**, 727-41.

Miyata, T., Kawaguchi, A., Saito, K., Kawano, M., Muto, T. and Ogawa, M. (2004). Asymmetric production of surface-dividing and non-surface-dividing cortical progenitor cells. *Development* **131**, 3133-45.

Miyata, T., Kawaguchi, D., Kawaguchi, A. and Gotoh, Y. (2010). Mechanisms that regulate the number of neurons during mouse neocortical development. *Curr Opin Neurobiol* **20**, 22-8.

Molnar, Z., Metin, C., Stoykova, A., Tarabykin, V., Price, D. J., Francis, F., Meyer, G., Dehay, C. and Kennedy, H. (2006). Comparative aspects of cerebral cortical development. *Eur J Neurosci* **23**, 921-34.

Molyneaux, B. J., Arlotta, P., Menezes, J. R. and Macklis, J. D. (2007). Neuronal subtype specification in the cerebral cortex. *Nat Rev Neurosci* **8**, 427-37.

Monteys, A. M., Spengler, R. M., Wan, J., Tecedor, L., Lennox, K. A., Xing, Y. and Davidson, B. L. (2010). Structure and activity of putative intronic miRNA promoters. *RNA* **16**, 495-505.

Morest, D. K. (1970). The pattern of neurogenesis in the retina of the rat. *Z Anat Entwicklungsgesch* **131**, 45-67.

Mourelatos, Z., Dostie, J., Paushkin, S., Sharma, A., Charroux, B., Abel, L., Rappsilber, J., Mann, M. and Dreyfuss, G. (2002). miRNPs: a novel class of ribonucleoproteins containing numerous microRNAs. *Genes Dev* **16**, 720-8.

Muotri, A. R., Chu, V. T., Marchetto, M. C., Deng, W., Moran, J. V. and Gage, F. H. (2005). Somatic mosaicism in neuronal precursor cells mediated by L1 retrotransposition. *Nature* **435**, 903-10.

Murakami, S., Kan, M., McKeehan, W. L. and de Crombrugghe, B. (2000). Up-regulation of the chondrogenic Sox9 gene by fibroblast growth factors is mediated by the mitogen-activated protein kinase pathway. *Proc Natl Acad Sci U S A* **97**, 1113-8.

Murchison, E. P., Partridge, J. F., Tam, O. H., Cheloufi, S. and Hannon, G. J. (2005). Characterization of Dicer-deficient murine embryonic stem cells. *Proc Natl Acad Sci U S A* **102**, 12135-40.

Naka, H., Nakamura, S., Shimazaki, T. and Okano, H. (2008). Requirement for COUP-TFI and II in the temporal specification of neural stem cells in CNS development. *Nat Neurosci* **11**, 1014-23.

Nakagawa, A., Shi, Y., Kage-Nakadai, E., Mitani, S. and Xue, D. (2010). Caspase-dependent conversion of Dicer ribonuclease into a death-promoting deoxyribonuclease. *Science* **328**, 327-34.

Nakashima, K., Yanagisawa, M., Arakawa, H., Kimura, N., Hisatsune, T., Kawabata, M., Miyazono, K. and Taga, T. (1999). Synergistic signaling in fetal brain by STAT3-Smad1 complex bridged by p300. *Science* **284**, 479-82.

Napoli, C., Lemieux, C. and Jorgensen, R. (1990). Introduction of a Chimeric Chalcone Synthase Gene into Petunia Results in Reversible Co-Suppression of Homologous Genes in trans. *Plant Cell* **2**, 279-289.

Nicholson, R. H. and Nicholson, A. W. (2002). Molecular characterization of a mouse cDNA encoding Dicer, a ribonuclease III ortholog involved in RNA interference. *Mamm Genome* **13**, 67-73.

Nielsen, J. A., Lau, P., Maric, D., Barker, J. L. and Hudson, L. D. (2009). Integrating microRNA and mRNA expression profiles of neuronal progenitors to identify regulatory networks underlying the onset of cortical neurogenesis. *BMC Neurosci* **10**, 98.

Nieto, M., Monuki, E. S., Tang, H., Imitola, J., Haubst, N., Khoury, S. J., Cunningham, J., Gotz, M. and Walsh, C. A. (2004). Expression of Cux-1 and Cux-2 in the subventricular zone and upper layers II-IV of the cerebral cortex. *J Comp Neurol* **479**, 168-80.

Noctor, S. C., Flint, A. C., Weissman, T. A., Dammerman, R. S. and Kriegstein, A. R. (2001). Neurons derived from radial glial cells establish radial units in neocortex. *Nature* **409**, 714-20.

Noctor, S. C., Martinez-Cerdeno, V., Ivic, L. and Kriegstein, A. R. (2004). Cortical neurons arise in symmetric and asymmetric division zones and migrate through specific phases. *Nat Neurosci* **7**, 136-44.

Noctor, S. C., Martinez-Cerdeno, V. and Kriegstein, A. R. (2008). Distinct behaviors of neural stem and progenitor cells underlie cortical neurogenesis. *J Comp Neurol* **508**, 28-44.

Nottrott, S., Simard, M. J. and Richter, J. D. (2006). Human let-7a miRNA blocks protein production on actively translating polyribosomes. *Nat Struct Mol Biol* **13**, 1108-14.

Nowakowski, T. J., Mysiak, K. S., Pratt, T. and Price, D. J. (2011). Functional dicer is necessary for appropriate specification of radial glia during early development of mouse telencephalon. *PLoS One* **6**, e23013.

Ochiai, W., Nakatani, S., Takahara, T., Kainuma, M., Masaoka, M., Minobe, S., Namihira, M., Nakashima, K., Sakakibara, A., Ogawa, M. et al. (2009). Periventricular notch activation and asymmetric Ngn2 and Tbr2 expression in pair-generated neocortical daughter cells. *Mol Cell Neurosci* **40**, 225-33.

Ohno, S. (2001). Intercellular junctions and cellular polarity: the PAR-aPKC complex, a conserved core cassette playing fundamental roles in cell polarity. *Curr Opin Cell Biol* **13**, 641-8.

Okano, H. and Temple, S. (2009). Cell types to order: temporal specification of CNS stem cells. *Curr Opin Neurobiol* **19**, 112-9.

Otto, S. J., McCorkle, S. R., Hover, J., Conaco, C., Han, J. J., Impey, S., Yochum, G. S., Dunn, J. J., Goodman, R. H. and Mandel, G. (2007). A new binding motif for the transcriptional repressor REST uncovers large gene networks devoted to neuronal functions. *J Neurosci* **27**, 6729-39.

Ozsolak, F., Poling, L. L., Wang, Z., Liu, H., Liu, X. S., Roeder, R. G., Zhang, X., Song, J. S. and Fisher, D. E. (2008). Chromatin structure analyses identify miRNA promoters. *Genes Dev* **22**, 3172-83.

Packer, A. N., Xing, Y., Harper, S. Q., Jones, L. and Davidson, B. L. (2008). The bifunctional microRNA miR-9/miR-9* regulates REST and CoREST and is downregulated in Huntington's disease. *J Neurosci* **28**, 14341-6.

Park, C. Y., Choi, Y. S. and McManus, M. T. (2010). Analysis of microRNA knockouts in mice. *Hum Mol Genet* **19**, R169-75.

Park, D., Xiang, A. P., Zhang, L., Mao, F. F., Walton, N. M., Choi, S. S. and Lahn, B. T. (2009). The radial glia antibody RC2 recognizes a protein encoded by Nestin. *Biochem Biophys Res Commun* **382**, 588-92.

Park, D., Xiang, A.P., Mao, FF., Zhang, L., Di, CG., Liu, XM., Shao, Y., Bao-Feng, M., Jae-Hyun, L., Kwan-Soo, H., Walton, N., Lahn, B.T.,. (2010). Nestin is required for proper self-renewal of neural stem cells. *Stem Cells*.

Parker, R. and Sheth, U. (2007). P bodies and the control of mRNA translation and degradation. *Mol Cell* **25**, 635-46.

Petersen, C. P., Bordeleau, M. E., Pelletier, J. and Sharp, P. A. (2006). Short RNAs repress translation after initiation in mammalian cells. *Mol Cell* **21**, 533-42.

Piccolo, S., Agius, E., Leyns, L., Bhattacharyya, S., Grunz, H., Bouwmeester, T. and De Robertis, E. M. (1999). The head inducer Cerberus is a multifunctional antagonist of Nodal, BMP and Wnt signals. *Nature* **397**, 707-10.

Pierfelice, T., Alberi, L. and Gaiano, N. (2011). Notch in the vertebrate nervous system: an old dog with new tricks. *Neuron* **69**, 840-55.

Pillai, R. S., Bhattacharyya, S. N. and Filipowicz, W. (2007). Repression of protein synthesis by miRNAs: how many mechanisms? *Trends Cell Biol* **17**, 118-26.

Pinto, L. and Gotz, M. (2007). Radial glial cell heterogeneity--the source of diverse progeny in the CNS. *Prog Neurobiol* **83**, 2-23.

Poche, R. A., Furuta, Y., Chaboissier, M. C., Schedl, A. and Behringer, R. R. (2008). Sox9 is expressed in mouse multipotent retinal progenitor cells and functions in Muller glial cell development. *J Comp Neurol* **510**, 237-50.

Pontes, O. and Pikaard, C. S. (2008). siRNA and miRNA processing: new functions for Cajal bodies. *Curr Opin Genet Dev* **18**, 197-203.

Pontious, A., Kowalczyk, T., Englund, C. and Hevner, R. F. (2008). Role of intermediate progenitor cells in cerebral cortex development. *Dev Neurosci* **30**, 24-32.

Price, D. J., Aslam, S., Tasker, L. and Gillies, K. (1997). Fates of the earliest generated cells in the developing murine neocortex. *J Comp Neurol* **377**, 414-22.

Quinn, J. C., Molinek, M., Martynoga, B. S., Zaki, P. A., Faedo, A., Bulfone, A., Hevner, R. F., West, J. D. and Price, D. J. (2007). Pax6 controls cerebral cortical cell number by regulating exit from the cell cycle and specifies cortical cell identity by a cell autonomous mechanism. *Dev Biol* **302**, 50-65.

Qureshi, I. A. and Mehler, M. F. (2009). Regulation of non-coding RNA networks in the nervous system--what's the REST of the story? *Neurosci Lett* **466**, 73-80.

Rakic, P. (1971). Guidance of neurons migrating to the fetal monkey neocortex. *Brain Res* **33**, 471-6.

Rakic, P. (1972). Mode of cell migration to the superficial layers of fetal monkey neocortex. *J Comp Neurol* **145**, 61-83.

Reynolds, B. A. and Weiss, S. (1996). Clonal and population analyses demonstrate that an EGF-responsive mammalian embryonic CNS precursor is a stem cell. *Dev Biol* **175**, 1-13.

Rice, D. S. and Curran, T. (2001). Role of the reelin signaling pathway in central nervous system development. *Annu Rev Neurosci* **24**, 1005-39.

Rice, D. S., Nusinowitz, S., Azimi, A. M., Martinez, A., Soriano, E. and Curran, T. (2001). The reelin pathway modulates the structure and function of retinal synaptic circuitry. *Neuron* **31**, 929-41.

Rowan, S. and Cepko, C. L. (2004). Genetic analysis of the homeodomain transcription factor Chx10 in the retina using a novel multifunctional BAC transgenic mouse reporter. *Dev Biol* **271**, 388-402.

Rowitch, D. H. and Kriegstein, A. R. (2010). Developmental genetics of vertebrate glial-cell specification. *Nature* **468**, 214-22.

Roy, K., Kuznicki, K., Wu, Q., Sun, Z., Bock, D., Schutz, G., Vranich, N. and Monaghan, A. P. (2004). The Tlx gene regulates the timing of neurogenesis in the cortex. *J Neurosci* **24**, 8333-45.

Rubenstein, J. L. (2011). Annual Research Review: Development of the cerebral cortex: implications for neurodevelopmental disorders. *J Child Psychol Psychiatry* **52**, 339-55.

Rubenstein, J. L. and Puelles, L. (1994). Homeobox gene expression during development of the vertebrate brain. *Curr Top Dev Biol* **29**, 1-63.

Rubenstein, J. L., Shimamura, K., Martinez, S. and Puelles, L. (1998). Regionalization of the prosencephalic neural plate. *Annu Rev Neurosci* **21**, 445-77.

Rybak, A., Fuchs, H., Hadian, K., Smirnova, L., Wulczyn, E. A., Michel, G., Nitsch, R., Krappmann, D. and Wulczyn, F. G. (2009). The let-7 target gene mouse lin-41 is a stem cell specific E3 ubiquitin ligase for the miRNA pathway protein Ago2. *Nat Cell Biol* **11**, 1411-20.

Rybak, A., Fuchs, H., Smirnova, L., Brandt, C., Pohl, E. E., Nitsch, R. and Wulczyn, F. G. (2008). A feedback loop comprising lin-28 and let-7 controls pre-let-7 maturation during neural stem-cell commitment. *Nat Cell Biol* **10**, 987-93.

Sahara, S. and O'Leary, D. D. (2009). Fgf10 regulates transition period of cortical stem cell differentiation to radial glia controlling generation of neurons and basal progenitors. *Neuron* **63**, 48-62.

Saito, T. (2006). *In vivo* electroporation in the embryonic mouse central nervous system. *Nat Protoc* **1**, 1552-8.

Sakakibara, S., Imai, T., Hamaguchi, K., Okabe, M., Aruga, J., Nakajima, K., Yasutomi, D., Nagata, T., Kurihara, Y., Uesugi, S., Miyata, T., Ogawa, M., Mikoshiba, K., Okano, H.,. (1996). Mouse Musashi-1, a neural RNA binding protein highly enriched in mammalian CNS stem cells. *Developmental Biology* **176**, 230 - 242.

Sakamoto, M., Imayoshi, I., Ohtsuka, T., Yamaguchi, M., Mori, K. and Kageyama, R. (2011). Continuous neurogenesis in the adult forebrain is required for innate olfactory responses. *Proc Natl Acad Sci U S A* **108**, 8479-84.

Santarelli, D. M., Beveridge, N. J., Tooney, P. A. and Cairns, M. J. (2011). Upregulation of dicer and microRNA expression in the dorsolateral prefrontal cortex Brodmann area 46 in schizophrenia. *Biol Psychiatry* **69**, 180-7.

Sayed, D. and Abdellatif, M. (2011). MicroRNAs in development and disease. *Physiol Rev* **91**, 827-87.

Schaefer, A., Poluch, S., Juliano, S., . (2008). Reelin is essential for neuronal migration but not for radial glial elongation in neonatal ferret cortex. *Developmental Neurobiology* **68**, 590 - 604.

Schmid, R. S., McGrath, B., Berechid, B. E., Boyles, B., Marchionni, M., Sestan, N. and Anton, E. S. (2003). Neuregulin 1-erbB2 signaling is required for the establishment of radial glia and their transformation into astrocytes in cerebral cortex. *Proc Natl Acad Sci U S A* **100**, 4251-6.

Schober, M., Schaefer, M. and Knoblich, J. A. (1999). Bazooka recruits Inscuteable to orient asymmetric cell divisions in Drosophila neuroblasts. *Nature* **402**, 548-51.

Schuurmans, C., Armant, O., Nieto, M., Stenman, J. M., Britz, O., Klenin, N., Brown, C., Langevin, L. M., Seibt, J., Tang, H. et al. (2004). Sequential phases of cortical specification involve Neurogenin-dependent and -independent pathways. *EMBO J* **23**, 2892-902.

Schuurmans, C. and Guillemot, F. (2002). Molecular mechanisms underlying cell fate specification in the developing telencephalon. *Curr Opin Neurobiol* **12**, 26-34.

Scott, C. E., Wynn, S. L., Sesay, A., Cruz, C., Cheung, M., Gomez Gaviro, M. V., Booth, S., Gao, B., Cheah, K. S., Lovell-Badge, R. et al. (2010). SOX9 induces and maintains neural stem cells. *Nat Neurosci* **13**, 1181-9.

Sengupta, S., Nie, J., Wagner, R. J., Yang, C., Stewart, R. and Thomson, J. A. (2009). MicroRNA 92b controls the G1/S checkpoint gene p57 in human embryonic stem cells. *Stem Cells* **27**, 1524-8.

Sessa, A., Mao, C. A., Hadjantonakis, A. K., Klein, W. H. and Broccoli, V. (2008). Tbr2 directs conversion of radial glia into basal precursors and guides neuronal amplification by indirect neurogenesis in the developing neocortex. *Neuron* **60**, 56-69.

Shawlot, W. and Behringer, R. R. (1995). Requirement for Lim1 in head-organizer function. *Nature* **374**, 425-30.

Shi, Y., Kirwan, P., Smith, J., Robinson, H. P. C. and Livesey, F. J. (2012) Human cerebral cortex development from pluripotent stem cells to functional excitatory synapses. *Nat Neurosci* advance online publication

Shibata, M., Kurokawa, D., Nakao, H., Ohmura, T. and Aizawa, S. (2008). MicroRNA-9 modulates Cajal-Retzius cell differentiation by suppressing Foxg1 expression in mouse medial pallium. *J Neurosci* **28**, 10415-21.

Shibata, M., Nakao, H., Kiyonari, H., Abe, T. and Aizawa, S. (2011). MicroRNA-9 regulates neurogenesis in mouse telencephalon by targeting multiple transcription factors. *J Neurosci* **31**, 3407-22.

Shibata, T., Yamada, K., Watanabe, M., Ikenaka, K., Wada, K., Tanaka, K. and Inoue, Y. (1997). Glutamate transporter GLAST is expressed in the radial glia-astrocyte lineage of developing mouse spinal cord. *J Neurosci* **17**, 9212-9.

Shimamura, K. and Rubenstein, J. L. (1997). Inductive interactions direct early regionalization of the mouse forebrain. *Development* **124**, 2709-18.

Shimojo, H., Ohtsuka, T. and Kageyama, R. (2008). Oscillations in notch signaling regulate maintenance of neural progenitors. *Neuron* **58**, 52-64.

Smart, I. H. (1973). Proliferative characteristics of the ependymal layer during the early development of the mouse neocortex: a pilot study based on recording the number, location and plane of cleavage of mitotic figures. *J Anat* **116**, 67-91.

Smart, I. H. (1976). A pilot study of cell production by the ganglionic eminences of the developing mouse brain. *J Anat* **121**, 71-84.

Smart, I. H., Dehay, C., Giroud, P., Berland, M. and Kennedy, H. (2002). Unique morphological features of the proliferative zones and postmitotic compartments of the neural epithelium giving rise to striate and extrastriate cortex in the monkey. *Cereb Cortex* **12**, 37-53.

Smirnova, L., Grafe, A., Seiler, A., Schumacher, S., Nitsch, R. and Wulczyn, F. G. (2005). Regulation of miRNA expression during neural cell specification. *Eur J Neurosci* **21**, 1469-77.

Soriano, P. (1999). Generalized lacZ expression with the ROSA26 Cre reporter strain. *Nat Genet* **21**, 70-1.

Srinivas, S., Watanabe, T., Lin, C. S., William, C. M., Tanabe, Y., Jessell, T. M. and Costantini, F. (2001). Cre reporter strains produced by targeted insertion of EYFP and ECFP into the ROSA26 locus. *BMC Dev Biol* **1**, 4.

Stefani, G. and Slack, F. J. (2008). Small non-coding RNAs in animal development. *Nat Rev Mol Cell Biol* **9**, 219-30.

Steinbeisser, H., De Robertis, E. M., Ku, M., Kessler, D. S. and Melton, D. A. (1993). Xenopus axis formation: induction of goosecoid by injected Xwnt-8 and activin mRNAs. *Development* **118**, 499-507.

Stolt, C. C. and Wegner, M. (2010). SoxE function in vertebrate nervous system development. *Int J Biochem Cell Biol* **42**, 437-40.

Stoykova, A., Fritsch, R., Walther, C. and Gruss, P. (1996). Forebrain patterning defects in Small eye mutant mice. *Development* **122**, 3453-65.

Sulik, K., Dehart, D. B., Iangaki, T., Carson, J. L., Vrablic, T., Gesteland, K. and Schoenwolf, G. C. (1994). Morphogenesis of the murine node and notochordal plate. *Dev Dyn* **201**, 260-78.

Takahashi, T., Nowakowski, R. S. and Caviness, V. S., Jr. (1995a). The cell cycle of the pseudostratified ventricular epithelium of the embryonic murine cerebral wall. *J Neurosci* **15**, 6046-57.

Takahashi, T., Nowakowski, R. S. and Caviness, V. S., Jr. (1995b). Early ontogeny of the secondary proliferative population of the embryonic murine cerebral wall. *J Neurosci* **15**, 6058-68.

Takahashi, T., Nowakowski, R. S. and Caviness, V. S., Jr. (1996). The leaving or Q fraction of the murine cerebral proliferative epithelium: a general model of neocortical neuronogenesis. *J Neurosci* **16**, 6183-96.

Tamamaki, N., Nakamura, K. and Kaneko, T. (2001). Cell migration from the corticostriatal angle to the basal telencephalon in rat embryos. *Neuroreport* **12**, 775-80.

Tao, W. and Lai, E. (1992). Telencephalon-restricted expression of BF-1, a new member of the HNF-3/fork head gene family, in the developing rat brain. *Neuron* **8**, 957-66.

Tarabykin, V., Stoykova, A., Usman, N. and Gruss, P. (2001). Cortical upper layer neurons derive from the subventricular zone as indicated by Svet1 gene expression. *Development* **128**, 1983-93.

Teixeira, D., Sheth, U., Valencia-Sanchez, M. A., Brengues, M. and Parker, R. (2005). Processing bodies require RNA for assembly and contain nontranslating mRNAs. *RNA* **11**, 371-82.

Theil, T., Alvarez-Bolado, G., Walter, A. and Ruther, U. (1999). Gli3 is required for Emx gene expression during dorsal telencephalon development. *Development* **126**, 3561-71.

Thermann, R. and Hentze, M. W. (2007). Drosophila miR2 induces pseudo-polysomes and inhibits translation initiation. *Nature* **447**, 875-8.

Tissir, F. and Goffinet, A. M. (2003). Reelin and brain development. *Nat Rev Neurosci* **4**, 496-505.

Tohyama, T., Lee, V. M., Rorke, L. B., Marvin, M., McKay, R. D. and Trojanowski, J. Q. (1992). Nestin expression in embryonic human neuroepithelium and in human neuroepithelial tumor cells. *Lab Invest* **66**, 303-13.

Trommsdorff, M., Gotthardt, M., Hiesberger, T., Shelton, J., Stockinger, W., Nimpf, J., Hammer, R. E., Richardson, J. A. and Herz, J. (1999). Reeler/Disabled-like disruption of neuronal migration in knockout mice lacking the VLDL receptor and ApoE receptor 2. *Cell* **97**, 689-701.

Uchida, N., Buck, D., He, D., Reitsma, MJ., Masek, M., Phan, TV., Tsukamoto, AS., Gage, FH., Weissman, IL.,. (2000). Direct isolation of human central nervous system stem cells. *Proceedings of the National Academy of Sciences of the USA* **97**, 15720 - 15725.

van Rooij, E., Sutherland, L. B., Qi, X., Richardson, J. A., Hill, J. and Olson, E. N. (2007). Control of stress-dependent cardiac growth and gene expression by a microRNA. *Science* **316**, 575-9.

Vasudevan, S., Tong, Y., Steitz, JA., . (2007). Switching from repression to activation: microRNAs can up-regulate transcription. *Science* **318**, 1931 - 1934.

Ventura, A., Young, A. G., Winslow, M. M., Lintault, L., Meissner, A., Erkeland, S. J., Newman, J., Bronson, R. T., Crowley, D., Stone, J. R. et al. (2008). Targeted deletion reveals essential and overlapping functions of the miR-17 through 92 family of miRNA clusters. *Cell* **132**, 875-86.

Visvanathan, J., Lee, S., Lee, B., Lee, J. W. and Lee, S. K. (2007). The microRNA miR-124 antagonizes the anti-neural REST/SCP1 pathway during embryonic CNS development. *Genes Dev* **21**, 744-9.

Vo, N., Klein, M. E., Varlamova, O., Keller, D. M., Yamamoto, T., Goodman, R. H. and Impey, S. (2005). A cAMP-response element binding protein-induced microRNA regulates neuronal morphogenesis. *Proc Natl Acad Sci U S A* **102**, 16426-31.

Voigt, T. (1989). Development of glial cells in the cerebral wall of ferrets: direct tracing of their transformation from radial glia into astrocytes. *J Comp Neurol* **289**, 74-88.

Walker, J. C. and Harland, R. M. (2009). microRNA-24a is required to repress apoptosis in the developing neural retina. *Genes Dev* **23**, 1046-51.

Wallace, V. A. and Raff, M. C. (1999). A role for Sonic hedgehog in axon-to-astrocyte signalling in the rodent optic nerve. *Development* **126**, 2901-9.

Wegner, M. (1999). From head to toes: the multiple facets of Sox proteins. *Nucleic Acids Research* **27**, 1409 - 1420.

Weimer, J., Yokota, Y., Stanco, A., Stumpo, DJ., Blackshear, PJ., Anton, ES.,. (2009). MARCKS modulates radial progenitor placement, proliferation and organisation in the developing cerebral cortex. *Development* **136**, 2965 - 2975.

Wilkie, A. L., Jordan, S. A., Sharpe, J. A., Price, D. J. and Jackson, I. J. (2004). Widespread tangential dispersion and extensive cell death during early neurogenesis in the mouse neocortex. *Dev Biol* **267**, 109-18.

Wodarz, A. and Huttner, W. B. (2003). Asymmetric cell division during neurogenesis in Drosophila and vertebrates. *Mech Dev* **120**, 1297-309.

Wodarz, A., Ramrath, A., Kuchinke, U. and Knust, E. (1999). Bazooka provides an apical cue for Inscuteable localization in Drosophila neuroblasts. *Nature* **402**, 544-7.

Wood, J. G., Martin, S. and Price, D. J. (1992). Evidence that the earliest generated cells of the murine cerebral cortex form a transient population in the subplate and marginal zone. *Brain Res Dev Brain Res* **66**, 137-40.

Woodhead, G. J., Mutch, C. A., Olson, E. C. and Chenn, A. (2006). Cell-autonomous beta-catenin signaling regulates cortical precursor proliferation. *J Neurosci* **26**, 12620-30.

Woods, A., Wang, G. and Beier, F. (2005). RhoA/ROCK signaling regulates Sox9 expression and actin organization during chondrogenesis. *J Biol Chem* **280**, 11626-34.

Wu, S., Mikhailov, A., Kallo-Hosein, H., Hara, K., Yonezawa, K. and Avruch, J. (2002). Characterization of ubiquilin 1, an mTOR-interacting protein. *Biochim Biophys Acta* **1542**, 41-56.

Xie, X., Lu, J., Kulbokas, E. J., Golub, T. R., Mootha, V., Lindblad-Toh, K., Lander, E. S. and Kellis, M. (2005). Systematic discovery of regulatory motifs in

human promoters and 3' UTRs by comparison of several mammals. *Nature* **434**, 338-45.

Yang, W., Chendrimada, T. P., Wang, Q., Higuchi, M., Seeburg, P. H., Shiekhattar, R. and Nishikura, K. (2006). Modulation of microRNA processing and expression through RNA editing by ADAR deaminases. *Nat Struct Mol Biol* **13**, 13-21.

Yi, R., Doehle, B. P., Qin, Y., Macara, I. G. and Cullen, B. R. (2005). Overexpression of exportin 5 enhances RNA interference mediated by short hairpin RNAs and microRNAs. *RNA* **11**, 220-6.

Yi, R., Qin, Y., Macara, I. G. and Cullen, B. R. (2003). Exportin-5 mediates the nuclear export of pre-microRNAs and short hairpin RNAs. *Genes Dev* **17**, 3011-6.

Yoo, A. S., Staahl, B. T., Chen, L. and Crabtree, G. R. (2009). MicroRNA-mediated switching of chromatin-remodelling complexes in neural development. *Nature* **460**, 642-6.

Yoo, A. S., Sun, A. X., Li, L., Shcheglovitov, A., Portmann, T., Li, Y., Lee-Messer, C., Dolmetsch, R. E., Tsien, R. W. and Crabtree, G. R. (2011). MicroRNA-mediated conversion of human fibroblasts to neurons. *Nature* **476**, 228-31.

Yoon, K., Nery, S., Rutlin, M. L., Radtke, F., Fishell, G. and Gaiano, N. (2004). Fibroblast growth factor receptor signaling promotes radial glial identity and interacts with Notch1 signaling in telencephalic progenitors. *J Neurosci* **24**, 9497-506.

Yoon, K. J., Koo, B. K., Im, S. K., Jeong, H. W., Ghim, J., Kwon, M. C., Moon, J. S., Miyata, T. and Kong, Y. Y. (2008). Mind bomb 1-expressing intermediate progenitors generate notch signaling to maintain radial glial cells. *Neuron* **58**, 519-31.

Yoshida, M., Suda, Y., Matsuo, I., Miyamoto, N., Takeda, N., Kuratani, S. and Aizawa, S. (1997). Emx1 and Emx2 functions in development of dorsal telencephalon. *Development* **124**, 101-11.

Yuan, A., Farber, E. L., Rapoport, A. L., Tejada, D., Deniskin, R., Akhmedov, N. B. and Farber, D. B. (2009). Transfer of microRNAs by embryonic stem cell microvesicles. *PLoS One* **4**, e4722.

Yun, K., Mantani, A., Garel, S., Rubenstein, J. and Israel, M. A. (2004). Id4 regulates neural progenitor proliferation and differentiation *in vivo*. *Development* **131**, 5441-8.

Zhao, C., Sun, G., Li, S. and Shi, Y. (2009). A feedback regulatory loop involving microRNA-9 and nuclear receptor TLX in neural stem cell fate determination. *Nat Struct Mol Biol* **16**, 365-71.

Zhao, Y., Ransom, J. F., Li, A., Vedantham, V., von Drehle, M., Muth, A. N., Tsuchihashi, T., McManus, M. T., Schwartz, R. J. and Srivastava, D. (2007). Dysregulation of cardiogenesis, cardiac conduction, and cell cycle in mice lacking miRNA-1-2. *Cell* **129**, 303-17.

Zhong, W., Jing, MM., Schonemann, MD., Meneses, JJ., Pedersen, RA., Jan, LY., Jan, YN.,. (2000). Mouse numb is an essential gene involved in cortical neurogenesis. *Proceedings of the National Academy of Sciences of the USA* **97**, 6844 - 6849.

Zhou, C. J., Borello, U., Rubenstein, J. L. and Pleasure, S. J. (2006). Neuronal production and precursor proliferation defects in the neocortex of mice with loss of function in the canonical Wnt signaling pathway. *Neuroscience* **142**, 1119-31.

Zhou, X., Ruan, J., Wang, G. and Zhang, W. (2007). Characterization and identification of microRNA core promoters in four model species. *PLoS Comput Biol* **3**, e37.

Zimmer, C., Tiveron, M. C., Bodmer, R. and Cremer, H. (2004). Dynamics of Cux2 expression suggests that an early pool of SVZ precursors is fated to become upper cortical layer neurons. *Cereb Cortex* **14**, 1408-20.